



**TSPM Science Document**

**Code:**

SCI/TSPM-PDR/001

**Issue:** 1.B

**Date:** 20/10/2017

**Pages:** 86



|                     |   |
|---------------------|---|
| <b>Authors:</b>     | Fernando Fabián Rosales Ortega (Project Scientist)<br>Jesús González<br>William Lee |
| <b>Revised by:</b>  |   |
| <b>Approved by:</b> |   |

### Contributors

|   |  |
|---|--|
| <i>Galactic and stellar astronomy</i><br>Carmen Ayala<br>Emmanuele Bertone<br>Mónica W. Blanco Cárdenas<br>Miguel Chávez Dagostino<br>Luis J. Corral<br>Arturo Gómez-Ruíz<br>Martin A. Guerrero<br>Silvana G. Navarro Jiménez<br>Manuel Nuñez<br>Lorenzo Olguín<br>Gerardo Ramos Larios<br>Mauricio Reyes Ruíz<br>Michael Richer<br>Carlos Román Zúñiga<br>Laurence Sabin<br>Miguel Ángel Trinidad<br>Roberto Vázquez Meza<br>Juan Luis Verbena Contreras | <i>Extragalactic astronomy &amp; Cosmology</i><br>Heinz Andernach<br>César A. Caretta<br>Alberto Carramiñana<br>Marcel Chow-Martínez<br>Deborah Dultzin Kessler<br>Héctor Javier Ibarra Medel<br>Simon N. Kemp<br>Omar López Cruz<br>Divakara Mayya<br>Daniel Rosa Gonzalez<br>Juan Pablo Torres Papaqui<br>Olga Vega<br><br><i>Future instrumentation</i><br>Edgar Castillo Domínguez<br>Perla Carolina García Flores<br>Sebastián F. Sánchez Sánchez<br>Laurence Sabin |
|---|--|



## TSPM Science Document

Code: SCI/TSPM-PDR/001  
Issue: 1.B  
Date: 20/10/2017  
Page: 3 of 86

### Distribution List

| Name      | Affiliation  |
|-----------|--------------|
| TSPM team | All partners |
|           |              |
|           |              |
|           |              |

### Document Change Record

| Issue | Date       | Section | Page | Change description   |
|-------|------------|---------|------|--|
| 1.A   | 17/09/2016 | All     | All  | First issue  |
| 1.B   | 20/10/2017 |         |      | Document updated from previous version. New science cases and instrumentation proposals included. Comments from the previous PDR panel considered. Comments and contributions from the TSPM Core Science Group included. |
|       |            |         |      |  |

### Applicable and Reference Documents

| N°  | Document Name                            | Code         |
|-----|--|--------------|
| R.1 | TSPM: List of acronyms and abbreviations | TEC/TSPM/001 |
|     |  |              |
|     |  |              |
|     |  |              |



**INDEX**

**1. SUMMARY ..... 6**

**2. OBJECTIVE ..... 6**

**3. SCOPE ..... 6**

**4. TOP LEVEL SCIENCE REQUIREMENTS..... 6**

**4.1 Key Science Drivers..... 7**

4.1.1 Complementarity for the current and future large telescopes ..... 7

4.1.2 Complementarity with the MMT..... 7

4.1.3 Time-domain astrophysics..... 8

**4.2 Science with the TSPM..... 8**

4.2.1 Galactic Astronomy..... 8

4.2.2 Extragalactic Astronomy and Cosmology ..... 11

4.2.3 Summary of science requirements..... 15

**Wavelength range, image quality and background ..... 18**

**Plate scale and focal stations..... 19**

**Science instruments ..... 19**

**Wide Field Corrector..... 20**

**5. PROPOSED SCIENCE CASES FOR A JOINT TSPM/MMT OBSERVATORY ... 21**

**5.1 Galactic and stellar astronomy..... 21**

5.1.1 Chromospheric activity and age of solar analogs in open clusters..... 21

5.1.2 Massive stars in nearby galaxies ..... 25

5.1.3 The impact of massive outflows in Galactic Star Formation ..... 28

5.1.4 Symbiotic systems and planetary nebulae: determination of physical parameters ..... 30

5.1.5 Molecular hydrogen of small scale structures in planetary nebulae..... 31

5.1.6 Observing Near Earth Objects using the 6.5m TSPM..... 33



|            |   |           |
|------------|---|-----------|
| 5.1.7      | High resolution spectroscopy and the abundance discrepancy problem in ionized plasmas                                 | 36        |
| 5.1.8      | Young star clusters and the structure of molecular clouds with the TSPM .....   | 37        |
| 5.1.9      | Determination of presence of shocks caused by PNe halo-ISM interaction .....  | 42        |
| <b>5.2</b> | <b>Extragalactic astronomy .....</b>  | <b>43</b> |
| 5.2.1      | Star formation histories of galaxies in the local Universe using the resolved bright stars in the near infrared ..... | 43        |
| 5.2.2      | H <sub>2</sub> ETGs: tracing accretion/SF/feedback in early-type galaxies with TSPM.....                              | 47        |
| 5.2.3      | Optical search and follow-up of gravitational waves counterparts .....  | 51        |
| <b>5.3</b> | <b>Cosmology .....</b>  | <b>53</b> |
| 5.3.1      | Peculiar velocities of clusters and groups of galaxies inside large scale structures .....                            | 53        |
| 5.3.2      | The evolving Universe of quasars .....  | 55        |
| 5.3.3      | The formation and evolution of cD galaxies .....  | 58        |
| 5.3.4      | The Butcher-Oemler Effect: Quenching vs. Ignition: A Scientific Case for TSPM and MMT                                 | 61        |
| <b>5.4</b> | <b>Future instrumentation .....</b>   | <b>67</b> |
| 5.4.1      | Wide-field imaging Fourier transform spectroscopy: a instrumentation proposal for the TSPM                            | 67        |
| 5.4.1.1    | <i>Technical challenges in the construction of an IFTS system .....</i>   | <i>74</i> |
| 5.4.1.2    | <i>Science with an IFTS instrument in a 6.5m class telescope: the case for TSPM...</i>                                | <i>76</i> |
| 5.4.2      | A (Spectro-)Polarimeter Unit for the TSPM: EspectroPol.....   | 81        |
| 5.4.2.1    | <i>EspectroPol: science with the TSPM .....</i>   | <i>84</i> |



## **1. SUMMARY**

The Telescopio San Pedro Mártir project (TSPM) will design, construct and operate a new wide-field 6.5m telescope at the Observatorio Astronomico Nacional in San Pedro Mártir, B.C., Mexico. It is a joint endeavor of the Mexican astronomical community, led by Universidad Nacional Autonoma de México (UNAM), and Instituto Nacional de Astrofísica, Óptica y Electrónica (INAOE) in Mexico, with the University of Arizona (UA) and the Smithsonian Astrophysical Observatory (SAO) in the United States. The TSPM project will take advantage of existing optical elements and instrumentation, particularly from the Magellan Observatory and the MMT at Mt. Hopkins, Arizona, operated by UA and SAO, and the goal is to operate both the TSPM and MMT as a joint bi-national astrophysics laboratory, with access to both communities and the implementation of complementary and large scale programs which will take advantage of the capabilities of each telescope.

## **2. OBJETIVE**

The purpose of this document is to identify the main scientific goals of the project and to provide a logical framework for the technical members of the team to develop the engineering requirements for the telescope system, considering that the telescope will likely be used in a wide range of ground-based optical and near-infrared astronomy areas over its lifetime.

## **3. SCOPE**

The TSPM Science Document describes the top level science requirements of the project, which include the present and future key science drivers for the TSPM, niches of opportunity and the proposed science cases for the TSPM/MMT joint observatory as of October 2017, gathering proposals from the members of the astronomical community in Mexico after a nation wide call.

## **4. TOP LEVEL SCIENCE REQUIREMENTS**

In compliance to the TSPM High Level Requirements, the TSPM shall be suitable for general science projects; in the understanding that the TSPM should have comparable flexibility to facilities such as MMT, Magellan, Keck, Gemini, VLT, and GTC, and not be a single-purpose facility such as LSST, Pan STARRS, and VISTA [RQ/TSPM/001]. At present, the TSPM science case is based almost entirely upon efforts and interests of the Mexican astronomical community. However, on the long-term, the goal is to operate both the TSPM and MMT as a joint bi-national astrophysics laboratory, with access to both telescopes by all of the communities involved in the TSPM project, and to take advantage of the specific capabilities of each telescope in order to perform specific and large-scale scientific programs.

During its first stage of operation (the so-called Day-One operation period), the TSPM is intended to provide a functionally equivalent telescope to the  $f/5$  Cassegrain configurations at the MMT and the



Magellan Clay telescopes, with a field of view (FoV) of one degree, and instrumentation composed by a suite of optical and infrared cameras, and potentially new instrumentation with spectroscopic and/or polarimetry capability. Subsequently, during a second stage of the project, the general goal is to implement additional Nasmyth focal stations in order to accommodate larger instruments and to provide versatility to the telescope, according to the needs and scientific interests of the partners.

#### **4.1 Key Science Drivers**

The TSPM project has identified the following key science goals:

##### **4.1.1 Complementarity for the current and future large telescopes**

In the future era of large telescopes, it is important to stress the scientific potential of a medium-size telescope like the TSPM, and its co-existence with future large facilities such as the LSST, TMT, GMT, E-ELT, and the JWST. The relation of mid-size telescopes with large ones is synergistic, each providing support for the other. Discoveries made at large telescopes can often be most effectively exploited on smaller ones. Current 8-10m class telescopes and the future giant telescopes (+25m) are neither designed nor intended to perform large sky surveys with enough depth that are important for several science programs. The extreme expenses of the giant telescopes strongly limits the observing time available to much less than could be profitably used by the astronomical community. Therefore, a 6.5m class telescope such as the TSPM will be a complementary instrument and will play an essential role in the forthcoming decades in the scenario of the large-scale astronomical infrastructures that will be deployed around the globe. A 6.5m class telescope with a one degree FoV –with spectroscopic and polarimetry capabilities– represents a significant niche and could potentially explore a selection of scientific initiatives that span the entire range of astronomical research: from the study of planetary systems, formation and evolution of stars, galaxy dynamics, to the evolution of the Universe at large scale.

##### **4.1.2 Complementarity with the MMT**

The operation of both telescopes as a joint observatory –each available for both communities– will optimize the use of both facilities considering the characteristics of each site and the configurations of both telescopes. SPM is a darker site, optimal for large field of view observations in the optical. The MMT has a modern adaptive optics system (AO) when the secondary mirror of the shortest field of view is deployed, which makes it suitable for the study of individual objects in the near infrared, where the sky brightness is not an important issue. The versatility given by having two telescopes that could mount complementary instrumentation is an important added value that could duplicate the scientific return and productivity. Furthermore, as has been the case for every previous increase in capability of any astronomical infrastructure, it is very likely that the scientific impact of the joint TSPM/MMT observatory will go far beyond what the project envisions today. Therefore, considering the functionality expected from the TSPM during its first stage of operation and the science drivers



described above, the niche opportunity for the TSPM would consist on exploiting the combination of the light gathering power of its 6.5-m primary mirror and the large FoV of the Day-One f/5 Cassegrain configuration.

#### **4.1.3 Time-domain astrophysics**

Every time a new domain in astronomy is explored –either in sensitivity or wavelength– astronomers have discovered staggering information about the content, origin and evolution of the Universe. However, there is an important domain that remains largely unexplored: the study of targets that modify their brightness and/or characteristics as a function of time. Despite important efforts in the community, we remain largely ignorant of rapidly variable and transient sources in the sky. This is a rapidly evolving field and will play a very important role in the understanding of the evolution of astrophysical systems and their observable properties. Next Generation Imaging Surveys (NGISs), such as Pan-STARRS and LSST, will soon routinely produce hundreds to thousands of transients per night. The phase space for new discoveries is enormous and the TSPM could position itself in the international arena to capitalize it. Monitoring variable objects, especially if full phase coverage is essential, requires telescopes with stable instrumentation and very flexible schedules. The TSPM project acknowledges that this is only possible during the envisaged second stage of the project, i.e. a telescope of a large field of view and the versatility offered by the implementation of additional Nasmyth and folded-Cass focal stations and new instrumentation. This potential configuration might open the verge of a whole new parameter space and will stand in the forefront of modern astronomy through revealing the time domain, making significant contributions in the field.

### **4.2 Science with the TSPM**

The TSPM could exploit its wide-field imaging capabilities during the Day-One operation period, and subsequently its potential spectroscopic and polarimetric capabilities within several forefront science areas:

#### **4.2.1 Galactic Astronomy**

**Protostars.** Protoplanetary disks and jets are an important part of the star formation process, and can provide insight into how planetary systems form. In this way, T-Tauri stars are among the youngest objects directly observed and their circumstellar environments are an ideal laboratory for studying the initial conditions of planet formation. In order to understanding protoplanetary disk evolution and how they are affected for the planet formation, a monitoring and study of the light curves of T-Tauri and intermediate-mass stars are required. Variability surveys in the near IR can probe stellar and circumstellar environments and provide information about the magnetic and accretion processes. In addition, this study will investigate the variability and periodicity of these objects and allow a classification of the different types of variability, e.g. periodic, stochastic and long-term variability.





**Nebulae around evolved stars.** A meaningful link between local heavy element enrichment and the global chemical evolution of galaxies can only be established by detailed studies of individual windblown bubbles in our Galaxy. Winds of evolved stars, and their surrounding bubbles (planetary nebulae, luminous blue variables, Wolf-Rayet ejects, supernovae remnants) are known to be globally enriched with products of nucleosynthesis. A complete survey of abundance, density, temperature and kinematic measurements in nebulae surrounding individual evolved stars or ionizing clusters, looking for non-homogeneities in the distribution of processed material (primarily nitrogen and oxygen), requires wide field imaging and spectroscopy with sufficient spatial and spectral coverage with the appropriate resolutions to perform such studies.

**NEOS and other minor bodies of the Solar system.** Asteroids are the leftovers of the rocky planet formation in our Solar system. They are important because they keep information of this early stage. Nowadays, more than seven hundred thousands asteroids are known and only less than one percent of them have been studied in detail. We can get information about the chemical composition, sizes and motion of asteroids by using a combination of optical and infrared technics. Reflectance spectroscopy is the only way to infer their surface chemical composition from ground. Besides, optical and infrared photometry allows us to calculate their rotation period and to infer their shape if multiepoch observations are used. Also, infrared photometry allow us to derive albedos and confident sizes. The TSPM spectroscopy and imaging capabilities are excellent suited to characterize thousands of faint asteroids ( $V > 17$ ). Near-Earth Objects (NEOs) includes all comets and asteroids that at some point in their orbit get closer than 1.3 AU from the Sun and enter in the Earth's neighborhood. Around 15000 NEOs are known and most of them are asteroids (99.3%). In order to assess the potential danger to Earth posed by NEOs, their orbital and physical properties must be known. Because of their rapid movement in the sky, in addition to their small size and low brightness, most NEOs are hardly studied in detail. The large collecting area of TSPM will offer a unique facility for fast spectral and photometrical observations of faint NEOs, aiming for the detailed characterization of their physical properties.

**Structure of Galactic HII regions.** Nebular emission lines from individual HII regions have been – historically– the main tool at our disposal for the direct measurement of the gas-phase abundance of the interstellar medium in galaxies, including the primordial helium abundance. Chemical, density and temperature inhomogeneities have been proposed as potential sources of error for the systematically underestimation of chemical abundances using collisionally excited lines as compared to optical recombination lines. In order to shed light into this problem, a complete spatial coverage of the HII regions is required. A large FoV, both in imaging and spectroscopy, offers the best opportunity for obtaining the required narrow band and/or spectral information of nearby Galactic HII regions with a complete spatial coverage, as well as the study of the impact of shock fronts originating from massive stellar winds and the kinematics of HII regions. This is an example of a program that will require wide-field imaging and spectroscopy with the best observing conditions such as those of SPM.



**Circumstellar discs and planet formation.** Circumstellar discs play a fundamental role in star evolution and planetary systems formation. The classical model of star formation naturally lead to a disc formation around protostars. As the secular evolution of a star takes place, the accretion rate decreases and the gas dissipates. In the disc dust remains and gradually coalesces into larger pieces. Planetesimals eventually form and planets are created by aggregation of multiple smaller bodies. Despite the large literature about the process, several gaps in circumstellar disc evolution remain. The study of large samples of stars and protostars to fill in the gaps are needed. TSPM equipped with Hectoechelle will be excellently suited for spectral characterization of stars fainter than  $V > 17$ .

**Properties of open stellar clusters.** Although hundreds of open clusters are known in the Galaxy, only for very few of them their main properties (size, distance, reddening age and metallicity) have been estimated. The angular extension of the cluster (of the order of 1 deg in some cases) is a limitation for obtaining spectroscopic data of a very large number of stars, and in cases of important crowding, the multi-fiber or multi-slit spectroscopy are not able to observe all the objects in the field at once. An imaging spectrograph with a large FoV will allow obtaining spectroscopic information on crowded stellar clusters with complete spatial coverage.

**Synergies with GAIA.** The Milky Way is the system for which we can hope to constrain in most detail the physical processes that play a role in the formation and evolution of galaxies. These mechanisms of formation and evolution are encoded in the location, kinematics and chemistry of stars. In order to understand the formation history of our own Galaxy, we need 6 dimensional phase space parameters (3D spatial, 3D velocity) for as many stars as possible, together with abundance determination to chemically tag the stars. Gaia is a European space mission that was launched in December 2013 which aim is to provide superb positional and proper motion data for a billion stars in the Milky Way during its 5 year mission (with a final catalogue scheduled for 2022). Gaia will determine position, parallax and proper motions (5 parameters) for  $10^9$  stars but radial velocities for only the brightest sources ( $10^8$ ,  $V < 17$ ) and abundances for  $V < 12$  mag. Considering the large FoV, light gathering power and potential multiplex spectroscopic capabilities, the TSPM could perform a large spectroscopic survey ( $10^6$  stars) in order to determine radial velocities of  $V > 17$  ( $R \sim 5000$ ) and abundances for  $V > 12$  mag ( $R \sim 20000$ ) Gaia stars, increasing considerably the parameter space statistics of Gaia targets. This complementary spectroscopic survey could provide important information in different science areas of Galactic astronomy, such as galaxy structure, dark matter potential, elemental abundances, star formation history, stellar populations, ages, open clusters, binary stars, star formation rate, and even an impact in areas such as the cosmic distance scale (Cepheids, RR Lyr), or time-domain astrophysics by providing candidates and alerts of transient events, one of the key science drivers for the TSPM.

**Milky Way halo.** The Galactic stellar halo keeps the record of the formation history of the Galaxy at different locations corresponding to different mixing timescales. Stellar streams can be detected as spatial over-densities in the outer halo (beyond 20–30 kpc), while the inner halo (within 10–20 kpc)



is better mixed and additional phase-space measurements as well as chemical abundances (e.g. Gaia) are needed to disentangle the remnants of old accretion events. The Galactic halo is large and diffuse, and therefore a telescope with high light gathering power and wide-field spectroscopic capabilities is necessary to carry out a global characterization of its chemodynamical properties. These observations will help to understand how much of the Milky Way stellar halo was formed in situ and how much was accreted, we could investigate the stellar mass contribution to the Galaxy out to 200 kpc, the clumpiness of the dark matter contribution within 20-50 kpc, and the shape of the Galaxy potential out to 50-100 kpc.

**Milky Way disc.** In addition to the merger history of the Milky Way, one of the main drivers of the evolution of the Galactic discs is the presence of non-axisymmetric perturbations such as bars and spiral arms. There are several questions open regarding the timescale of these features in our Galaxy and other galaxies, about their detailed structure and dynamics and their influence on secular processes such as stellar radial migration. These features, together with other dynamical components of the disc (such as radial and vertical structures) are essential elements for a better understanding of the chemo-dynamical evolution of our Galaxy, and of galaxies in general. Again, the phase space distribution of disc stars and abundance analysis are required to chemo-dynamically tag the stellar disc component of the Galaxy, and a wide-field spectroscopic survey complementary to Gaia would be of paramount importance for this purpose.

#### **4.2.2 Extragalactic Astronomy and Cosmology**

**Stellar astrophysics in the Local Group of galaxies.** The Local Group of galaxies can be used as laboratories to study the influence that metallicity and other environmental factors have over the evolution of stars, principally massive stars. With a FoV of about  $1^\circ$  and with instrumentation like Binospec, TSPM can be used to map the kinematics and metallicity of a complete sample of the massive stars of the associations in nearby galaxies. It will be possible to observe a complete sample of stars with few settings using the multi-slit capacity of the instrument. Even if the resolution of the spectra is relatively low ( $\sim 3000$ ) it will be possible to get the stellar parameters comparing the spectra with a grid of models using intelligent artificial techniques. This information can be used to find the characteristics of the initial mass function (IMF) and details of the evolutionary tracks of massive stars, among other studies. Some of the advantages of studying individual stars in external galaxies are that they have similar extinction and distances, and a span of around a factor of 20 in the metallic content that give us the opportunity to study of the stellar evolution with cosmological characteristics.

**Extragalactic globular clusters.** With moderate-to-high resolution multiplexing spectroscopy of extragalactic globular clusters, integrated light chemical abundances of globular clusters can be measured in nearby galaxies. Metal-poor globular clusters are essentially the only way to study the chemical abundances of stellar halos. With similar data but at lower signal-to-noise, velocity dispersions and thence mass-to-light ratios can be measured of large samples of extragalactic globular



clusters. This is an example of a program that would require a telescope with spectroscopic capabilities over a large FoV.

**Local Group dwarf Spheroidals.** Surveys of the kinematics and chemical abundances of low luminosity dwarf spheroidal satellites address critical questions on the nature of dark matter and the nature of early galaxy formation. For example, whether the recently discovered low luminosity dwarfs are the last remnants of the primordial population that perhaps formed prior to reionization; or whether their detailed chemistry differs from the field halo and the more luminous dwarfs and the reasons of each scenario. Although many new systems are certain to be discovered via NIGs (e.g. Pan-STARRS, LSST), no instrument exists on current telescopes to undertake a major program of spectroscopy on hundreds of stars per galaxy. This could be a niche opportunity for the TSPM considering its large FoV and potential spectroscopic capabilities.

**Low redshift galaxies.** Most of the conclusions drawn so far on the chemical evolution of galaxies are based on integrated spectra of galaxies (e.g. SDSS, 2dF) or based on restricted or inhomogeneous data: galaxies studied with long-slit, MOS or fiber-fed IFUs are restricted by their small field of view or a tiny fraction of the total surface of their targets. Fabry-Pérot or interference filter data usually cover a single line and so they are not able to produce line profiles and obtaining information through a wide spectral range. A telescope with a large FoV and imaging and spectroscopic capabilities is the ideal instrument to study the chemical abundances, kinematics and stellar populations of nearby galaxies with superb detail. Deep, high spectral resolution ( $\sim 10,000$ - $20,000$ ) observations of large samples of nearby galaxies with the TSPM could potentially revolutionize the study of galaxy chemical evolution.

**Groups and clusters of galaxies.** Several observational approaches have been adopted to address the study of galaxies in clusters. The most efficient ones are based on wide field imaging with broad or narrow band filters, allowing to cover fields of the order of  $0.25 \text{ deg}^2$  to  $1 \text{ deg}^2$  in a single exposure, completely covering spatial regions corresponding to the virial radii for nearby ( $z < 0.04$ ) clusters with reasonable observing times. In addition, the large densities of galaxies in the central regions of clusters provide data on large numbers of galaxies and thus the obtained results benefit from statistical significance. Broad band imaging can provide valuable information on galaxy morphologies and on variations of the star formation history (SFH) in timescales of  $\sim 10^9$  yr. Narrow band imaging can provide information on the recent SFR of cluster galaxies (usually through the  $H\alpha$  emission line), information on other emission lines (like  $H\beta$ ) is required to decontaminate for the dust attenuation. The main advantage of the wide field imaging is the complete spatial coverage of the studied regions, not limited to pointed observations of galaxies, which allows the study of serendipitous discoveries of structures of tidal origin or due to the action of the intergalactic medium (IGM) which are thought to be a common feature of clusters of galaxies and that can be used to impose constraints to the models of cluster formation and evolution. A different approach to the study of galaxies in clusters is the spectroscopic observations of selected targets (usually previously imaged). These observations can



be obtained for large FoV in an efficient way using either fiber-fed Integral Field Units (IFU) or multi-object spectroscopy (MOS). Wide-field spectroscopy of nearby galaxies clusters, coupled with the gathering power of a 6.5m telescope such as the TSPM could provide an overall view, including not only the galaxies but also the tidal and other environmentally produced features which are common in these dense environments and that can shed light on the physical processes governing the evolution of cluster galaxies.

**The formation and evolution of galaxies at  $z \sim 1$ .** The local galaxy population ( $z < 0.1$ ) is now well surveyed thanks to pioneering surveys of nearby galaxies (SDSS, 2dF), however redshift removes the effects of projection, reveals the cosmic web, and allows conversion of observed fluxes and sizes to physical rest-frame quantities. Galaxy redshift surveys targeting objects at  $z \sim 1$  (e.g. Keck/DEEP2) remain limited by cosmic variance because of their small survey volumes. Because galaxy properties correlate with large-scale structure, one must map much wider areas of the sky at  $z \sim 1$  and beyond to construct a coherent picture of galaxy evolution, to understand the interplay of star formation, stellar mass build-up, accretion through mergers, feedback from stars and AGN, and the effects of environment over cosmic time. Such efforts demand long integration, wide-field, low-dispersion spectroscopy for hundreds or thousands of targets across  $0.5$  to  $1 \text{ deg}^2$ , a program suitable for the TSPM characteristics, considering its large FoV and potential spectroscopic capabilities.

**The formation and evolution of Seyfert galaxies.** One of the main contributions of an exhaustive analysis of a sample of Seyfert type 1.0, 1.2, 1.5, and 2.0 from the Data Release 7 of the Sloan Digital Sky Survey (SDSS) is that all type of galaxies Seyferts contain an important young star formation in their nucleus. Using new infrared diagnostic diagrams support this analysis. This result requires a deep study of present AGN models considering that the light coming from Seyfert type 1.0 nuclei is dominated by a spatially unresolved component. The detection of recent star formation of all types of Seyfert galaxies constitutes a strong evidence of some kind of connection between Starburst and Seyfert activity, although it is still not clear that necessarily a Starburst is present in all AGN. If such a connection exists, it would bring important implications for the theory of formation of the AGN as well as its role in the formation and evolution of Seyfert galaxies and mainly Unified Model of AGN. To this is necessary obtaining a large spectroscopic sample for thousands of Seyfert galaxies across  $0.03 < z < 0.5$ , a program suitable for the TSPM.

**Studies of black holes.** Studies on elliptical galaxies and spiral bulges have lead to the discovery that most such galaxies contain a super-massive black hole (SMBH). Methods based on photometry and spectroscopy to find the masses of super-massive Black Holes on a sample of galaxies elliptical galaxies and spiral bulges were applied, but the initial results differ in several orders of magnitude between photometry and spectroscopy methods. A telescope with imaging and spectroscopic capabilities is the ideal instrument to study the different photometry and spectroscopy methods and the most important with the same setup. Also analyze the correlations obtained between the SMBH and the physical properties of galaxies in the nearby universe as well as their possible formation and





evolution. The main result will be to obtain one relation to determinate the mass of black hole for any kind of photometry or spectroscopy observation.

**Synergies with wide-field radio surveys.** The next generation radio surveys will be targeting continuum sources over hundreds of square degrees (e.g. LOFAR, APERTIF, SKA) up to  $z \sim 2$  or further. This radio source population will be extremely diverse, biased towards emission line galaxies and radio-quiet AGNs at cosmological distances. Wide-field spectroscopy over 1 degree FoV could obtain redshifts for tens of thousands of emission-line galaxies detected by these next generation radio surveys at  $z < 1.3$  ([OII]) and  $z > 2.3$  (Ly $\alpha$ ). Moreover, radio continuum fluxes obtained by these surveys plus the determination of their redshift by means of optical spectra will provide unbiased star formation rates over a large range of cosmic time. Special programs could obtain deep spectra of a selection of targets in order to obtain metallicities and even stellar velocity dispersions.

**Time-domain astrophysics (TDA).** There are several representative TDA science areas of broad interest in which the TSPM with its large light gathering power and FoV could greatly contribute: variable stars, stellar bursts, evolution of AGN jets, black hole tidal disruption events, etc. These should be found by NGISs by the dozens in the next few years, offering a new window of potential discovers in the variable time-domain astrophysics. TSPM observations could provide crucial spectroscopic confirmation, redshifts, and monitoring of emission-line diagnostics and variability over timescales of weeks to months of these targets.

**Optical search and follow-up of gravitational waves counterparts.** Mergers of compact objects are considered the prime sources of gravitational waves (GW), finding electromagnetic (EM) counterparts of GW sources will be of significant in order to fully understand their nature. Coincident EM-GW signals could potentially be used to build independent cosmological distance ladder, to probe the central engines of supernovae and gamma ray bursts, as well as to study the evolution of massive stars and formation of compact objects such as black-holes (BHs) and neutron stars (NSs), to study galaxy-super massive black hole (SMBH) symbiosis and evolution, and even to measure neutron star equation of state. Many of the mergers giving rise to GW events could be explosive and would drive blast waves, relativistic or nonrelativistic, into the surrounding medium and shine as bright radio transients. The light curve evolution of radio supernovae and afterglows from compact object mergers would look alike. Therefore distinguishing the two classes from each other observationally will be important, which could be done at early time by optical spectroscopy. However, GW events are poorly localized (uncertainties with areas of tents to hundreds of square degrees), with bright but rapidly fading optical afterglows. Telescopes suited to perform extremely wide-field searches of transient events, such as the NGISs, the GROWTH network or the future Zwicky optical transient facility are needed in order to cover the GW error boxes. Nevertheless, these imaging surveys will need telescopes with enough light gathering power and FoV to detect and follow-up GW transient candidates for an adequate time to obtain spectral features and to study the physical properties of the counterparts. The detection of EM (optical) counterparts of GW events would enable extremely



exciting advances in what is already a groundbreaking new field, a niche of opportunity for TSPM considering its collecting area, FoV, pointing overhead time and accuracy, and potential spectroscopic capabilities.

**Magnetic fields in astrophysics:** The study of polarization, which describes the geometry of the electromagnetic waves arriving to the observer from astrophysical phenomena, provides a large amount of information on the nature and particularities of the emitting objects. Among the physical processes of interest directly obtained from polarimetric studies we can cite the magnetic fields. The latter are known to play an important role in a wide range of astrophysical objects. In the case of stars, magnetic activity can be found from the fully convective ones at the bottom of the HR diagram, in solar type stars, or hot stars with a spectral type A and B locate in the upper part of the HR diagram. On the other hand, linear polarization studies can help investigate astrophysical phenomena such as AGNs, shocks, jets, synchrotron emission, morphology and binarity in various objects (blazars, binary stars, protoplanetary discs, etc). Although considerable progresses have been made in the development of theoretical models, data analysis techniques and magneto-hydrodynamical codes; more accurate and more numerous observational data are still missing. Detecting and measuring magnetic fields is a difficult task considering the challenging detection thresholds that hampers their accurate study. The possibility of exploring weak magnetic field regimes using high resolution spectropolarimetry in a large light gathering telescope would be a huge breakthrough, as it would open a new door for the community involved in the TSPM (and particularly the Mexican one). Totally unexplored groups of objects would now be accessible.

#### 4.2.3 Summary of science requirements

The table below summarizes the relation between the science examples given in the previous section and the main properties that the telescope and potential instrumentation must have (at the different operational periods) in order to comply with the scientific requirements. Note that many of the science programs listed in the second stage of operation could be developed if spectroscopic and/or polarimetric instruments become available during Day-One stage operations. Indeed, many other science areas could be proposed as the project evolves, especially with the expected involvement of the astronomical community from UA and SAO.

#### Day-One operation period (f/5 Cassegrain):

| Science Programs | Telescope properties                 |
|------------------|--------------------------------------|
| Protostars       | • Wide-field (0.5 - 1 deg) coverage. |



**TSPM Science Document**

Code: SCI/TSPM-PDR/001  
 Issue: 1.B  
 Date: 20/10/2017  
 Page: 16 of 86

|   |  |
|---|--|
| NEOS and minor bodies of the Solar system<br>Properties of open stellar clusters<br>Milky Way halo<br>Groups and clusters of galaxies<br>Magnetic fields in evolved intermediate mass stars | <ul style="list-style-type: none"> <li>• Optical and near IR imaging.</li> <li>• Broad wavelength coverage.</li> <li>• Wide-field broad-band and narrow-band imaging.</li> <li>• High light gathering power.</li> <li>• Superb observing conditions of SPM.</li> </ul> |
|---|--|

**Second stage operation period:**

(Nasmyth + folded-Cass focal stations + spectroscopic + polarimetry + multiplexing)

| <b>Science Programs</b>   | <b>Telescope properties</b>   |
|---|---|
| Stellar astrophysics in the Local Group<br>Protostars<br>Nebulae around evolved stars<br>NEOS and minor bodies of the Solar system<br>Structure of Galactic HII regions<br>Circumstellar discs and planet formation<br>Properties of open stellar clusters<br>Synergies with GAIA<br>Milky Way halo<br>Milky Way disc<br>Extragalactic globular clusters<br>Local Group dwarf Spheroidals<br>Low redshift galaxies<br>Groups and clusters of galaxies<br>(continues...) | <ul style="list-style-type: none"> <li>• Wide-field (0.5 - 1 deg) coverage.</li> <li>• Optical and near IR imaging.</li> <li>• Wide-field broad-band and narrow-band imaging.</li> <li>• Wide-field optical and near IR spectroscopy.</li> <li>• Multiplexing spectroscopic capabilities.</li> </ul> (continues...) |
| The formation and evolution of galaxies at $z \sim 1$<br>The formation and evolution of Seyfert galaxies<br>Studies of black holes<br>Synergies with wide-field radio surveys<br>Time-domain astrophysics<br>Optical search and follow-up of gravitational waves counterparts<br>Magnetic fields in evolved intermediate mass stars<br>Spectropolarimetry of AGN  | <ul style="list-style-type: none"> <li>• 6.5m class telescope light gathering power.</li> <li>• Fast pointing and accuracy.</li> <li>• Superb observing conditions of SPM.</li> </ul>   |

*Table 1: Relation between the proposed science programs and TSPM properties.*





## TSPM Science Document

Code: SCI/TSPM-PDR/001  
Issue: 1.B  
Date: 20/10/2017  
Page: 17 of 86

The top-level science requirements for the telescope that emerges from the above table are:

1. The TSPM should achieve an image quality equal to the best conditions of the site. SPM at 2800m elevation, is regarded as one of the best astronomical sites in the world with over 60% of nights being photometric and 80% spectroscopic, 0.5 arcsec median seeing (10th-percentile @ 500 nm), and 2 mm typical level of water vapor. The TSPM optics and instrumentation should be designed to exploit the excellent observing conditions of SPM.
2. The TSPM will belong to a joint international facility serving a large community of users, although it will be initially commissioned with a small number of capabilities, in a f/5 Cassegrain configuration, provisions for future upgrades or modifications should be taken.
3. The science programs will be carried out with the TSPM and their auxiliary instruments working as a system. The instruments and telescope together determine the ultimate scientific capabilities of the TSPM.
4. For full realization of its scientific potential, the TSPM must provide a broad wavelength coverage and high throughput from ultraviolet wavelengths longer than 0.35  $\mu\text{m}$  through the visible and infrared bands to at least 2.5  $\mu\text{m}$ .
5. The TSPM must provide a Day-One imaging mode offering at least 0.5 degree diameter field of view in the Cassegrain focal station.
6. The TSPM must provide a Day-One spectroscopic mode offering a 1 degree diameter field of view in the Cassegrain focal station.
7. The TSPM instrumentation during its first stage of operation and thereafter, should consider optical and near infrared broad-band and narrow-band imaging capabilities.
8. The TSPM instrumentation during its second stage of operation and thereafter, should consider wide-field multiplexing spectroscopy over a 1 degree diameter field of view.
9. The TSPM must provide accessible focal stations at which the instruments can be located. They must provide adequate space and weight carrying capacity for mounting the instruments as well as necessary data links, power, and cryogenics.
10. The TSPM should be designed so that upgrades and new instrumentation can be accommodated in the future; in particular, the following future capabilities shall be taken into account: TSPM shall permit upgrades to provide Nasmyth and Folded Cassegrain focal stations that are compatible with those presently at Magellan and MMT, namely f/5 Nasmyth and Gregorian f/11 configurations, each with an additional secondary and tertiary mirrors,



**TSPM Science Document**

Code: SCI/TSPM-PDR/001  
Issue: 1.B  
Date: 20/10/2017  
Page: 18 of 86

mechanical de-rotator, guide sensor and WFS similar to the existing sensors in the Day-One f/5 Cassegrain corrector.

11. The TSPM design shall permit an upgrade to an optical configuration making use of Nasmyth ports that allows a spectroscopic mode offering at least a 1 degree diameter field of view.
12. The TSPM design shall permit an upgrade to an optical configuration making use of Folded Cassegrain ports that allows a spectroscopic mode offering at least a 0.5 degree diameter field of view.
13. To achieve maximum scientific productivity for TDA and changing sky conditions, the TSPM design for the future Nasmyth and Folded Cassegrain ports should permit a rapid change between mounted instruments. This capability could lower operational costs through a reduced demand for installing and removing instruments.
14. Future upgrades of the TSPM in its optical configurations and instrumentation should consider instrumental versatility in order to be competitive in the field of time-domain astrophysics (TDA).
15. The TSPM shall provide a high stability focal station in the telescope pier for instruments requiring high thermal stability and constant gravity orientation.
16. None scientific requirement has been identified for use of the prime focus.

The TSPM High Level Requirements, Optical Configurations and System Specification are in full compliance with the top level science requirements described above, namely:

| <b>Req ID</b> | <b>TSPM HIGH LEVEL REQUIREMENTS</b>   |
|---------------|---|
| <b>3</b>      | <b>GENERAL REQUIREMENTS</b>   |
| <b>3.1</b>    | <b>Project Development</b>  |
| 3.1.1         | The TSPM shall be suitable for general science projects; in the understanding that the TSPM should have comparable flexibility to facilities such as MMT, Magellan, Keck, Gemini, VLT, and GTC, and not be a single-purpose facility such as LSST, Pan STARRS, and VISTA [RQ/TSPM/001]. |
| <b>3.2</b>    | <b>Wavelength range, image quality and background</b>   |
| 3.2.1         | TSPM shall be optimized from the near ultraviolet to the near infrared (0.35 -2.5 $\mu\text{m}$ ).  |



**TSPM Science Document**

Code: SCI/TSPM-PDR/001  
 Issue: 1.B  
 Date: 20/10/2017  
 Page: 19 of 86

|            |  |
|------------|--|
| 3.2.2      | The effective thermal emissivity of the telescope at the Cassegrain focus shall be less than 10% of that from a blackbody at the ambient temperature and should be less than 7%.   |
| <b>3.3</b> | <b>Plate scale and focal stations</b>  |
| 3.3.1      | TSPM shall start operations with an f/5 secondary and a wide-field corrector at a Cassegrain station   |
| 3.3.2      | TSPM shall use the existing secondary and wide-field corrector now in operation at Magellan  |
| 3.3.4      | TSPM shall permit upgrades to provide at least two Nasmyth focal stations compatible the f/5 Nasmyth and Gregorian f/11 configurations described at the corresponding optical design requirements documents [...].   |
| 3.3.5      | TSPM shall permit upgrades to provide at least four folded Cassegrain focal stations compatible the f/5 Nasmyth and Gregorian f/11 configurations described at the corresponding optical design requirements documents [...].  |
| <b>3.4</b> | <b>Science instruments</b>   |
| 3.4.1      | The TSPM f/5 Cassegrain station shall permit the use of at least the following science instruments presently in use at or under construction for the f/5 Cassegrain stations of MMT and Magellan: MEGACAM, MMIRS, BINOSPEC, SWIRC and MAESTRO.   |
| 3.4.2      | TSPM shall be commissioned and initially operate with the following f/5 Cassegrain instruments: MEGACAM and MMIRS.   |
| 3.4.3      | After initial operations with the existing f/5 Cassegrain instruments, TSPM should not preclude future dedicated or long-term projects, other specialized or general instrumentation, or other observing modes such as classical, queued, remote or robotic modes.   |
| 3.4.4      | TSPM shall not exclude future instruments that maintain it at the frontier of competitive astronomical research.   |
| 3.4.5      | TSPM shall not exclude the future development of the capacity to use multiple Nasmyth and Folded-Cassegrain stations in one night [...].   |
|            | <b>TSPM OPTICAL CONFIGURATIONS</b>   |
| <b>3</b>   | <b>TSPM F/5 CASSEGRAIN CONFIGURATION</b>   |
|            | In its initial (base) configuration, TSPM is to: 1) Use an existing 6.5 meters honeycomb primary mirror (M1) cast by the UA Mirror Lab and polished to the same prescription and specifications as the primaries of the MMT and the Magellan telescopes. 2) Adopt the existing F/5 secondary from the Magellan telescope, together with its wide-field corrector |



**TSPM Science Document**

Code: SCI/TSPM-PDR/001  
Issue: 1.B  
Date: 20/10/2017  
Page: 20 of 86

|            |   |
|------------|---|
|            | (WFC) [...]. Therefore, the optical design of the f/5 Cassegrain configuration is already fixed [...].  |
| <b>3.3</b> | <b>Wide Field Corrector</b>   |
|            | TSPM will adopt either the existing WFC at MMT or at Magellan [...]. The f/5 corrector has two configurations: (1) the spectroscopic mode offers a telocentric 1° diameter field of view with a curved focal surface, (2) the imaging mode offers a flat 0.5° diameter field of view [...]. |

*Table 2: TSPM High Level Requirements, Optics Configuration and System Specifications that are in compliance with the TSPM science requirements.*



## **5. PROPOSED SCIENCE CASES FOR A JOINT TSPM/MMT OBSERVATORY**

This section contains specific science cases considered as October 2017 for the TSPM/MMT joint facilities, persuasively made in individual proposals prepared by astronomers of the Mexican community. They span a very wide range of interests, from stellar and Galactic studies to cosmology, using techniques from single object spectroscopy to deep optical and near-infrared surveys. To realize all of these science cases will require a greater diversity of instrumentation, other than the one that will be available at Day-One at the TSPM or shortly thereafter, but that could capitalized the instrumentation available at MMT. The goal of jointly operating the TSPM and MMT is a quick path toward making the required instrumentation available and to use efficiently the advantages and capabilities of each site.

### **5.1 Galactic and stellar astronomy**

#### **5.1.1 Chromospheric activity and age of solar analogs in open clusters**

Open clusters represent a most valuable laboratory for understanding the physics of stars. Having a common origin, member stars are usually considered coeval and initially chemically homogeneous. The age of the cluster can be therefore easily and quite precisely obtained (once the chemical abundances are known) by isochrone fitting. On the contrary, age determination methods for field stars are usually affected by larger uncertainties (see, for instance, the excellent review on this topic by Soderblom 2010). For this reason, stars in clusters are excellent targets to calibrate the connection between age and age-dependent stellar properties, correlations that can be eventually applied to field stars. In this context, Hectochelle, with its multi-object capability coupled to the large collecting area of a 6.5 m telescope, represents a ideal instrument for the study of the resolved stellar population of Galactic stellar clusters: it will efficiently gather high-quality spectra of fainter stars in the CMD diagrams of more distant objects (the lower-resolution Binospec spectrograph can be also useful for fainter and younger clusters, where the Ca HK lines presumably are more intense). As we shall see below, observations of main sequence (MS) stars will be feasible on systems up to several kiloparsecs.

Of particular interest is the study of solar analogs. In fact, the discovery of hundreds of extrasolar planets in the recent years has renewed the interest of the astrophysical community on solar-like stars, which for a long time were not considered attractive astronomical targets. In the last decade, however, there has been a flourishing of studies, which also revealed some important relations between the presence of a planetary system and the properties of the host stars. One of the most relevant has been the work of Valenti & Fischer (2005), who found that extrasolar giant planets are more likely to form around metal-rich stars ( $[Fe/H]>0$ ). More recently, Israelian et al. (2009) have found a negative correlation between the stellar lithium abundance and the existence of a planetary system, a correlation that is still under a vivid discussion. A detailed characterization of MS stars (atmospheric



parameters and age) is therefore fundamental in the understanding of planet formation and evolutionary status of the circumstellar disks of material that originate them.

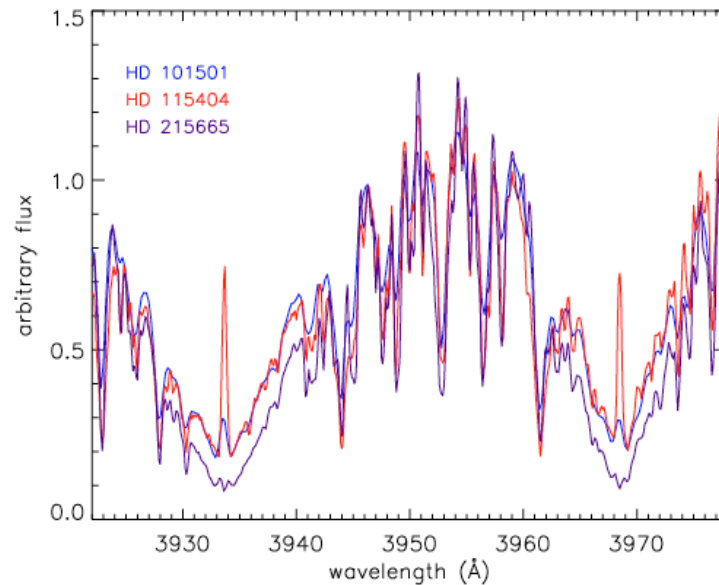


**Figure 1:** The Ca H and K lines for three stars presenting different level of chromospheric activity. Spectral resolution is  $R = 20,000$ . [data from Montes et al. 1997].

In the case of intermediate- and late-type MS stars, chromospheric activity has been widely used as a clock (other methods include nucleocosmochronometry, asteroseismology, kinematic analysis, lithium depletion, etc.), since the magnetic activity in the upper atmospheric layers is correlated with rotational period. Rotational periods are expected to decay as an effect of mass loss during the stellar lifetime. One of the most used indicators of chromospheric activity is the emission of the Ca H and K lines at 3969 and 3933 Å which is usually expressed as  $R_{\text{HK}} = L_{\text{HK}}/L_{\text{bol}}$ , where  $L_{\text{HK}}$  is the luminosity within the emission lines and  $L_{\text{bol}}$  is the bolometric luminosity of the star. These transitions produce a strong photospheric absorption in solar-like stars but in an optically thin chromosphere, due to the temperature inversion, they generate emission lines (see Figure 1). The strength of this (sometimes very tiny) emission at the very center of a strong absorption feature has been correlated with age, by means of observations of stars in clusters of known age.

The recent  $R_{\text{HK}}$ –age calibration of Mamajek & Hillenbrand (2008), which is shown in Figure 2, has been obtained from a collection of literature data for just about 200 stars of 13 open clusters (plus a small number of field stars of Valenti & Fischer (2005), whose age has been obtained by isochrone placement). They claim to have reached a relative precision of 60% for the age of solar analogs (in the age interval 0.6–4.5 Gyr).

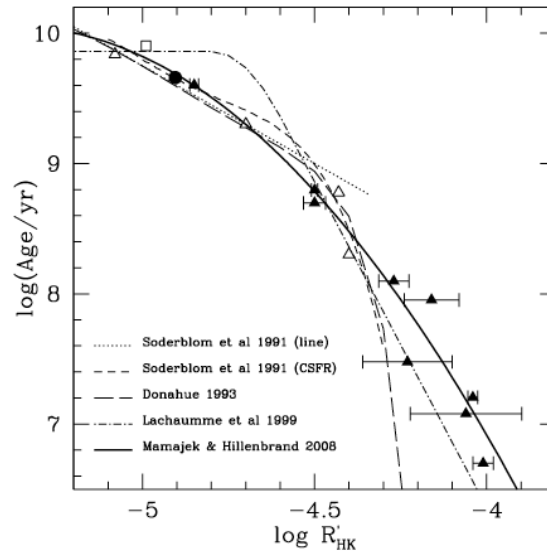


**Figure 2:** The chromospheric activity–age calibration from Mamajek & Hillenbrand (2008), compared with previous calibration from different authors. The triangles show the mean  $\log R'_{HK}$  values of star in cluster vs. cluster age; the square indicates the mean value for the sample of solar-type dwarfs from Valenti & Fischer (2005); the circle is the Sun.

We propose to observe the Ca HK spectra of solar-type stars in a selected sample of 22 open clusters. These observations will considerably increase the number of cluster stars with a well measured  $R_{HK}$ . This would allow to significantly decreasing the uncertainty of the activity–age calibration, that we can be applied to field stars. The sample of open clusters has been extracted from the WEBDA catalog (Mermilliod J.-C. 2005), applying the following criteria:

- $B \leq 18.5$  for a G2V type star;
- a total number of stars with  $B - V$  color typical of solar analogs (G0–G3 types) greater than 200;
- a declination  $\text{dec} \geq -20$  deg.

The sample of the target open clusters is described in Table 1, where we report the name of the cluster along with the coordinates, the density of solar analogs, the diameter, the age, and the distance. It is worth noticing that our sample includes 6 clusters with age  $> 1$  Gyr. This age interval is critical, since the Mamajek & Hillenbrand (2008) calibration is based only on one bona-fide cluster in this range, since these objects are usually located at large distances from the Sun. The observations of a large number of stars in these evolved systems will greatly increase the precision of age determination for older stars.



As a first step, we plan to homogeneously derive the age of the clusters by using the latest Padova stellar tracks (Bressan et al., in preparation) to perform the isochrone fitting of the clusters' CMDs. The Padova group has recently revised their stellar evolution code, by including up-to-date physical ingredients (e.g., opacities, equation of state, nuclear reaction rates, chemistry, microscopic and turbulent diffusion, neutrino energy loss), and they have computed a new library of evolutionary tracks in a large range of age and metallicity ( $0.15M_{\text{sun}} < M < 120M_{\text{sun}}$  y  $0.0001 < Z < 0.05$ ). An extremely important property of these tracks is that they adopted the solar abundances from Ludwig et al. (2010), which has been obtained from 3D modeling of solar atmosphere and result in a total metallicity of  $Z_{\text{sun}} = 0.01533^*$ . Since for MS stars is the chemical composition (and not age) that defines their location on the CMD, the use of a new set of isochrones, based on different reference solar abundances, will give rise to a modified chronology, which will affect the stellar activity vs. age calibration.

| Cluster name   | RA       | Dec       | targets<br>(#/arcmin <sup>2</sup> ) | diam. (arcmin) | log Age | d<br>(pc) |
|----------------|----------|-----------|-------------------------------------|----------------|---------|-----------|
| 1 Stock 24     | 00 39 42 | +61 57 00 | 108.5                               | 5              | 8.08    | 2818      |
| 2 Berkeley 62  | 01 01 00 | +63 57 00 | 80.2                                | 5              | 7.18    | 1837      |
| 3 NGC 381      | 01 08 19 | +61 35 00 | 102.5                               | 6              | 8.51    | 1148      |
| 4 NGC 581      | 01 33 23 | +60 39 00 | 295.3                               | 5              | 7.34    | 2194      |
| 5 NGC 654      | 01 44 00 | +61 53 06 | 86.5                                | 5              | 7.15    | 2041      |
| 6 Berkeley 7   | 01 54 12 | +62 22 00 | 57.5                                | 4              | 6.60    | 2570      |
| 7 King 5       | 03 14 36 | +52 43 00 | 68.7                                | 5              | 9.00    | 1900      |
| 8 Berkeley 17  | 05 20 36 | +30 36 00 | 115.4                               | 7              | 10.08   | 2700      |
| 9 IC 2157      | 06 05 00 | +24 00 00 | 103.9                               | 5              | 7.80    | 2040      |
| 10 Saurer 1    | 07 18 18 | +01 53 12 | 116.2                               | 4              | 9.85    | 1970      |
| 11 Trumpler 32 | 18 17 30 | -13 21 00 | 91.0                                | 5              | 8.48    | 1720      |
| 12 NGC 6611    | 18 18 48 | -13 48 24 | 75.9                                | 6              | 6.88    | 1749      |
| 13 NGC 6631    | 18 27 11 | -12 01 48 | 195.7                               | 6              | 8.60    | 2600      |
| 14 Basel 1     | 18 48 12 | -05 51 00 | 66.1                                | 5              | 7.89    | 2178      |
| 15 NGC 6705    | 18 51 05 | -06 16 12 | 63.7                                | 13             | 8.30    | 1877      |
| 16 NGC 6819    | 19 41 18 | +40 11 12 | 123.5                               | 5              | 9.17    | 2360      |
| 17 NGC 6834    | 19 52 12 | +29 24 30 | 72.2                                | 5              | 7.88    | 2067      |
| 18 NGC 6996    | 20 56 30 | +45 38 24 | 54.9                                | 8              | 8.54    | 760       |
| 19 Berkeley 54 | 21 03 12 | +40 28 00 | 198.5                               | 4              | 9.60    | 2300      |
| 20 NGC 7235    | 22 12 25 | +57 16 12 | 50.8                                | 5              | 7.07    | 2823      |
| 21 King 11     | 23 47 48 | +68 38 00 | 59.3                                | 5              | 9.05    | 2892      |
| 22 NGC 7790    | 23 58 24 | +61 12 30 | 133.3                               | 5              | 7.75    | 2944      |

*Table 3: Properties of the target open clusters.*

**Observations.** Hectochelle will be used with the Ca41 filter, at a spectral resolution  $R \leftarrow 32000$ , which is very suitable for detailed observations of emission at the core of the Ca HK lines (Fig. 1). With four hour exposure time observations, we should reach a  $\text{SNR} > 10$  for the Ca HK emission line





even for the faintest stars of our sample and weak chromospheric activity. The observation of the full sample of 22 clusters should use therefore about 100 hours (plus overheads) of telescope time.

**Stellar atmospheric parameters.** The spectra collected by the Hectochelle, in addition to the Ca HK chromospheric emission, will contain a wealth of information that can be exploited for determining the atmospheric parameters of all the observed stellar targets. The density of absorption lines in late-type stars is maximum in the blue interval and the  $R \sim 32,000$  spectral resolving power, even if it is not enough to perfectly separate all individual lines, will certainly allow to define a set of line indices, that measure both the equivalent widths (or suitable Lick-like indices) and line flux ratios (e.g., Rose 1994; Liu et al. 2008), which have proved to be very sensitive to the main atmospheric parameters: effective temperature, surface gravity, and overall metallicity. The observed indices will be matched with those computed from a new library of suitable theoretical stellar spectra (Bertone et al., in preparation), which are being computed using the same solar partition of Ludwig et al. (2010) used to compute the new Padova evolutionary tracks. Before this comparison, however, the theoretical indices will be calibrated against the observations, using a suitable sample of well known reference stars.

\*The Ludwig et al. values  $Z_{\text{sun}} = 0.0153$  is intermediate between the one proposed by Grevesse & Sauval (1998) ( $Z = 0.0171$ ) and the one obtained by Asplund et al. (2005) ( $Z = 0.0122$ ). However, the value of  $Z = 0.0171$  is not compatible with the most recent observations, while the Asplund solar metallicity is in conflict with helioseismological results

Asplund, M., Grevesse, N., & Sauval, A. J. 2005, *Cosmic Abundances as Records of Stellar Evolution and Nucleosynthesis*, 336, 25

Grevesse, N., & Sauval, A. J. 1998, *Space Sci. Rev.*, 85, 161

Liu, G. Q., Deng, L., Chávez, M., et al. 2008, *MNRAS*, 390, 665

Ludwig, H.-G., Caffau, E., Steffen, M., et al. 2010, *IAU Symposium*, 265, 201

Mamajek, E. E., & Hillenbrand, L. A. 2008, *ApJ*, 687, 1264

Mermilliod, J.-C. 1995, *Information and On-Line Data in Astronomy*, 203, 127

Montes, D., Martin, E. L., Fernandez-Figueroa, M. J., Cornide, M., & de Castro, E. 1997, *A&AS*, 123, 473

Rose, J. A. 1994, *AJ*, 107, 206

Soderblom, D. R. 2010, *ARA&A*, 48, 581

Valenti, J. A., & Fischer, D. A. 2005, *ApJS*, 159, 141

### 5.1.2 Massive stars in nearby galaxies

Massive stars are the origin of several highly energetic phenomena. Born with masses exceeding eight times the solar mass, they are one of the main sources of the chemical and dynamic evolution of galaxies. Its evolution is very fast, and during their life time releases large amounts of nuclear-



processed material through fast and dense stellar winds. As a very powerful source of high-energy photons, they are responsible of the heating and ionization of interstellar material. They will die as supernovae at the end of his life, injecting more chemical enriched material and turbulent energy to the interstellar medium. The remnants are neutron stars or black holes and some of them can produce Gamma Ray Bursts.

Massive stars are also very luminous and can be studied individually on nearby galaxies, they can use as standard candles to find their distance. The evolutionary process varies with the physical properties of the stars, like the initial mass, metallicity and rotation velocity. Metallicity depends on the galaxy that hosts the stars and in some of the nearby galaxies the properties that we found are close to those in the early Universe. This give the chance to understand the process that took place when the universe was young and the first stars was formed. When we observe distant galaxies we have the contributions of many type of stars integrated in the radiation, therefore is necessary to study massive stars with different evolutionary stages in several nearby galaxies that cover a variety of these parameters.

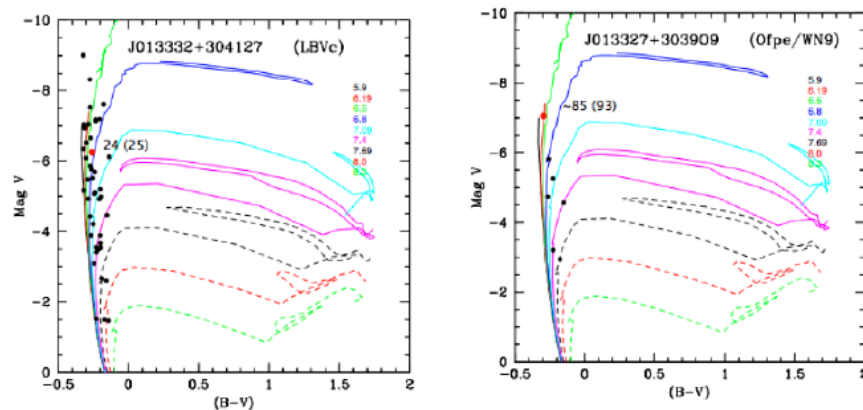


**Figure 3:** HR diagrams of two clusters with a LBVc member (in red) of M 33. The tracks are isochrones calculated by Lejeune & Schaerer (2001) and the masses are the initial mass of the objects.

One of the stages of the evolution of massive stars is known as Luminous Blue Variables (LBV). These are a group of irregular variables characterized by their intrinsic high luminosities, blue colors, their photometric behavior and their related spectroscopic changes. Members of this group have been identified not only in the Milky Way, but also in nearby galaxies as well. LBV is a term coined by Conti (1984) that covers member of the S Dor variable, the Hubble-Sandage variable and the P Cygni variable classes. Reviews of LBV can be found in Humphreys & Davidson (1994), and in Bohannon (1997). In M 33 there are at least 6 known LBV. Four of them were identified first by their variability: Var B, Var C, Var 2 ( Hubble & Sandage 1953 ) and Var 83 ( van den Bergh et al. 1975). Recently



three more LBV have been identified in M33: B 324, UIT 003 and B 416. (Monteverde et al. 1996, Massey et al. 1996 and Shemmer et al. 2000).

Some stars with the same, or at least related, spectroscopic characteristics of LBV, but without any reported variation in historical times, are known as LBV-candidates (LBVc). There are at least 15 stars classified as such in the literature that belong to M33 (see Massey et al. 1996 and Corral 1996). The importance of the number of LBV in a particular galaxy, is that this number is directly related with the lifetime of this evolutionary stage. Is during this phase that the strongest mass loss rates are found in the evolutionary track of massive stars (Humphreys & Davidson 1994), and is believed that the LBV phase is previous to the WR phase in some of the most massive stars. The masses of WR found in binaries are in the order of 5 to 10 Msun, but objects in the previous phases are in the order of 20 Msun or more. Is expected that during the LBV phase at least 5 (or even 10) Msun are lost, making a great contribution to the input of momentum and chemical enrichment to the interstellar medium. We want to determine the mass and age of these objects learn if all the massive stars go through this stage or only the most massive ones.

A well known method of understanding the nature of evolved stars is to determine the turn-off luminosities on the HR diagrams of clusters containing such objects (Johnson & Sandage 1955; Schwarzschild 1958) and with evolutionary theory results determining the age of the cluster. This was first applied by Sandage (1953) to get the masses of RR Lyrae stars in the globular clusters M3 and M92 (Sandage 1956). In a previous work (Corral et al. in preparation) we found the HR diagrams of massive star clusters and associations with an LBV or LBVc members. Using evolutionary tracks calculated by Lejeune & Schaerer (2001) we found that photometrically they show a variety of masses (from 25 to > 100 Msun). We need to study the members of the cluster spectroscopically to better determine their parameters (mass, log g, metallicity, mass loss rate and rotational velocity) and discard those objects that are binaries (or multiples) in order to get a better understanding of the evolution. These studies can be done with BINOSPEC. Their multi object spectroscopic capability, the wide field of view (16 x 15 arcmin) and high throughput ( 30% @ 5000 Å) make it a very useful instrument to this kind of studies. We propose to observe a good sample of the member of the cluster and found their parameters comparing the spectrum with models calculated with the code CMFGEN.

Bohannon, B., in *Luminous Blue Variables: Massive Stars in Transition*, 1997, ASP Conf. Series, 120, Nota, A., Lamers, H.J.G.L.M. eds.

Conti, P.S., in *Observational tests of the stellar evolution theory*, 1984, IAU symp. 105, ed. Maeder & Renzini (Kluwer, Dordrecht), p. 233

Corral, L.J., 1996, *AJ*, 112, 1450

Herrero, A., et al., 1994, *A&A*, 287, 885

Hubble, E. & Sandage, A., 1953, *ApJ*, 118, 353

Humphreys, R. & Davidson. K., *PASP*, 1994, 106, 1025

Johnson, H. L., & Sandage, A. R. 1955, *ApJ*, 121, 616



Lejeune J. & Schaerer D. 2001, A&A, 366, 538  
Massey, P., Bianchi, L., Hutchings, J.B., Stecher, T.P., 1996, ApJ, 469, 629  
Monteverde, M., Herrero, A., Lennon, D., Kudricki, R., 1996, A&A, 312, 24  
Sandage, A. 1953, Mem. Soc. Roy. Sci. Liege, 14, Ser. 4, 254  
Shemmer, O, Leibowitz, E. M., Szkody, P., 2000, MNRAS, 311, 698  
van den Bergh, S., Herbst, E., Kowal, Ch., 1975, ApJS, 29, 303

### **5.1.3 The impact of massive outflows in Galactic Star Formation**

Understanding the formation of High-Mass stars is one of the main problems of the modern astrophysics. In recent years, unbiased surveys in the Mid-IR and Sub-mm have given us new samples of candidates of High-Mass Protostars in the earliest phase of formation. Systematic studies trying to characterize such objects are underway. An example of these is the GLIMPSE (Galactic Legacy Infrared Mid-Plane Survey Extraordinaire) survey in the Mid-Infrared (Mid-IR), from which different star-formation phenomena have been revealed, from Ultra Compact HII regions to bipolar outflows.

A new catalog of massive outflows has been published by Cyganowski et al. (2008), based on the GLIMPSE survey with the IRAC camera. The finding method consisted in displaying three color images (3.6, 4.5 and 8.0  $\mu\text{m}$ ) of the GLIMPSE survey area and look for Green Extended Objects (EGOs, with the 4.5  $\mu\text{m}$  band coded as green). Observationally, the excess in the 4.5  $\mu\text{m}$  band is interpreted as a shock tracer based on comparisons with Near-IR H<sub>2</sub> narrow-band images and the presence of the H<sub>2</sub> lines and CO band heads in this band (Davis et al. 2007). The gas temperatures implicated are  $> 1000$  K, and therefore tracing very energetic outflows (Ybarra & Landa, 2009). This extended emission is interesting as a new diagnostic for Massive Protostars, in particular the outflows related with them. This catalog compile around 300 extended 4.5  $\mu\text{m}$  sources, most of them new massive outflow candidates, not studied before in any other outflow tracer. Recently, Chen et al. (2013) added about one hundred more newly identified EGOs from the GLIMPSE II survey.

**Near- and mid-IR observations of massive outflows with SPMT.** The relevance of such EGOs is that those sources with an excess in the 4.5 micron band could be related with the earliest phases of massive star formation, as well as revealing very energetic outflows which could have a very important impact in the ISM as a whole: shock-induced chemistry and shocks as a feedback process. Follow up observations have started trying to characterize EGOs by using several star formation tracers. In particular, Cyganowski et al. (2009, 2011a,b) have presented interferometric observations of centimeter continuum emission, CH<sub>3</sub>OH masers, CO, SiO, and HCO<sup>+</sup> transitions in a sub-sample of about 20 EGOs, tracing ionized regions and molecular outflows, suggesting that EGOs are related with massive outflows (see Fig. 3). In the infrared, the most complete study comes from Lee et al. (2013), whose narrow band H<sub>2</sub> and continuum near-infrared observations in about 90 EGOs showed that only half of them were related with H<sub>2</sub> outflows (considering the H<sub>2</sub> outflows incompleteness),



while the rest comes from scattered continuum from the embedded young stellar object. The discrepancy between the radio/mm and NIR observations may come from the different optical depths each tracer is sensitive to and/or the low statistics in the radio/mm data. These results therefore call for further investigations in the radio/mm, NIR, and Mid-IR wavelengths, in the latter case with direct spectroscopy of the  $4.5\mu\text{m}$  band.

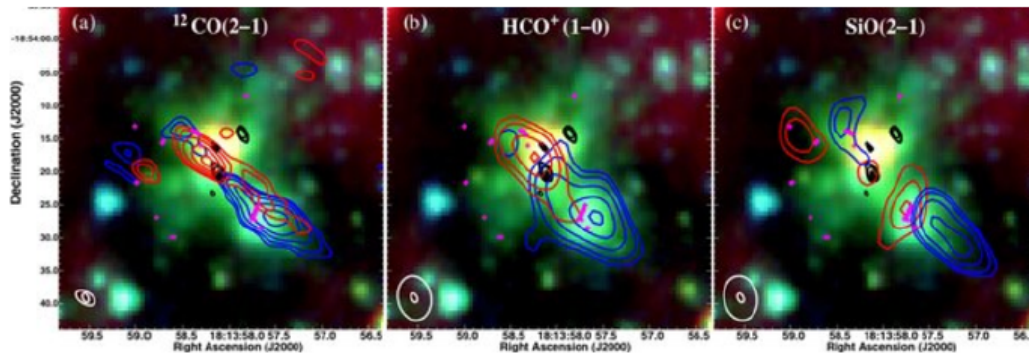


**Figure 4:** The three color image from the GLIMPSE/IRAC survey showing an Extended Green Object, while the contours show molecular line observations demonstrating that EGOs are tracing molecular outflows (from Cyganowski et al 2011a). An image similar to these could be provided by data from the SPMT and the LMT (at infrared and millimeter wavelengths, respectively).

NIR observations with a 6-m class telescope will be key to complete the  $\text{H}_2$  survey towards this sample of massive outflows candidates, for example with an instrument like the MMIRS. With its sensitivity and angular resolution, detailed analysis of the emission structures can be made, and faster than with previous observations. These observations will complement an observing campaign our group at INAOE will undertake with the Large Millimeter Telescope in molecular lines. The synergy between these two facilities will provide an advantage in the data analysis. However, what would be really new is to enable the 6-m SPMT with mid-IR spectrographs, in order to provide direct spectroscopy in the  $4.5\mu\text{m}$  band, which has been barely tried until now, at least in these objects.

In general, the 6-m SPMT will be a very important facility which can work very well in synergy with the LMT, since in the particular case of outflows studies infrared data is key for the development of the next generation models that try to explain the mechanisms behind the outflow phenomenon in star formation. Therefore, the SPMT together with the LMT will provide an important advantage to Mexican community working in this field.

Chen et al. 2008, MNRAS, 396, 1603

Chen et al. 2013, ApJS, 206, 9

Cyganowski et al. 2011a, ApJ, 729, 124



Cyganowski et al. 2011b, ApJ, 743, 56  
Cyganowski et al. 2008, ApJ, 136, 2391  
Cyganowski et al. 2009, ApJ, 702, 1615  
Davis et al. 2007, MNRAS, 374, 29  
Ybarra & Lada, 2009, ApJ, 695, L120

#### **5.1.4 Symbiotic systems and planetary nebulae: determination of physical parameters**

Symbiotic systems are binary systems that undergo mass transfer episodes in their evolution history, producing in some cases accretion disks, and in many of these objects are observed collimated mass ejection. Planetary nebulae are the result of the evolution of low and medium mass stars, when the evolved star are part of a binary system, it could transfer mass to the companion when it transform into an AGB or Mira variable. The physical process in both type of objects are very similar and many authors coincide in the probable evolutionary relation between them. The binary periods determined for some of these objects are very different: from few months or years for PNe to more than ten years for SS.

In the other hand, many PNe shows multiple rings and structures that may be the result of multiple mass loss episodes and, in many cases the interaction between material from them produce shocks. The analysis of the emission lines observed in these objects:  $\lambda\lambda$  4363 and 5007, from [OIII], H $\beta$ , H $\alpha$  and  $\lambda\lambda$  6548 and 6583 from [NII] and their quotients may give us an idea of the process producing these lines (photoionization or shocks) throughout the construction of diagnostic diagrams. The weak emission from the rings and halos in PNe demand the use of a large telescope (in the range of 6 to 10 m) with image and spectral capabilities, for this reason BINOSPEC will be the ideal instrument.

The recent results of the IPHAS project (Viironen et al. 2009, Sabin et al., 2014. ) produce a good number of candidates to PNe many of them with weak emission lines. The possibility to use a 6.5m telescope let us to obtained reliable spectroscopy that could confirm such classification and permit us to obtain the physical parameters of each nebula.



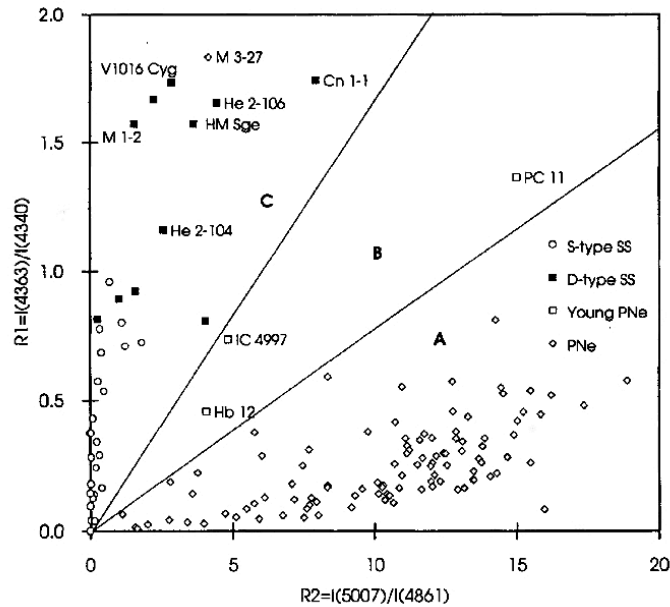


*Figure 5: The Diagram from Gutierrez-Moreno et al. (1995) where the clear separation of PNe and symbiotic is shown*

The analysis of the emission lines observed in these type of objects, and the construction of the appropriate diagnostic diagrams can separate the Symbiotic systems from the PNe:  $5007/4363$  vs  $4363/4340$  (Gutierrez-Moreno et al. 1995) (Figure 4) Another diagrams can give evidence for shocks in this objects. The determination of electron density ( $n_e$ ) and temperature ( $T_e$ ) can be made from the  $\lambda\lambda$  4363 and 5007, [OIII] lines,  $H\beta$ ,  $H\alpha$ ,  $\lambda\lambda$  6548 and 6583 [NII] lines, and  $\lambda\lambda$  6717 and 6730 [SII] emission lines, using the equations from Osterbrock & Ferland, 2006.

Gutierrez-Moreno A., Moreno, H. & Cortes. 1995. PASP, 107, 462.

Osterbrock, D.E. & Ferland G. J., 2006. Astrophysics of gaseous nebulae and active galactic nuclei

Sabin, L.; Parker, Q.A.; Corradi, R.L.M.; et al. 2014. MNRAS 443, 3388

Viironen, K.; Greimel, R.; Corradi, R.L.M.; et al. 2009. A&A, 504, 291

### **5.1.5 Molecular hydrogen of small scale structures in planetary nebulae**

One of the most attractive and interesting aspect of the study of Planetary Nebulae (PNe), which are the product of the evolution of low and intermediate mass stars (0.8M 8Msun), resides in their outstanding morphologies. The observed shapes originate from the successive mass loss events occurring during the PN formation process (coupled with other physical mechanisms), which



ultimately led to the formation of an extensive ionized nebula (Kwok 2000). The latter will then slowly dissipate into the interstellar medium (ISM).

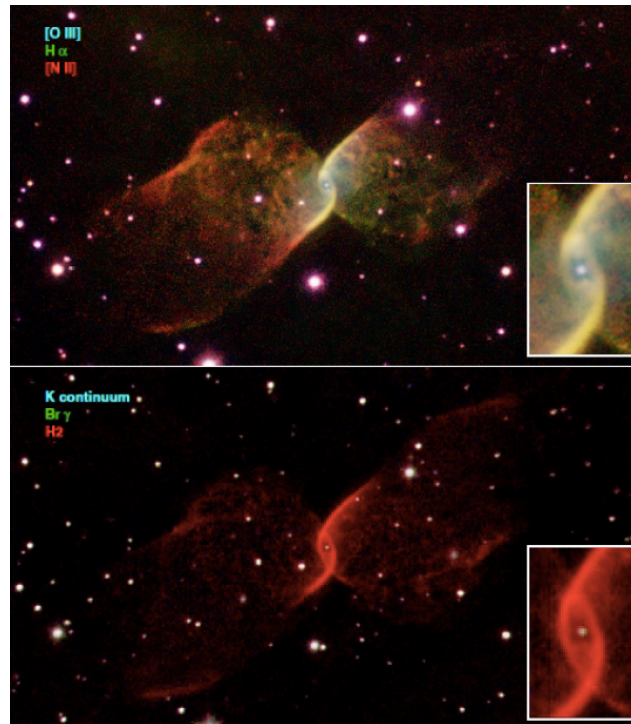


**Figure 6:** The NOT telescope color composite optical (top) and WHT telescope near IR (bottom), narrow band pictures of PN Kn 26. The narrow band filters and colors assigned to each picture are labeled on them. The FoV is 150" X 85". In both pictures north is up, east to the left (Guerrero et al. 2013).

The morphological analysis (of macro and micro structures) of these nebulae has been at the centre of various investigations related to the creation of morphological catalogues (e.g. Sahai et al. 2011) underlying the wide variety of shapes and therefore the occurrence and implication of (a) distinctive shaping mechanism(s); the determination of the kinematics of the ionised ejecta (e.g. Lopez et al. 2012) or the analysis of the faint ejecta (halos) from the Asymptotic Giant Branch phase which are sometime still observable around PNe (e.g. Ramos Larios & Phillips 2009, Corradi et al. 2003).

While most of these morphological investigations were generally made using deep optical images focusing on emission lines such as H $\alpha$ , [N II] 6584 and [O III] 5007, it has been noted that PNe can also be well imaged using molecular lines in the near infrared such as H<sub>2</sub>. This weak emission line has the advantage not only to indicate the bipolar nature of PNe (Kastner et al. 1996) by underlying the contours of the dark lane or the disk/torus where H<sub>2</sub> is not dissociated; but also to delineate the





transition zone between the ionised and molecular regions in the nebulae. In this framework several investigations have been realized and we can cite as an example the works by Cox et al. 2001, Volk et al. 2004, Matsuura et al. 2009 and Marquez Lugo et al. 2013, Guerrero et al. 2013 [and references therein], which mainly targeted large and/or bright PNe.

The aim of this proposal is to search for H<sub>2</sub> (1-0) S(1), H<sub>2</sub> (2-1) (S1) and Bry line emission in the near IR K band of small scale low ionisation structures of PNe in order to assess the origin of the mid IR emission and to derive line ratios in the H<sub>2</sub> lines to study the excitation mechanisms: ionized gas would imply Bry emission, molecular material would result in the detection of H<sub>2</sub> emission, and dust would result in neither detection of Bry nor H<sub>2</sub> emission. With these observations we expect to achieve several goals: corroborate for the first time the presence (or absence) of molecular hydrogen in small or distant PNe and then identify the nature of the emission at distinctive locations, compare the optical and Near IR morphologies in the case of a positive detection as well as evaluate the evolution of H<sub>2</sub> for PNe presenting similar morphologies but different evolutionary stage.

Corradi R. L. M., et al., 2003, MNRAS, 340, 417

Cox, P., et al, Post-AGB Objects as a Phase of Stellar Evolution, Proceedings of the Torun Workshop held July 5-7, 2000. Edited by R. Szczerba and S. K. Gorny. Astrophysics and Space Science Library Vol. 265, ISBN 07923-71453. Publisher: Kluwer Academic Publishers, Boston/Dordrecht/London, 2001.

Guerrero, M. A., Miranda, L. F., Ramos-Larios, G., Vázquez, R., A&A 2013, 551, A53

Kastner, J., Weintraub, D., Gatley, I., Merrill, K. M., Probst, R., ApJ, 1996, v.462, p.777

Kwok, S. Asymmetrical Planetary Nebulae II: From Origins to Microstructures, ASP Conference Series, Vol. 199. Edited by J. H. Kastner, N. Soker, and S. Rappaport. ISBN: 1-58381-026-9, 2000, p. 9

López, J. A., et al., Revista Mexicana de Astronomía y Astrofísica, 2012, Vol. 48, pp. 3-7

Marquez-Lugo, R.A., Ramos-Larios, G., Guerrero, M.A., Vázquez, R. MNRAS 2013, 429, 973

Matsuura, M., et al., ApJ, 2009, Volume 700, Issue 2, pp. 1067-1077

Ramos-Larios, G., Phillips, J.P., MNRAS, 2009, 400, 575

Sahai, R., Morris, M., Villar, G., AJ, 2011, 141, 134 (31pp)

Volk, K., Hrivnak, B., Kwok, S., ApJ 2004, Volume 616, Issue 2, pp. 1181-1187

### **5.1.6 Observing Near Earth Objects using the 6.5m TSPM**

The Near Earth Objects (NEOs) are defined as those minor bodies of the Solar System with orbits close to our Planet (0.983 to 1.3 AU) and its population is constituted by different type of objects: meteoroids, asteroids, comets, interstellar dust, and interplanetary dust particles (Binzel et al. 2002). The study of NEOs has relevant implications for the international astronomical community. First, some of these objects preserve properties of the primordial conditions of the Solar System, as has been revealed by in situ measurements and astronomical observations. Moreover, the exploration of space mining is opening a new window in this research area, through the resource exploitation of



nearby asteroids. On the other hand, as they reach and/or cross the orbit of the Earth, the possibility of impact must be considered as we trace contingency plans and make a detailed evaluation of the damages that these events may produce.

It has been estimated that nearly 50 to 150 tons of dust and small objects break through the atmosphere each day without any catastrophic consequences, however, those big enough to produce craters have impacted the Earth before and they are associated with massive extinctions (e.g. the 10 Km Chicxulub crater in Yucatan, Mexico). Furthermore, even when small objects of few tens of meters go through the atmosphere and disintegrate without a collision with the ground, considerably local damage may be provoked (e.g. Tunguska and Chelyabinks on 1908 and 2013, respectively).

The NEOs are classified by its chemical composition, like the asteroids, and, due to these chemical properties, they can be highly reflective or obscured at optical wavelengths and, above all, knowing its chemical composition is critical to understand the damages generated in case of collision with the Earth. Nowadays, more than 11,000 NEOs have been discovered thanks to the effort of several missions devoted to this task. However, those with diameters below 140 m and likely a high fraction of the reddest (low albedo objects and, thus, strong infrared emitters) remain unknown. Therefore, to properly characterize these objects several studies may be performed.

In this context, taking advantage of the construction of the 6.5 m telescope in San Pedro Mártir (hereafter referred as TSPM) we have explored the possibilities of using this powerful telescope to study NEOs. In the following lines, we describe three projects to detect and characterize NEOs using the Magellan/MMT/TSPM instruments approved for the collaboration.

**Deep NEOs survey.** Due to its 6.5 m aperture, the TSPM operating with the wide field camera MEGACAM (field of view 24'x24') offers a valuable opportunity to accomplish a deep survey of NEOs focused in the study of the statistical properties of the orbital distribution of these objects, as well as their sizes. One of the most important parameters of the NEOs is the absolute magnitude  $H$ , which is related to the size of the object and its albedo. The usage of MEGACAM/TSPM will allow to seek and observe smaller NEOs, down to few tens of meters in size, due to its higher sensitivity, compared with the rest of the surveys devoted to this effort. In comparison with other surveys, such Catalina sky Survey (CSS), Pan-STARRS, and the forthcoming Large Synoptic Survey Telescope (LSST), the MECAM/TSPM deep survey will focus in a limited field or in a group of fields (a.k.a. pencil-beam survey), accordingly to the observing time granted to this project. Further, the sensitivity will be greater than the sensitivity achieved by Pan-STARRS and by the pencil-beam survey DECam (Dark Energy Camera NEO Search Program, CTIO). The main goals of this survey are: 1) To detect less brighter NEOs, because of their small size, their low albedo or because they are away on its orbit and 2) To determine the orbital distribution by means of statistics and their sizes with the highest sensitivity possible. Both quantities are fundamental to know the impact probability and the risks that



the NEOs population may imply. Finally, we have investigated possible observation strategies leading us to an estimation of several hundreds of NEOs discovered by this deep survey.

**Rapid-response taxonomy.** As was mentioned before, knowing the chemical composition of NEOs is vital to prevent and to trace contingency plans in case of impact. The surveys dedicated to detect NEOs have a magnitude limit of  $V=20$ , the objects bright around this magnitude, typically during several weeks, until they diminish its bright just before they are not observable at all. Thus, the only way to characterize these objects is to observe them immediately after their discovery. One of the most used methods to inspect the composition of NEOs is to perform photometry in different bands to infer some properties of the reflectance spectrum of these objects. The 8-color classification system proposed by Tholen (1984) is one of the most used and provides a preliminary and useful overview of the composition of these objects. The instrument MMIRS mounted in the TSPM will allow to perform these photometric observations in the Y, J, H, and K near infrared bands for the more obscured NEOs, since they are strong infrared emitters, helping us to constrain their albedo, a critical parameter to estimate the size of these objects. A significant improvement to the MMIRS observations devoted to this project would be to acquire a z filter, without substantial expenses and easy to implement as well. Finally, it is worth to mention that the MMIRS/TSPM project will complement the LSST project, providing the missing infrared information of the LSST.

**Characterization of NEOs.** To precisely determine the mineralogy of NEOs, optical and infrared spectroscopic observations are required. Considering the 1st generation of instruments of the TSPM, the usage of MMIRS on its long-slit observing mode will offer a valuable opportunity to achieve a fine characterization of most obscured NEOs. Beside a red slope on their reflectance spectrum, carbonaceous and metallic NEOs show considerable differences at near infrared wavelengths. For example, the presence of absorptions at 1 and 2 microns indicate a silicate mineralogy, and their relative abundances and centers tells us what kind of silicate (olivines and piroxenes) dominates the composition of the NEO observed. Furthermore, NEOs with sizes down to 500 m have no spectral information at all. The NEOs characterization project using MMIRS/TSPM will open a new and excellent opportunity to contribute to the international efforts to the knowledge of the properties of the NEO population. Finally, the execution of all these projects are planned in the queue observation mode proposed for the operation of the TSPM.



### **5.1.7 High resolution spectroscopy and the abundance discrepancy problem in ionized plasmas**

Ionized gas is used to infer chemical abundances throughout the universe. Usually, these abundances are derived from observations of strong, collisionally-excited emission lines. However, in the local universe, it has long been known that the abundances derived from these lines differ from those derived from recombination lines, at least for the common ions  $C^{++}$ ,  $N^{++}$ ,  $O^{++}$ , and  $Ne^{++}$  (Wyse 1942; Peimbert & Peimbert 2006; Liu 2010). This problem is known as the abundance discrepancy problem. Typically, in H II regions, the abundances inferred from recombination lines are about a factor of two larger than those inferred from collisionally-excited lines. In planetary nebulae, the same situation holds for about 80% of the objects studied thus far, but the remaining objects have larger discrepancies, exceeding a factor of five (Liu 2010). There is presently no completely satisfactory explanation for this abundance discrepancy. Although it is impossible to study this problem in the more distant universe in the spectra of active galaxies, since their internal kinematics smear the spectra too much to distinguish the individual recombination lines, there is no reason to expect that it does not exist, leading Ferland (2003) to classify the issue among the big, unsolved problems facing nebular astrophysics and our understanding of the chemical abundances in ionized plasmas throughout the universe. This issue is not trivial, since these elements are among the most common in the universe, but are created in stars. The implications therefore extend beyond nebular astrophysics to the understanding of both stellar evolution (and perhaps structure) and the cycling and accumulation of matter within the galaxies they inhabit.

Thus far, most studies of the abundance discrepancy problem have used low-resolution spectroscopy. While this has permitted the problem to be characterized in many objects, it has the consequence of integrating the physical conditions (and the physics) along the line of sight through the objects studied. High-resolution spectroscopy can and should be pursued vigorously, as it can take advantage of the internal kinematics to resolve the H II regions and planetary nebulae of interest along the line of sight and also allow the study of the physical conditions locally, resolved along the line of sight.

Recently, we used high-resolution spectroscopy obtained with the UVES spectrograph at the VLT to compare the kinematics of recombination and collisionally-excited emission lines through NGC 7009 (Richer et al. 2013), finding an additional kinematic component emitting in recombination lines, but with no counterpart in collisionally-excited lines. In other recent studies (Peimbert & Peimbert 2013, Peimbert et al. 2014), we have used low-resolution spectroscopy to compare the temperatures, densities, and pressures inferred from recombination and collisionally-excited lines in H II regions and planetary nebulae, including NGC 7009, finding rather similar physical conditions for both types of lines. Since the first study is nearly unique, its results cannot be generalized yet and so must be repeated in more objects to understand whether its result is typical. The second type of study has already been applied to a number of objects, so its results are clearly more general, but it would be useful to study some of the same objects at high spectral resolution to determine whether the results



hold both locally and globally (resolved and integrated along the line of sight, respectively). Both types of studies would provide crucial information to better understand the conditions under which the recombination and collisionally-excited emission lines are emitted in ionized plasmas, both in the local and distant universe.

For both types of studies, which provide crucial information to understand the origin of the abundance discrepancy problem, access to a world-class, high-resolution spectrograph is necessary. The Maestro spectrograph, used with the atmospheric dispersion corrector at the  $f/5$  focus of the MMT, should be a capable of undertaking the required studies. The spectrograph s design optimizes its performance in the UV and blue parts of the spectrum, coinciding with the wavelength range that includes the majority of the emission lines of interest.

Ferland, G. J. 2003, *ARA&A*, 41, 517

Liu, X.-W. 2010, in *NewVision 400: Engaging Big Questions in Astronomy and Cosmology Four Hundred Years after the Invention of the Telescope*, ed. D. G. York, O. Gingerich, S.-N. Zhang & C. L. Harper, Jr.

Peimbert, M., & Peimbert, A. 2006, in *IAU Symp. 234, Planetary Nebulae in our Galaxy and Beyond*, ed. M. J. Barlow & R. H. Méndez (Cambridge: Cambridge Univ. Press), 227

Peimbert, A., & Peimbert, M. 2013, *ApJ*, 778, 89

Peimbert, A., Peimbert, M., Delgado-Inglada, G., García-Rojas, J., & Peña, M. 2014, *RMxAA*, 50, 329

Richer, M. G., Georgiev, L., Arrieta, A., & Torres Peimbert, S. 2013, *ApJ*, 773, 133

Wyse, A. B. 1942, *ApJ*, 95, 356

### **5.1.8 Young star clusters and the structure of molecular clouds with the TSPM**

A majority (70-90%) of the stars in our Galaxy –and most likely in other galaxies too– form in relatively numerous groups (typically, hundreds to thousands of members). These stellar nurseries are known as embedded clusters (Lada & Lada, 2003). They are typically detected through surveys of Giant Molecular Cloud complexes with active star formation, where they are usually still forming a fraction of their members while still being surrounded by the remnant of the parental gas clumps from which they formed. Embedded star clusters are difficult to observe in optical wavelengths due to the copious amount of dust usually present in the cluster envelopes, but they are usually very bright – prominent, in fact– at infrared wavelengths.

To understand the processes of formation and early evolution of these young stellar systems is a problem that sits at the very backbone of modern astrophysics, relating two fundamental, unsolved puzzles: the process of star formation, and the process by which galaxies assemble from the stars formed in the clusters. To understand embedded star clusters takes us to understand basic questionings like: why are stars preferentially formed in numerous groups and not in small or isolated systems?, how important is the influence of local environment to define the properties of the clusters they form



(Román-Zúñiga 2014), how is that star clusters have so similar Initial Mass Function (IMF) despite forming in completely independent regions (Bastian et al 2010), is the IMF assembled since the fragmentation of the molecular cloud itself (Alves et al 2007). The answers we can give to these questions is what eventually will lead us to tackle more complex problems, like what were the process by which globular clusters or dwarf galaxies were assembled (Kissler-Patig et al 2006), how massive clusters can be formed in very small galaxies with relatively little gas (de Grijs 2013).

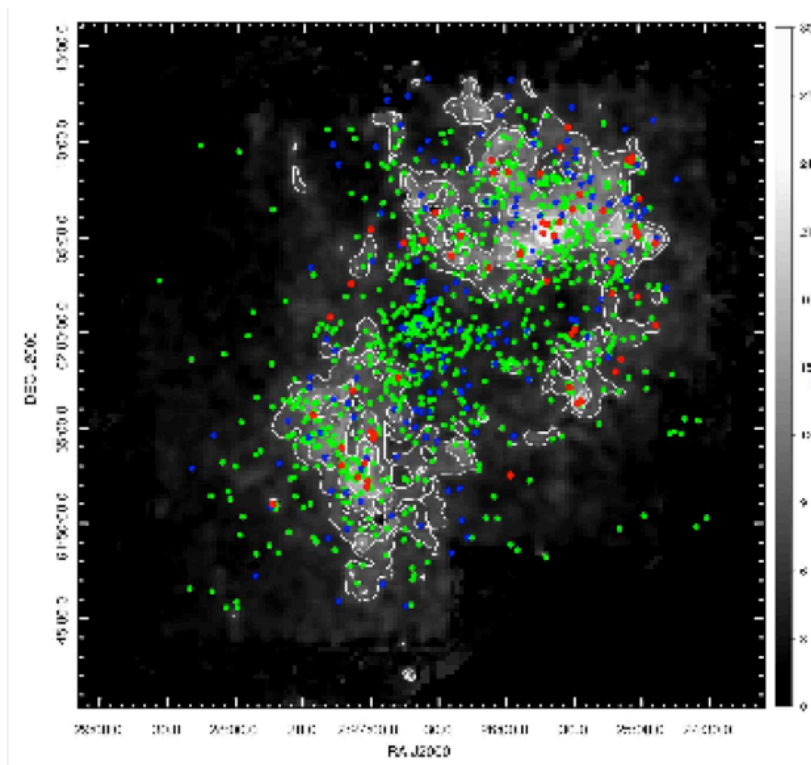


**Figure 7:** Gray scale and contours show a dust extinction map of the W3 complex. Dot symbols indicate locations of candidate young star members at different evolutive stages (red: protostars, green: stars with prominent circumstellar disks, blue: stars with receding circumstellar disks).

There is also one particularly tricky problem that has come to light recently and it is worth mentioning: how is that older stellar aggregations like Globular Clusters present evidence of hosting members with distinct metallicity, i.e. evidence that at some point, a fraction of the stars in a given cluster formed from gas with a richer content of metals. This could mean that along the history of the cluster, some of the massive stars died and enriched the interstellar medium, from which a new generation of stars formed and mixed with the older generation of longer-lived low-mass stars. This problem of “self-enrichment” in stellar cluster (see e.g. Schiavon et al. 2013; Bastian et al. 2015) currently lacks a satisfactory explanation, and it may be possible that the only way to provide one is





to understand how massive clusters form in the first place, and if they can indeed, self-enrich. One requirement for self-enrichment would be for clusters to keep a reservoir of gas to form subsequent generations. Are there other mechanisms to be considered? For instance, could it be possible that chemical abundances vary in the right proportions within a single giant molecular complex, forming mixed population clusters from the merging of smaller clusters forming at different epochs? Studying the chemical evolution of young, massive clusters is still an unexploited niche in current Astrophysics, and may be accessible to a 6.5m class telescope like the TSPM provided access to Echelle spectroscopy (e.g. MAESTRO, Hectochelle) to study bright members in massive star clusters, located at distances of 1-5 kpc.

To date, embedded clusters in relatively nearby active star forming complexes, like Orion, Perseus or Taurus, have been studied with meticulous detail. In those nearby ( $d < 500$  pc) complexes we can resolve binary or multiple systems, or detect very low mass sources, even with relatively small telescope apertures. For instance, class 2-4m equipped with sensitive infrared cameras are enough to sample the mass spectrum of a nearby embedded cluster down to the brown dwarf regime (0.005 – 0.02  $M_{\text{sun}}$ ). The problem is that, at smaller distances, the area of a cluster with 10<sup>3</sup>-10<sup>4</sup> members can easily span from a few to a few tens of square degrees. Thus, global studies in complexes like Orion or Perseus, aimed to study environmental process or the interaction between clusters, require of capital observational effort. For that reason, global studies of molecular complexes that consider entire “families” of clusters are better suited for more distant regions (e.g. the Rosette Molecular Cloud, W3; Román-Zúñiga et al. 2008, 2015). Class 4-6m or 6-8m telescopes are nowadays being used to augment the level of detail in complexes at distances of 1 to 2 kpc.

Surveys of numerous star cluster forming regions have been done from both earth and space-based facilities. However, most of these studies do not include high resolution spectroscopy data, capable of providing radial velocities to trace the internal kinematics of the clusters. Only a handful of studies have succeeded at this task so far (e.g. Fűrész et al. 2006, 2008; Cotaar, 2015). These data are crucial to understand one essential aspect: how a few embedded clusters survive to become bound open clusters while the rest do not (the so called “infant mortality”, Lada & Lada 2003). Two aspects of this problem are important: a) the removal of the gravitational potential formerly provided by the parental gas once it is removed, and b) the effect of tides both from the cloud and nearby clusters (the so called “cruel cradle” effect, Kruijssen) and from the gravitational potential of the Galaxy. Also, this could help to attack another poorly understood aspect: the evolution of star clusters -manifested as variations in their size, density and morphology from sub-virial states.

UNAM is already actively participating in a systematic large scale study of nearby ( $d < 500$  pc) young star cluster kinematics in the “Young Clusters and Young stars” goal science group (Covey et al. 2013) of the APOGEE-2 survey of the fourth phase of the Sloan Digital Sky Survey (SDSSIV). However, this survey, performed with the Apache Point 2.5m telescope, is limited to the brightest population ( $H[1.6 \mu\text{m}] < 12.5$  mag) of the clusters. An instrument like Hectochelle, would allow,



undoubtedly, to perform similar systematic studies of the velocity dispersion in young clusters both down to the low mass end in nearby clusters, or to extend the reach to more distant ( $1 < d < 3$  kpc) regions. To date, studies like those of Fűrész et al. (2006, 2008) show clearly the feasibility of such projects down to 1 kpc. In Fig. 5 we show an image of the W3 complex (Román-Zúñiga et al 2015), where we can see the spatial distribution of over a thousand young stars with ages between 1 and 3 Myr, identified and classified from multi-wavelength photometry catalogs (infrared plus X-rays). The approximate diameter of this region is 1 degree, ideal for Hectochelle (to measure radial velocities) or Hectospec (to classify spectral types and/or determine stellar masses). The difference respect to studies of nearby regions is that we would be able to study the interaction between different clusters and the relation to the molecular cloud as it is being evacuated from the complex. Moreover, Echelle spectroscopy will provide abundances, so that we could take a dive into the problem of self-enrichment. If self-enrichment is actually primordial diversity of abundances within a molecular complex in scales of tens of parsecs, we may be able to prove it.

Nowadays, Hectochelle is in doubt for being included in the package of  $f/5$  instruments to be moved to the TSPM. One of the main reasons for this is the current status of the fiber positioning system and head, which is possibly reaching the end of its operating life. However, we would like to propose here a possible solution to the problem: the idea is that, based on the experience we are acquiring from APOGEE-2, we could consider to design and construct a replacement, simpler system of exchangeable fiber-plug plates for Hectochelle. This system could be implemented by the Mexican partners, under technical advise from MMT and also from SDSS. With a well put proposal and a strong instrumentation team, it may be possible to adapt a fiber-plug plate system to Hectospec/Hectochelle for the TSPM, so that the lifespan of the instrument is increased, even if its field reconfiguration efficiency is reduced by the requirement of positioning fibers by hand.

**3-D Structure of Molecular Gas in the Milky Way.** Characterizing the structure of molecular clouds down to the scales of pre-stellar cores is key to understanding the initial conditions of star formation. The structure of molecular gas clouds is not easy to determine, as molecular Hydrogen ( $H_2$ ) cannot be observed directly because it lacks a permanent dipole moment and its rotational transitions are very weak. Molecular emission from tracers like CO used to be the preferred trace surrogates, and they work well for the inter-clump medium and the relative diffuse external layers of clouds, but they are severely depleted in the dense regions where stars form (Bergin et al. 2002). A more direct tracer is dust, which obscures clouds and comprises about 1% of the cloud mass. Dust can be fairly assumed to be uniformly distributed in the gas (e.g. Whittet, 2003), and observations have shown that the column density is linearly dependent to the reddening of background stars by dust grains. At near-infrared wavelengths, clouds can be penetrated to reveal the background sources, each working as an individual measurement of reddening: By averaging stellar reddening within an aperture and scanning across a field, we can map the variations of dust extinction across a cloud and construct maps of  $H_2$  column density with resolutions comparable of those obtained with radio telescopes. This Near-Infrared Color-Excess technique or NICE (Lada et al. 1994) became a practical





way of using photometry in a minimum of two bands to map the structure of molecular clouds. The NICE technique was optimized as a multi-band technique (NICER) (Lombardi et al. 2001), has also recently been improved with complex noise reduction techniques (Lombardi et al. 2009) and can even include extragalactic sources as individual measurements of reddening by dust (Foster et al. 2008). The same technique has also been used to map extinction at unprecedented levels of  $70 < AV < 100$  visual magnitudes (Román-Zúñiga et al 2009). The color excess technique is thus ideal for the construction of deep, highly detailed two-dimensional maps of molecular clouds at a relatively low observational cost. Other methods, like the Raleigh-Jeans Color Excess (RJCE) technique (Majewski et al. 2011), which make use of multi-band catalogs that include Spitzer or WISE space telescopes photometry at  $3.5\text{-}5\ \mu\text{m}$  have been recently shown to map extinction at even more complex regions where dense and diffuse material is present.

Now, by combining accurate mapping of molecular clouds with increasing quality parallax measurements of foreground stars, it is possible to estimate distance to a cloud with precisions of the order of only tens of parsecs. Studies like those of Knude et al 2008, Lombardi et al (2008) and others, show how a simple Bayesian inference method can be applied to estimate distance-extinction relations at a given line of sight. The success of the GAIA mission will imply that parallax measurements will be improved by orders of magnitude in only a few years, and that the precision to estimate distances to a cloud will also be improved. Knude et al already shown how with relatively little effort, it could be possible to estimate distances even within a single cloud, and thus the door to tridimensional mapping of molecular complexes is already open. A wide-field near-IR detector like MMIRS at TSPM, with the quality of the SPM at infrared wavelengths to make imaging surveys, will surely allow the construction of exquisitely detailed maps of different molecular cloud complexes - the resolution of pre-stellar core scales will depend of distance to the cloud and the density of background sources, but the uniformity of the map will be directly related to the depth and precision of the photometry.

If MMIRS or a similar instrument is not available, then MEGACAM could also do the trick: recent studies like those of Sale et al (2009) showed the feasibility of the Mapping Extinction Against Distance (MEAD) technique using data from the IPHAS survey (Drew et al 2005). The MEAD technique shows that optical colors from  $r$ ,  $i$  and  $H\alpha$  photometry, plus parallaxes, can be used to construct distance-extinction relations of high precision. While less suitable for molecular clouds, these methods can be used to estimate the tri-dimensional structure of the molecular gas in the spiral arms of the galaxy. An instrument like MEGACAM at the TSPM could easily improve the IPHAS catalogs in quality and sensitivity and, in synergy with GAIA could provide fantastic insight into this problem.

Alves, J., Lombardi, M. & Lada, C. J. 2007, *A&A*, 462, L17

Bastian, N., Covey, K. R. & Meyer, M. R. 2010, *Annu. Rev. Astro. Astrophys*, 48, 339

Bergin, E. A., Alves, J., Huard, T. & Lada, C. J. 2002, *ApJ*, 570, L101



- Covey, K. et al. "APOGEE-2 Young Cluster Science Requirements Document", Sloan Digital Sky Survey IV  
de Grijs, R., Anders, P., Zackrisson, E. & Östlin, G. 2013, MNRAS, 431, 2917  
Drew, J. E., Greimel, R., Irwin, M. J., et al. 2005, MNRAS, 362, 753-776  
Foster, J. B., Roman-Zúñiga, C. G., Goodman, et al. 2008, ApJ, 674, 831  
Foster, J., Cottaar, M., Covey, K. et al. 2015, ApJ, 799, 136  
Fűrész, G., Hartmann, L. W., Szentgyorgyi, A. H., et al. 2006, ApJ, 648, 1090  
Fűrész, G., Hartmann, L. W., Megeath, et al. 2008, ApJ, 676, 1109  
Kissler-Patig, M., Jordán, A. & Bastian, N. 2006, A&A, 448, 1031  
Knude, J. & Nielsen, A. S. 2001, A&A, 373, 714-719  
Kruijssen, J. M. D., Maschberger, T., Moeckel, N., et al. 2012, MNRAS, 419, 841  
Lada, C. J., Lada, E. A., Clemens, D. P. & Bally, J. 1994, ApJ, 429, 694  
Lada, C. J. & Lada, E. A. 2003, Annu. Rev. Astro. Astrophys, 41, 57  
Lombardi, M. & Alves, J. 2001, A&A, 377, 1023  
Lombardi, M., Lada, C. J. & Alves, J. 2008, A&A, 480, 785  
Lombardi, M. 2009, A&A, 493, 735  
Majewski, S. R., Zasowski, G. & Nidever, D. L. 2011, ApJ, 739, 25  
Román-Zúñiga, C. G., Elston, R., Ferreira, B. & Lada, E. A. 2008, ApJ, 672, 861-887  
Román-Zúñiga, C. G., Lada, C. J. & Alves, J. F. 2009, ApJ, 704, 183  
Román-Zúñiga, C. G., Ybarra, J., Megias G. et al. 2015, AJ  
Sale, S. E., Drew, J. E., Unruh, Y. C., et al. 2009, MNRAS, 392, 497  
Whittet, D. 2003, Dust in the galactic environment, IOP Publishing, 2003 Series in Astronomy and Astrophysics, ISBN 0750306246

### **5.1.9 Determination of presence of shocks caused by PNe halo-ISM interaction**

A shock in a PNe causes the electronic temperature  $T_e$  to increase, which in turn causes an enhancement of the [OIII] emission. On the other hand, a decrease in the electronic density  $N_e$  will cause a decrease in the  $H\alpha$  emission (Guerrero et al. 2013). Because of this effects, we can search for evidence of shocks caused by the interaction between the ISM, and the outer envelope of PNe, which we can then model using hydrodynamics simulations. In this project we want to search for shocks as evidence of interaction between the ISM and PNe halo. We are most interested in the  $H\alpha$  line at  $6563.8 \text{ \AA}$ , which is known to be a detectable line in the objects and regions of interest of this proposal, and the [OIII] line at  $5007 \text{ \AA}$ . The [OIII]/ $H\alpha$  ratio will give us evidence of shocks in the region. This emission is usually very weak in the halo, thus we are in need of a telescope sensitive enough as to reduce the integration time needed to achieve a decent signal to noise ratio. This sensitivity can be achieved with the 6.5 meter telescope.

We will observe as many regions of each PN halo in as many directions as possible, where we expect to see different line ratios due to the direction of motion of the object with respect to the ISM and the shocks we expect to be caused by this. Examples of the objects we plan to observe are the following:



| Object   | Right Ascension | Declination     |
|----------|-----------------|-----------------|
| Cn 1-5   | 18h 29m 11.659s | -31° 29' 59.16" |
| NGC 2438 | 07h 41m 50.51s  | -14° 44' 07.7"  |

The choice of objects has been based on the coordinates, as well as the fact that we have photometry that suggests an enhancement in the H $\alpha$  emission in the halo, as can be seen in Figure 7. We still don't have spectral information that will help us understand if we have shocks and thus interaction that we can model with a hydrodynamics code we have already produced. Several hours of observing time are required to make sure a good signal to noise ratio is reached, giving us confidence in then results and more robust data for our simulations.

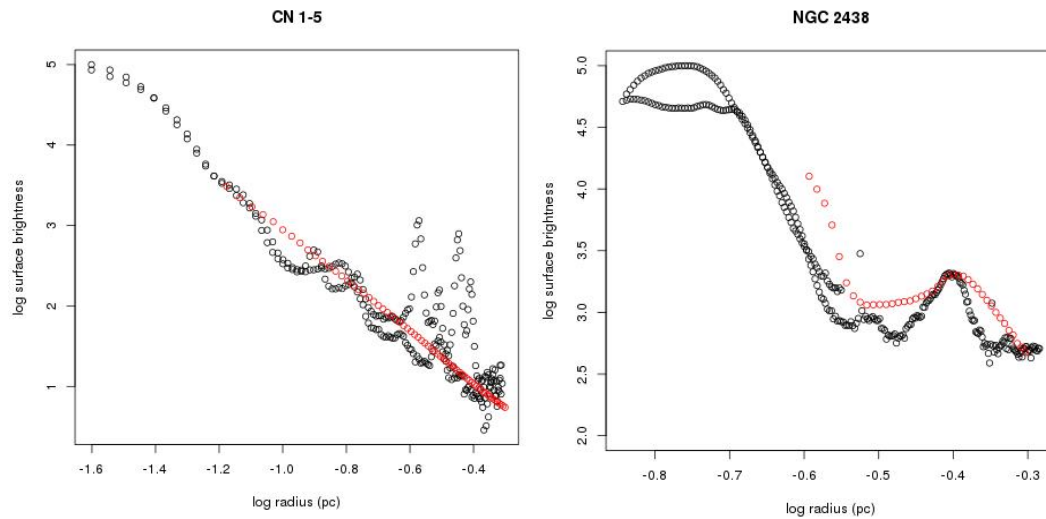


**Figure 8:** NGC 2438 and CN 1-5. In red we show the modeling assuming no interaction and in black we show the actual observations.

Guerrero M.A., et al, 2013, A&A, 557, A121, 12

## 5.2 Extragalactic astronomy

### 5.2.1 Star formation histories of galaxies in the local Universe using the resolved bright stars in the near infrared

According to the currently popular hierarchical model of galaxy formation, galaxies grow by successive merging of low mass galaxies (Ellis & Silk 2007). On the other hand, in the classical monolithic collapse model, galaxies evolve by transforming their gas into stars at rates set by their



initial masses. The predicted star formation histories (SFHs) are expected to be vastly different in the two scenarios: in the former case it is expected to be spiky, with each spike related to a merger event, whereas in the latter case, it is expected to be smooth. Hence, obtaining the SFH over the entire Hubble time has the potential to distinguish these two scenarios. The traditional method of determining SFHs using the Population Synthesis Techniques (Bruzual & Charlot 2003) has sensitivity only to the most dominant stellar population, and hence not useful in obtaining SFH over the entire Hubble time.

Resolved stellar populations are the best tracers of the SFH of a galactic region, and their color-magnitude diagram (CMD), the best tool to exploit the tracers (Tosi 2009). This is due to the well-established fact that the location of any individual star in a CMD is uniquely related to its mass, age and chemical composition. Thus from the CMD, we can directly obtain these parameters. In the case of simple stellar populations, i.e. coeval stars with the same chemical composition, isochrone fitting is the most frequently used method to infer the age of the system. In the case of galaxies, with rather complicated mixtures of different stellar generations, the diagram can be used to derive SFH, as illustrated in the left panel of Figure 8.

The technique of determination of SFH of external galaxies through the use of resolved stellar population is made possible through the unprecedented resolving power of the images obtained by the WFPC2 and ACS aboard the Hubble Space Telescope (HST). Since its launch almost 2 decades ago, SFHs are obtained for most of the *dwarf* galaxies in the local group (Tosi 2009), and also in the group of M81 (Weisz et al. 2008). However, study of *massive, high surface brightness* galaxies is crucial in order to understand galaxy formation. The ACS Nearby Galaxy Survey Treasury (ANGST; Dalcanton 2008) project is aimed to do this in galaxies within a distance of 4 Mpc. Even with the HST resolution, crowding becomes an issue in the inner regions of nearby giant galaxies. In addition, there are only a handful of giant galaxies closer to 4 Mpc, making it necessary to look for techniques that can be used to investigate SFH of giant galaxies at distances greater than this. As will be discussed below, use of infrared bright stars in a near infrared (NIR) CMD promises to allow the determination of SFHs to distances up to 6 Mpc even using ground based telescopes. The increased volume over which the sample can be chosen gives a great opportunity to understand the formation of galaxies.

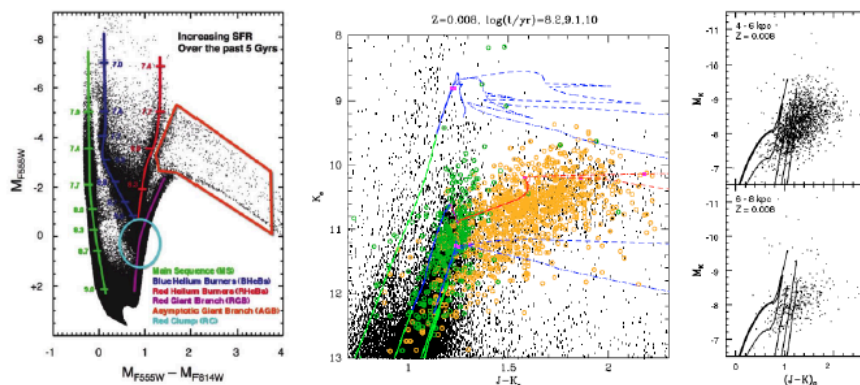




**Figure 9:** The (left) Illustration of determination of SFH using CMDs from Weisz et al. (2008). The plot shows a simulated CMD of increasing SF over the past 5 Gyr. Important features on the CMD are highlighted. The logarithmic ages of stars are overlaid for the main sequence, blue Helium burners and red Helium burners. (middle) Comparison of recent isochrones of Marigo et al. (2008) with the data for the LMC. Three sets of isochrones at log ages (in yr) 8.2, 9.1 and 10.0 are shown (brighter at smaller ages) for two different prescriptions of circumstellar dust. The symbols show spectroscopically confirmed M (green) and C-stars (orange). (right) Illustration of obtaining SFH using CMDs in M82 disk from Davidge (2008). The two plots show the CMDs for the stars detected at two consecutive radial bins. The plotted isochrones correspond to log ages (in yr) 7.5, 8.0, 8.5 and 9.0 from Girardi et al. (2002; 2004). These tracks do not include the C-star phase during which  $J - K$  colors become redder than 1.3 mag. By a comparison of the  $J - K$  colors of M82 and LMC stars, it can be inferred that many of the detected stars in M82 are C-stars.

**Star formation histories of nearby galaxies using TSPM.** In recent years, several NIR surveys (i.e. DENIS, 2MASS, SAGE, and S3MC data for the Magellanic Clouds) have clearly demonstrated that the Thermally Pulsing Asymptotic Giant Branch (TP-AGB) stars account for most of the bright-infrared (IR) objects in resolved galaxies (Cioni et al. 1999; Bolatto et al. 2007). These red stars have the potential to facilitate the determination of the SFHs through the use of NIR CMDs, and theoretical isochrones (Marigo et al. 2008). An example of this for the resolved stars in the LMC is shown in Figure 8 (middle panel).

The following special properties make the NIR CMDs very useful for the study of SFH in nearby galaxies:

- *Identification of TP-AGB and Carbon stars:* Only stars that attain colors redder than  $J - K > 1.3$  mag are the C-stars, which represent a short-lived phase in the TP-AGB evolution. These stars can be un-ambiguously identified among the population of resolved stars. Only stars of initial mass less than 7 Msun pass through the Carbon-rich phase of the AGB. The corresponding age of the stars is  $>200$  Myr. Successively lower mass stars reach this phase at later times, and they are systematically fainter. Hence, the SFH can be derived by counting the relative number of stars in successive magnitude bins.
- *Detection from ground-based telescopes:* Detection of individual stars in galaxies depends on the contrast a star offers in the background of other stars. The main contributors to the background are the low-mass main sequence stars. At infrared wavelengths, the AGB stars are 5–10 mag brighter than the background star, which facilitates their easy detection even with the ground-based telescopes. It may be noted that the horizontal branch (HB) stars, critical for the determination of SFH using the optical CMDs, are only 2–3 mag brighter than the stars that make up the background, and hence it is necessary to resolve the background-contributing population for their detection.



- *The time-resolution and the look-back times of the derived SFH:* The TP-AGB stars span a limited range of magnitudes ( $\leftarrow 3$ ) in the K-band, with the brightest stars reaching  $M_K = -10$ . The faintest of the TP-AGB stars have  $M_K = -7$  mag, which are associated with stellar populations as old as 10 Gyr. Observations that can detect stars of  $M_K = -7$  mag can infer the SFHs all the way up to the Hubble time. The time resolution of the SFH depends on the size of the magnitude bin. For magnitude bins of around 0.2 mag, one can hope to achieve time resolutions of  $\leftarrow 1$  Gyr for look back times greater than a gigayear and much better at earlier epochs. This compares favorably with what is possible these days for galaxies in the local group using HST-derived optical CMDs.  $M_K = -7$  mag corresponds to  $K = 22$  at a distance of 6 Mpc. TSPM, in combination with a NIR instrument such as MMIRS will be able to reach these limiting magnitudes with net exposure times of 2 hours. Hence, TSPM/MMIRS combination promises to obtain the SFH spanning the entire Hubble time for all galaxies that are nearer than 6 Mpc.

**Illustration of SFH through NIR CMD in the nearby galaxy M82.** An insight of what can be achieved with TSPM/MMIRS can be obtained from a study of the nearby high surface brightness galaxy M82 by Davidge (2008) (see Figure 8). All the bright stars detected in the disk of M82 from deep images obtained with WIRCAM at CFHT are plotted. Stars with  $J - K > 1.3$  mag in this diagram are C-stars of ages between 0.1 to 1 Gyr. More importantly the CMD rules out the existence of stars younger than 0.1 Gyr, consistent with a disk-wide burst model for this galaxy proposed by Mayya et al. (2006). The observations had a 50% completeness limit up to  $K=20$  ( $M_K \approx -8$ ), with a net exposure time of 40 minutes. By going down by 1 mag for this galaxy, one could definitely establish the SFH over the entire Hubble time. With TSPM, it would be possible to do that in only a few minutes of observing time. M82 is located in the M81 group at a distance of 3.6 Mpc (distance modulus of 27.8 mag). TSPM will allow similar studies to be carried out up to a distance of  $\sim 6$  Mpc. The increased volume would allow the SFHs to be determined in several massive galaxies, thus providing the key to understand the galaxy formation.

- Bolatto, A.D., Simon, J.D., Stanimirovic, S. et al. 2007, ApJ, 655, 212  
Bruzual, G. & Charlot, S. 2003, MNRAS, 344, 1000  
Cioni, M.-R.L., Girardi, L., Marigo, P., & Habing, H. J. 2006, A&A, 448, 77  
Dalcanton, J. 2008, in Galaxies in the Local Volume, ed. B. S. Koribalski & H. Jerjen, Astrophysics and Space Science Proceedings (Springer)  
Davidge, T. J. 2008, ApJ, 136, 2502  
Ellis, R. & Silk, J. 2007 astro-ph/0712.2865  
Girardi, L., Bertelli, G., Bressan, A., et al. 2002, A&A, 391, 195  
Girardi, L., Grebel, E.K., Odenkirchen, M. & Chiosi, C. 2004, A&A, 422, 205  
Mayya, Y.D., Bressan, A., Carrasco, L., & Hernandez-Martinez, L. 2006, ApJ, 649, 172  
Tosi, M. 2009, The Ages of Stars, Proceedings of the International Astronomical Union, IAU Symposium, Volume 258, p. 61-72





Weisz, D. et al. 2008, ApJ, 689, 160

### **5.2.2 H<sub>2</sub>ETGs: tracing accretion/SF/feedback in early-type galaxies with TSPM**

Early type galaxies (ETGs) have long been considered to be inert, red and dead stellar systems, essentially devoid of gas and dust. This view is radically changed since a number of imaging and spectroscopic studies have revealed the presence of a multiphase interstellar medium (ISM). Starting with the pioneering work of Phillips et al. (1986), optical spectroscopic studies have revealed that the emission line ratios in ETGs are typical of Low-Ionization Nuclear Emission-line Regions (LINERs, Heckman 1980). However, after about three decades of studies, there is still strong debate about the excitation mechanism in LINERs. The three most viable mechanisms are: a) low accretion-rate AGN (e.g. Kewley et al. 2006; Ho 2009); b) photoionization by old, post-asymptotic giant branch (PAGB) stars (e.g. Trinchieri & di Serego Alighieri, 1991; Binette et al. 1994; Stasinska et al. 2008; Sarzi et al. 2010; Capetti & Baldi 2011); c) shocks (e.g. Koski & Osterbrock 1976; Dopita & Sutherland 1995; Allen et al. 2008).

In the study of the optical emission lines in a sample of 65 ETGs, Annibali et al. (2010) have demonstrated that optical diagnostic diagrams (e.g., [OIII]/H $\beta$  vs [NII]/H $\alpha$ ) can not discriminate between low accretion-rate AGNs and shocks, moreover Annibali et al. show that PAGB stars can explain only the observed nuclear emission in the 22% (the fainter tail) of the studied LINERs.

The mid infrared (MIR) window adds new clues to the ETGs/LINERs investigation and in principle it is able to well separate LINERs powered by SF (9% have class-3 spectra in RSA). Vega et al. (2010), Panuzzo et al. (2011), and Rampazzo et al. (2013) shown that the MIR-spectra of ETGs fall into five MIR classes (see left panel in Figure 8), ranging from AGN (class-4), star forming (SF) nuclei (class-3, lines + PAHs with normal ratios), transition class-2 (lines + PAHs with anomalous ratio), class-1 (lines, no-PAHs) to passively evolving nuclei (class-0, no PAH, no emission lines).

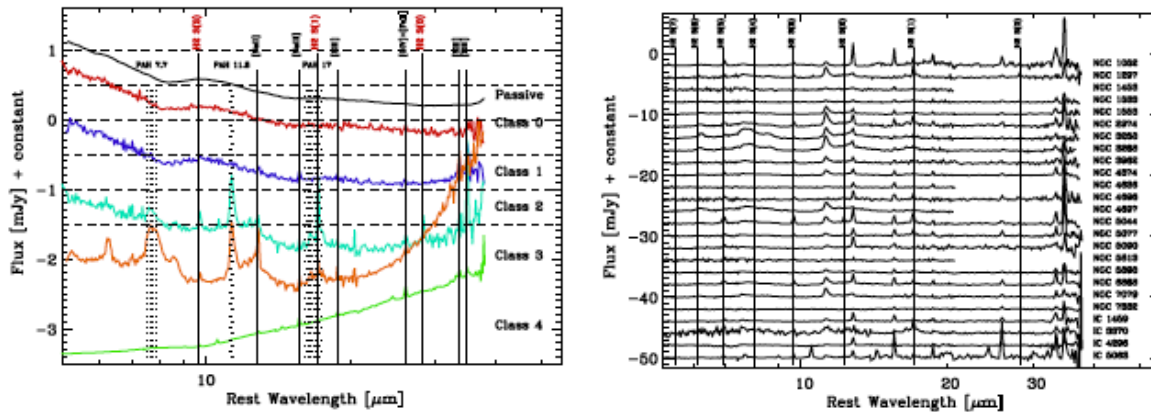


**Figure 10:** Left panel: MIR spectra of ETGs representative of the five classes defined in Panuzzo et al (2011). The thicker black lines mark the positions of the main H<sub>2</sub> rotational lines. Right panel: Spitzer-IRS spectrum of some H<sub>2</sub>ETGs in our sample.

Demographic studies of the morphology and kinematics, presence of dust-lanes and emission from radio to X-ray, supports the view that the MIR classes are connected to a recent accretion episode. Each MIR class may represent a snapshot of the evolution in the inner regions of the ETGs/LINERs, starting from, and ending with a passively evolving (MIR class-0) spectrum (see Fig.11 in Panuzzo et al. 2011).

One interesting result from this analysis is the extremely intense H<sub>2</sub> emission found in ETGs (34 % of Es and 51% of S0s in RSA, see right panel in Fig. 9). Most of them are LINERs and show anomalous low 7.7 $\mu$ m/11.3 $\mu$ m PAH ratio, indicating that the emission is not powered by star formation (Vega et al. 2010), i.e. only a small fraction of H<sub>2</sub> bright ETGs (H<sub>2</sub>ETGs) are excited via UV fluorescence in photo-dissociation regions (PDRs). Other proposed excitation mechanisms of H<sub>2</sub> are X-ray illumination (e.g. Maloney 1996) and shocks (e.g. Hollenbach & McKee 1989; Vega et al. 2010). Some studies suggest that neither diffuse X-ray emission (see e.g. Roussel et al. 2007) nor X-ray illumination from AGN (see e.g. Ogle et al. 2010) are efficient enough to produce the large observed H<sub>2</sub> emission. The [NeIII]15.5 / [NeII]12.8 $\mu$ m vs. [SIII]33.5 / [SiII]34.8 $\mu$ m MIR diagnostic diagram shows that H<sub>2</sub>ETGs fall in the shock regions (Panuzzo et al. 2011).

However, a degeneracy persists with the AGN models if a spread in the dust content of the narrow-line region is allowed. Jet and accretion driven flows are both viable mechanisms to produce shocks in LINERs (Dopita & Sutherland 1995; Nagar et al 2001; Dopita et al.1997; Crawford & Fabian 1992) as well as turbulent motions of gas clouds within the potential well of the galaxy (Ho 2009; Annibaldi et al. 2010 and references therein). Shocks may also be due to supernova remnants or outflows in a region where a starburst has occurred (see van der Werf 2000). Figure 10 shows our total sample of H<sub>2</sub>ETGs compared with other nearby galaxies showing H<sub>2</sub> emission: it is evident the





difficulty in discriminating among various mechanisms of excitation at work from such diagnostic diagrams. Moreover, radically different 2D geometries of the H<sub>2</sub> emission are expected in the case of PDR, shocks or AGN excitation mechanisms (e.g. Donahue et al. 2000).

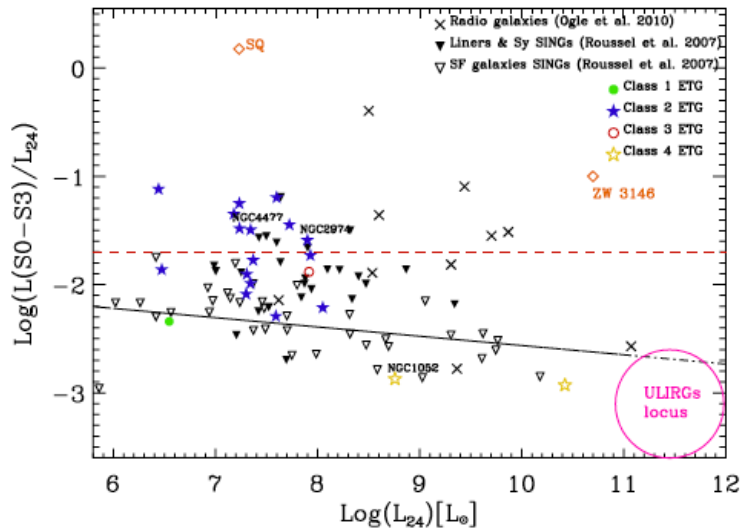


**Figure 11:** Ratio of the pure rotational H<sub>2</sub> emission lines luminosity to the IR luminosity at 24 μm. Our H<sub>2</sub>ETGs (stars, belonging to different MIR classes) are shown in comparison with radio (Ogle et al. 2010), LINERs, Sy and SINGs Star Forming galaxies in (Roussel et al. 2007) and the Stefan’s Quintet (SQ) intergalactic shock (Cluver et al. 2010). Some objects in class-2 (NGC 4477 and NGC 2974) and in class-4 (NGC 1052) are indicated. Class-3 ETGs lie among star forming SINGs spirals. The dashed (red) line separates normal H<sub>2</sub> emission from MOHEG (MOlecular Hydrogen Emission-line Galaxies). The latter have a high H<sub>2</sub>/7.7 PAH ratio (> 0.04), implying an excitation not fully justified by a pure UV heating (Ogle et al. 2010). The solid (black) line is the fit of Star Forming galaxies. Different powering mechanisms are at work in the nuclei of H<sub>2</sub>ETGs, that can be disentangled via the morphological study of H<sub>2</sub> emission and the study of gas kinematics.

The proposed spectroscopic study between 1.25-2.45 μm will allow to detect not only the H<sub>2</sub> line (2.122 μm) but also the [FeII]1.644 μm and the Brγ 2.16 μm emission lines. The [FeII]1.64 μm line is favored in zones of partially ionized gas that are large when the gas is heated by X-rays (power-law photoionization) or by shocks (Mouri et al. 2000). The [FeII]1.64/Brγ ratio is typically a factor ~ 50 higher in shocked regions than in AGNs (see models by Allen et al. 2008 and Groves et al. 2004). Thus a measure of that ratio will allow us to separate shock regions from regions where AGN photoionization dominate. Therefore, to directly investigate the different mechanisms for the excitation of H<sub>2</sub>, high resolution NIR- H<sub>2</sub> narrow-band imaging and NIR spectroscopy are the most suitable observations.



We foresee to use these data-set to constrain our chemo-photometric smoothed-particle hydrodynamics (SPH) simulations providing the global evolution of these ETGs in a fully consistent picture (e.g. Mazzei et al. 2014 and references therein). We also simulate the (thermo)dynamical evolution of molecular clouds in the nuclei of our host ETGs to study the properties of shocks. MMIRS at the TSPM or Atlas at MMT could be suitable instruments to carry out the spectroscopic part of this investigation. We would also request narrow band H2 filters to observe the different H2 emission geometries needed in this work.

We suggest that MIR classes mark evolutionary phases during an accretion episode that may induce SF, and/or AGN activity/feedback. H<sub>2</sub>ETGs and a large fraction of nearby LINERs may represent the final (cooling) phases before the galaxy came back to a passive evolution. Optical diagnostic diagrams alone are unable to disentangle mechanisms at work and 2D studies are rare. The high resolution H2 images plus spectroscopic information accurately modeled will allow us to disentangle the gas powering mechanism/s (shock, AGN, SF) and their interplay as drivers of the evolution in ETGs/LINERs.

Allen et al. 2008, ApJS, 178, 20  
Annibali et al. 2010, A&A 519, A40  
Binette et al. 1994, A&A, 292, 13  
Capetti & Baldi 2011, A&A, 529, A126  
Cluver et al. 2010, ApJ, 710, 248  
Crawford & Fabian 1992, MNRAS, 259, 265  
Donahue et al. 2000, ApJ, 545, 670  
Dopita & Sutherland 1995, ApJ, 455, 468  
Dopita et al. 1997, ApJ, 490, 202  
Groves et al. 2004, ApJS, 153, 9  
Heckman 1980, A&A, 87, 152  
Ho 2009, ApJ, 699, 626  
Ho 2009, ASR, 23, 813  
Hollenbach & McKee 1989, ApJ, 342, 306  
Kewley et al 2006, MNRAS, 372, 961  
Koski & Osterbrock 1976, ApJL, 203, L49  
Mazzei et al. 2014, ASR, 53, 950  
Maloney 1996, ApJ, 466, 561  
Mouri et al. 2000, ApJ, 528, 186  
Nagar et al 2001, ApJL, 559, L87  
Ogle et al. 2010, ApJ, 724, 1193  
Panuzzo et al. 2011, A&A, 528, 10  
Phillips et al. 1986, AJ, 91, 1062  
Rampazzo et al. 2013, MNRAS, 432, 364  
Roussel et al. 2007, ApJ, 669, 959  
Sarzi et al. 2010, MNRAS, 402, 2187



Stasinska et al. 2008, MNRAS, 391, L29

Trinchieri & di Serego Alighieri, 1991, AJ, 101, 1647

van der Werf 2000, in Molecular Hydrogen in Space eds. F. Combes & G. Pineau des For. eds, Cambridge Univ. Press

Vega et al. 2010, ApJ, 721,1090

### **5.2.3 Optical search and follow-up of gravitational waves counterparts**

**Rationale:** Mergers of compact objects are considered the prime sources of gravitational waves (GW), finding electromagnetic (EM) counterparts of GW sources will be of significant in order to fully understand their nature, as proved by the recent gravitational wave event GW170817 followed by electromagnetic detection (Abbott et al. 2017). Coincident EM-GW signals could potentially be used to build independent cosmological distance ladder, to probe the central engines of supernovae and gamma ray bursts, as well as to study the evolution of massive stars and formation of compact objects such as black-holes (BHs) and neutron stars (NSs), to study galaxy-super massive black hole (SMBH) symbiosis and evolution, and even to measure neutron star equation of state. Many of the mergers giving rise to GW events could be explosive and would drive blast waves, relativistic or nonrelativistic, into the surrounding medium and shine as bright radio transients. The light curve evolution of radio supernovae and afterglows from compact object mergers would look alike. Therefore distinguishing the two classes from each other observationally will be important, which could be done at early time by optical spectroscopy. However, GW events are poorly localized (uncertainties with areas of tents to hundreds of square degrees), with bright but rapidly fading optical afterglows. Telescopes suited to perform extremely wide-field searches of transient events, such as the NGISs, the GROWTH network or the future Zwicky optical transient facility are needed in order to cover the GW error boxes. Nevertheless, these imaging surveys will need telescopes with enough light gathering power and FoV to detect and follow-up GW transient candidates for an adequate time to obtain spectral features and to study the physical properties of the counterparts. The detection of EM (optical) counterparts of GW events would enable extremely exciting advances in what is already a groundbreaking new field, a niche of opportunity for TSPM considering its collecting area, FoV, pointing overhead time and accuracy, and potential spectroscopic capabilities.

**Optical search and follow-up of gravitational waves counterparts:** With the discovery detection of gravitational waves (GW) in black holes and neutron star mergers during the first run (O1) of advanced LIGO, the need to search of electromagnetic counterparts of GW events has materialized. The first two events found, GW150914 and GW151226, consisted of unexpected mergers of binary black hole system of  $36+29$  MSun and  $14+7$ MSun, respectively. These gravitational data provide information about the distance to these now merged black holes (BH), 410Mpc and 440Mpc respectively, with a very poor localization by the two LIGO detectors.



Finding electromagnetic (EM) counterparts of this type of GW sources is of significant relevance in order to fully understand their nature: do these binary BH happen within a host galaxy? What are the properties of these galaxies? Do BH mergers have EM counterparts? Answering these questions requires the ability to make rapid and deep optical and NIR follow-up observations of these events. With the continuous upgrade of LIGO and VIRGO, and the incorporation of new GW detectors in Japan (KAGRA), India (InDIGO) and potentially in the Southern hemisphere, gravitational wave astronomy is poised to open vast new ground. VIRGO is currently in operations together with the LIGO O2 run, forming the second generation network able to provide error boxes of  $< 20 \text{ deg}^2$  for about 40% of hundreds of binary BH events expected to be detected in the next five years. The now planned observatories are to join the current ones within the next years, forming a global network of GW detectors that should be able to find the signals of binary neutron star mergers.

The GW network of the mid 2020s will be the base to search for coincident EM-GW signals, which would allow building independent cosmological distance ladder, and could potentially be used to probe the central engines of supernovae and gamma ray bursts, as well as to study the evolution of massive stars and the formation of compact binary BH systems and neutron stars, to study galaxy-super massive black hole (SMBH) symbiosis and evolution, and even to measure neutron star equation of state. Some merger events producing GW could be explosive and would drive blast waves, relativistic or nonrelativistic, into the surrounding medium and shine as bright radio transients. The light curve evolution of radio supernovae and afterglows from compact object mergers would look alike. Distinguishing the two classes observationally, which could be done at early time by optical spectroscopy, will be of particular importance.

However, even in the 2020s GW events will be poorly localized, with uncertainties of the order of ten square degrees expected to contain a bright and rapidly fading optical counterpart. Telescopes suited to perform extremely wide-field searches of transient events, such as the NGISs, the GROWTH network or the future Zwicky optical transient facility are needed in order to cover the GW error boxes. Nevertheless, these imaging surveys will need telescopes with enough light gathering power and FoV to detect and follow-up GW transient candidates for an adequate time to obtain spectral features and to study the physical properties of the counterparts. The detection of EM (optical) counterparts of GW events would enable extremely exciting advances in what is already a groundbreaking new field, a niche of opportunity for TSPM considering its collecting area, FoV, pointing overhead time and accuracy, and potential spectroscopic capabilities.

LIGO Scientific Collaboration and VIRGO Collaboration:  
Abbot, B.P., et al. 2016, Phys. Rev. Lett. 116, 061102  
Abbott, B.P., et al. 2017, Phys. Rev. Lett. 119, 161101



## 5.3 Cosmology

### 5.3.1 Peculiar velocities of clusters and groups of galaxies inside large scale structures

The biggest coherent structures in the Universe are the superclusters of galaxies. By coherent one means, in such a context, that these large scale structures are expected to be gravitationally bound, hosting some virialized structures (like some galaxy cluster cores), but overall in a dynamically young state, perhaps even still expanding with the Hubble flow, albeit at a decelerated rate. This implies that the superclusters of galaxies still preserve the memory of their formation, in such a way that the study of their structure, internal dynamics and composition may give important clues about the evolution of the Large Scale Structure of the Universe. Bulk flows have already been measured for the Local Supercluster surroundings (e.g. Dressler et al. 1987; Hudson 1993; Lavaux et al. 2010; Pomaredé et al. 2013, Tully et al. 2013), which made possible to measure, for example, our motion towards the “Great Attractor” (e.g. Lynden-Bell et al. 1988), and also streaming motions of individual groups and clusters (e.g. Bernardi et al. 2002; Hudson et al. 2004; Springob et al. 2007; Mutabazi et al. 2014). On the other hand, very few Abell clusters, which are members of superclusters in the Local Universe, have distance estimates for a number of individual galaxies. In this project we intend to study the internal dynamics and evolution of nearby ( $z \leq 0.05$ ) superclusters of galaxies by measuring peculiar radial velocities for the clusters, substructures and groups of galaxies they host. In order to obtain peculiar motion of these systems we need first to measure directly the distance for a certain number of individual member galaxies, by using methods such as the Tully-Fisher and Fundamental Plane relations. With these distances we can estimate the mean Hubble flow velocity of their systems and, by combining this information with radial velocity data we can calculate their peculiar motion.

The steps for this challenging work are:

1. identify the clusters and groups of galaxies that compose the superclusters of galaxies;
2. study the internal structure and galaxy membership for each cluster, substructure and group of the sample;
3. check the literature for existing data for such member galaxies (direct distance measurements, spectroscopically measured radial velocities, photometric data on luminosities, diameters, etc., and spectroscopic data on central stellar velocity dispersions or maximum rotation velocities);
4. select unobserved member galaxies, in a number enough for completing the individual cluster/groups subsamples in order to measure their peculiar velocities to an acceptable level of uncertainties;
5. obtain the complementary photometric and spectroscopic data for these unobserved member galaxies;
6. calculate the peculiar radial velocity for each system (cluster, substructure and group);



7. study the internal dynamics of each supercluster of the sample.

The state of art of such endeavor is:

1. We have already selected the superclusters of galaxies and their member clusters and groups (e.g. Chow-Martínez et al. 2014).
2. We have advanced on the study of the internal structure and membership for some of the member clusters and groups (Caretta et al., in preparation).
3. There are already some data available on direct distance measurements for galaxies in the Local Universe (e.g. Springob et al. 2007; Tully et al. 2013; Campbell et al. 2014), and many databases with photometric and spectroscopic data for galaxies that are in our subsamples of cluster/group members.
4. We have already estimated the number of individual member galaxies we need for each system in order to obtain a reliable estimation of its peculiar velocity. We have also selected some target samples that need new photometric and spectroscopic observations.

For achieving an adequate level of photometric quality and signal to noise, deeper enough for covering the subsamples we have selected in a reasonable amount of time, we need a medium-large telescope, like the 6.5m telescope planned for San Pedro Mártir Observatory, and an instrument with both photometry and spectroscopy capability. Optical and/or NIR may be used both for photometry and spectroscopy, the first with the advantage of being already widely used for photometric parameters and line widths, while the second allows, as have been pointed in the last decades, sharper distance relations (taking advantage of the smaller k-corrections and interstellar extinction together with the more direct connection with the stellar component of galaxies). An adequate instrument, for example, is the MMIRS. Usually the targeted galaxies are among the 30 brightest members of each cluster/group, and cover a magnitude range between 9 and 15 in the H band. A 30' FOV is ideal for covering even the brightest galaxies of the sample with enough field for measuring their background. For spectroscopy an intermediate resolution is needed for measuring the line strengths of relatively bright lines.

Bernardi, M., Alonso, et al., 2002, AJ, 123, 2159  
Campbell, L.A., et al., 2014, MNRAS, 443, 1231  
Chow-Martínez, et al., 2014, MNRAS 445, 4073  
Dressler, A., et al., 1987, ApJ, 313L, 37  
Hudson, M.J.; 1993, MNRAS, 265, 72  
Hudson, M.J., et al., 2004, MNRAS, 352, 61  
Lavaux, G., Tully, R.B., Mohayaee, R. Colombi, S.; 2010, ApJ, 709, 483  
Lynden-Bell, D., et al., 1988, ApJ, 326, 19  
Mutabazi, T., et al., 2014, MNRAS, 439, 3666  
Pomaredé, D., Courtois, H., Tully, R.B.; 2013, IAUS, 289, 323  
Springob, C.M., et al., 2007, ApJS, 172, 599



Tully, R. B., et al., 2013, AJ, 146, 86

Tully, R.B., et al., 2014, Nature, 513, 71

### 5.3.2 The evolving Universe of quasars

Several ongoing and planned surveys will provide an unprecedented wealth of distant type-1 quasar samples, boosting the population of known quasars at  $i \approx 21.5 - 22$ , and even reaching down to  $i \approx 26$  (see e.g. reviews in Chapter 8 of D'Onofrio et al.). Do we need to study more quasars and especially faint quasar at high redshift? The answer is a strong yes.

At low redshift, quasar UV, optical and IR rest-frame properties are not simply scattering randomly around an average but can be organized along a sequence that is conceptually analogous to the stellar main sequence in the H-R diagram (the so-called Eigenvector 1 sequence, Boroson & Green 1992; Sulentic, Marziani, & Dultzin-Hacyan 2000; Shen & Ho 2014). The main governing parameters are thought to be luminosity-to-black hole mass ratio ( $L/M$ ) along with black hole mass and viewing angle. Black hole spin and gas metal contents are also playing an important role. Estimating these parameters for each individual quasar requires high S/N and intermediate dispersion spectroscopy (spectral resolution 1000 and continuum  $S/N > 20$ ; i.e., Sulentic et al., 2014).

At high redshift, we expect to find quasar populations with significantly different properties. Even the deepest present-day survey provides a biased view of quasar populations. Fig. 11 shows that a flux limit introduces a strong selection effect on quasar sampling for a fixed absolute magnitude range (left) as well as on a key physical parameter like Eddington ratio (right). Current studies infer a down-sizing in black hole growth, but we actually know very little (if anything) of any small black hole mass population of quasars at high  $z$ .



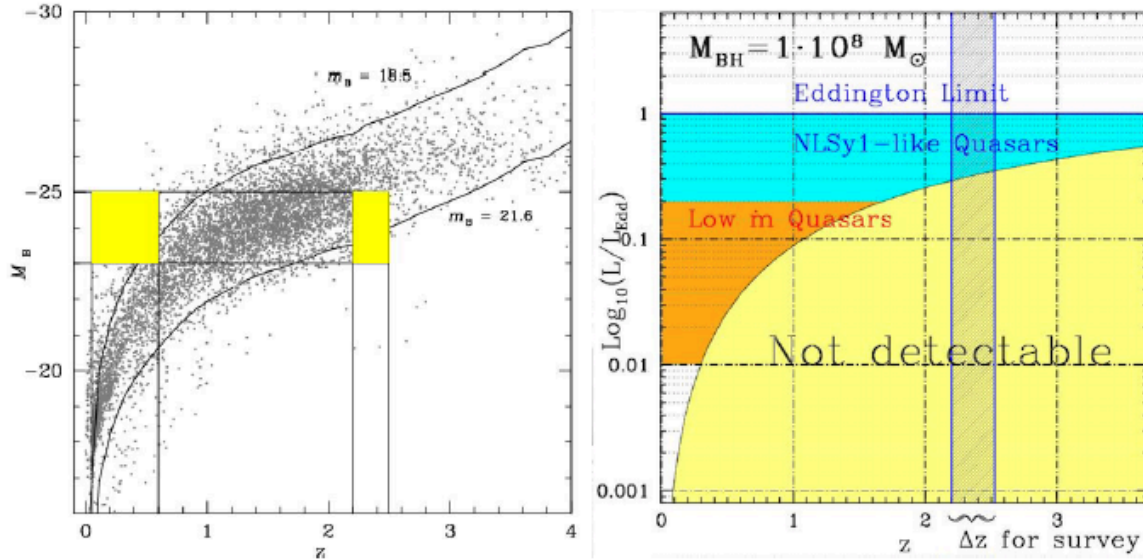


**Figure 12:** Left: Bias in sampling of quasars for a fixed absolute magnitude range, in the local Universe and in a hypothetical pencil beam quasar survey in the  $z$  range 2.2 – 2.5. At low  $z$ , the absolute magnitude range –23 to –25 includes the most luminous quasars. At high  $z$ , in the same absolute magnitude range there is a loss of sources at the faint end due to the magnitude limit at 21.6: fainter quasars are not yet discovered. Right: Eddington ratio as a function of redshift, with the area of undetectable sources below a limiting magnitude  $m_B$  21.5 colored yellow. The redshift range of an hypothetical pencil beam quasar survey is identified by a dashed strip. From Sulentic et al. 2014.

The ongoing optical and IR surveys will provide the identification of quasars that will still need intermediate resolution high S/N spectra for a quantitative empirical parameterization, a proper contextualization within the Eigenvector 1 sequence as well as within a physical parameter space that includes  $M$ , Eddington ratio, orientation metallicity, etc. The availability of a large aperture telescope of the 6 m class is vital to this endeavor. If performing like GTC OSIRIS, Binospec will allow high S/N observations ( $\geq 20$ ) in the rest frame UV of quasars in the redshift range  $1.5 < z < 4$ . Considering an expected quasar surface density at  $g < 22$ , 50 – 100 quasars per square degree, some multiplexing advantage will be offered by the field-of-view  $\approx 0.03$  square degrees (i.e., up to 3 quasars per fields could be simultaneously observed). A great wealth of physical information can be extracted from the  $H\beta$  spectral range: source placement in the Eigenvector 1 sequence, reliable estimates of BH mass from the  $H\beta$  line profile,  $L/M$  (Eddington) ratio). The IR spectrometer MMIRS will allow to cover  $H\beta$  up to K band i.e., up to redshift 3.8.

High S/N observations of faint quasars are instrumental to unbiased studies of black hole mass and accretion rate evolution, as well as gas chemical enrichment history in the host galaxies. Understanding quasar evolution is also a necessary step to build a satisfactory scenario of structure evolution in the Universe. Quasar mass outflows and radiation forces (whose prominence is a function



of the quasar location in the Eigenvector 1 sequence) are expected to produce a strong effect on the host gas content, star formation rates as well as on its structure and dynamics (e.g. Fabian 2012).

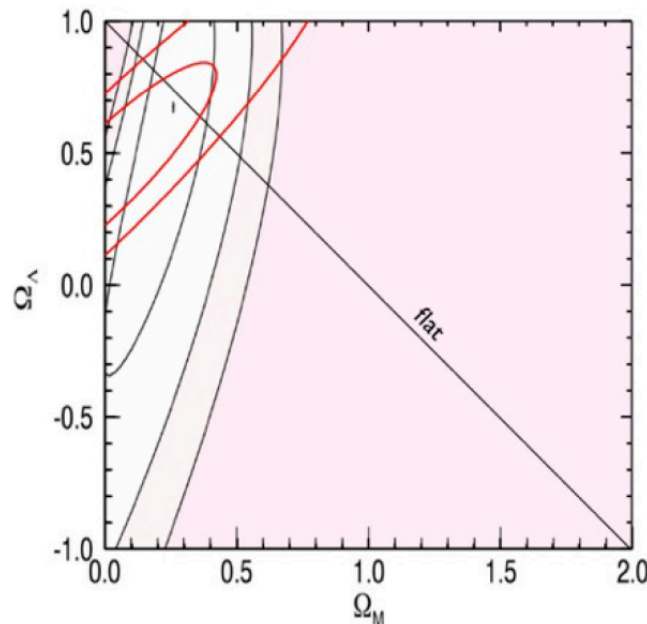


**Figure 13:** Constraints set by the supernova photometric survey described by Campbell *et al.* 2013, *ApJ*, 763, 88 (black filled lines show confidence intervals are at 1 and 2 $\sigma$ ) and by a mock sample (red; 1, 2, 3  $\sigma$ ). Only statistical errors are included in both cases.

**Quasars for cosmology.** Quasars radiating close to the Eddington limit (hereafter referred to also as extreme quasars) show distinguishing spectral properties that can be recognized in major surveys. Our research group developed a particular approach based on the Eigenvector 1 of quasars that enabled us to identify and isolate extreme accretors with Eddington ratio (proportional to the luminosity-to-mass ratio) close to 1 once an optical or UV rest-frame spectrum is available (Marziani & Sulentic 2014). If the Eddington ratio is known, it is then possible to derive distance-independent luminosities by computing the black hole mass. Extreme quasars with  $z < 3 - 4$  might be used as “Eddington ratio standard candles”. This possibility gave rise to a fledgling but booming field of research: several major papers in the past 2 years stressed the possibility of using extreme quasars as distance indicators (among them, Wang *et al.* 2013; La Franca *et al.* 2014).

Extreme quasars offer the non-negligible advantage that they can be found in large numbers. Their redshift distribution can be made statistically unbiased up to  $z \sim 3 - 4$ , where the most reliable distance indicators are not available and the effects of the energy density of matter is dominant. The assessment of systematic effects will lead to a fully independent measure of  $\Omega_M$ , will permit to significantly



constrain  $\Omega_\Lambda$ , and will offer the possibility of studying the cosmic evolution of the equation of state of dark energy. Expected constraints on  $\Omega_M$  from a sample of 400 quasars, compared to a recent supernova survey, are shown in Figure 12. Much larger samples ( $\geq 1000$  sources) can be pre-selected from low signal to noise spectra.

Dedicated observations in the optical and NIR with a large aperture telescope are needed to define the spectral energy distributions and emission line properties of highly accreting quasars, and to measure virial line widths to derive black hole masses. Extreme quasars occupy a very well defined place in the so-called quasar Eigenvector 1 sequence (Marziani & Sulentic 2014), but intrinsic dispersion in physical properties of these sources and eventual trends with redshift and luminosity have to be precisely known if these source are to be used as distance indicators. Binospec and MMIRS would provide suitable measurements for highly accreting quasars up to  $z \sim 4$ .

Current issues go beyond the existence of the dark energy and focus more on its properties. The simplest model for dark energy is a cosmological constant with a fixed equation of state ( $p = w\rho$ , with fixed  $w = -1$ ). However, the dark energy density may depend weakly upon time, according to many proposed models of its nature (Carroll, S. 2005): a general scalar field predicts  $w$  to be negative and evolving with redshift. The ability to build the Hubble diagram uniformly covering a broad  $z$  range makes highly accreting quasars suitable probes for testing whether the dark energy equation of state is constant or is evolving as a function of redshift (following e.g., Piedipalumbo, E., et al. 2014; Capozziello S., et al. 2011).

- Boroson & Green 1992, ApJS 80, 109  
Capozziello S., et al. 2011, Phys.Rev. D84 124061  
Carroll, S. 2005, ASP CS, 339, 4  
D’Onofrio, Marziani, Sulentic, 50 years of quasars, Berlin:Springer  
Fabian 2012, ARA&Ap 50, 455  
La Franca et al. 2014, ApJ, 787, L12  
Marziani & Sulentic 2014, MNRAS 442, 1211  
Piedipalumbo, E., et al. 2014, MNRAS, 441, 3643  
Shen & Ho 2014, Nat 513, 210  
Sulentic, Marziani, & Dultzin-Hacyan 2000, ARevA&Ap, 80, 521  
Sulentic et al., 2014, A&Ap, 570, A96  
Wang et al. 2013, PhRev Lett., 110, 1301

### 5.3.3 The formation and evolution of cD galaxies

This is a project that will take advantage of the sensitivity of the TSPM 6.5m telescope to faint haloes of giant galaxies to investigate mechanisms of formation and evolution of these galaxies and compare with current ideas of galaxy formation and evolution, usually involving the hierarchical assembly of



structures (e.g. Ascaso et al. 2014, Cooper et al. 2014) cD galaxies are supergiant elliptical galaxies found usually in the centres of rich clusters. They have an extended halo-like component (envelope) and an underlying de Vaucouleurs-Sérsic elliptical galaxy-like component. The envelope can reach radial distances of  $< 500$  kpc (Oemler 1976, Schombert 1988). There have been many theories to explain the formation of these envelopes. These include tidal stripping (Gallagher & Ostriker 1972), where material is stripped from neighboring galaxies in the cluster, falling into the gravitational potential of the cD; mergers, where the envelope is built up hierarchically by successive major and minor mergers with cluster galaxies; primordial origin (Merritt 1984), where the envelope is formed simultaneously with the rest of the elliptical galaxy (which appears to be related to recent theories of *downsizing* (Neistein et al. 2006) and early formation of the largest galaxies); and cooling flows (Fabian et al. 1982), clusters with X-ray emission from hot gas frequently have a minimum in temperature in the centre which can be interpreted as a flow of cooling gas towards the central regions, and if the gas cools sufficiently it could form stars, and hence form the envelope populations.

The colours of the stars in the envelopes will be affected by their process of formation and subsequent evolution. We carried out a programme of deep surface photometry on a sample of 10 cD envelopes using the 2.1m and 1.5m telescopes at San Pedro Mártir, Baja California, Mexico, obtaining 30-90 min total exposure per filter. For the majority of the galaxies we obtained very flat colour profiles within the errors, varying by no more than  $\pm 0.1$  mag in  $B - V$  (Kemp et al. 2009). The flat profiles imply similar stellar populations in the underlying galaxy and the envelope, maybe formed at the same time. This could favour the primordial origin or downsizing hypothesis, and implies that any subsequent evolution that the galaxy experiences does not usually dominate its global colours.

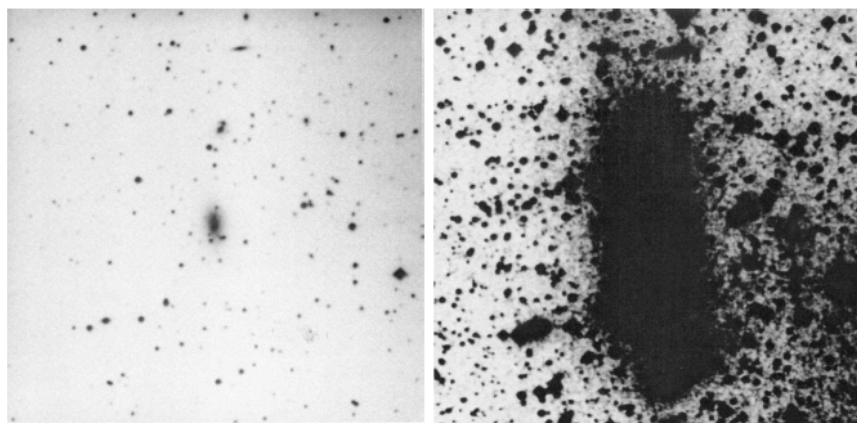


**Figure 14:** The cD in Abell 3571 at low and high contrast (12 x 12 arcmin field)

Variations in age and metallicity of the stellar populations with position could produce similar colours. We have carried out a programme of medium-resolution spectroscopy of cDs at the 2.1m in



San Pedro Mártir to obtain age and metallicity of stellar populations of our cD sample. We obtained spectra of the central regions of each galaxy and various radial positions along the slit up to re (Pérez-Hernández 2014), but with an adequate S/N only until the interface between the underlying elliptical and envelope. In general galaxies with flat red colour profiles have old populations of near-solar metallicity though there are exceptions (A2589 has young populations 2–6 Gyr in all positions with metallicity of 0.3– 0.4, in spite of also having a flat, red, colour profile) while A2199 has younger ages at larger radii corresponding to the observed bluer colours, but slightly sub-solar metallicities.

In general the spectroscopy seems to confirm photometric results, but not always, and it is necessary to obtain a good spectral S/N in the region of the envelope to properly investigate the stellar populations there. A larger sample is also necessary to explore the different types of objects classed as cDs and their differing evolutionary histories. The new 6.5m telescope TSPM and the first generation instrumentation will be ideal to carry out such a project as the good S/N needed in the faint halo regions for both imaging and spectroscopy will be obtainable in a reasonable exposure time. Going by previous experience with 2m telescopes we will ask for 5–10 min total exposures in gri filters and 30 min total in u using Megacam, and carry out spectroscopy with Binospec ( $R = 1000$ ) with up to  $\sim 3$  hour total exposures for positions in the faintest parts of the envelope, lesser exposures for more central positions. The observed colours and Lick spectral indices will be used with several stellar evolution codes to obtain the stellar populations in each position in the galaxy.

We have also carried out analysis in 2 dimensions of galaxy profiles using GALFIT to fit components to the underlying galaxy and envelopes. The main result so far is that the extended halo component frequently has a Sérsic index of close to 1, i.e. an exponential fall off with radius, similar to the results of Donzelli et al. (2011). We will extend this project considerably with the new imaging data from Megacam. The shape and Sérsic index of the halo component will influence the modeling of the formation and subsequent evolution of this component.

Ascaso, B.; et al., 2014, MNRAS, 442, 589

Cooper, A., et al., 2015, MNRAS, 451, 2703

Donzelli, C. J.; Muriel, H. & Madrid, J. P. ApJS, 195, 15

Fabian, A. C., Nulsen, P.E.J., & Canizares, C.R. 1982, MNRAS, 201, 933

Gallagher, J.S., & Ostriker, J.P. 1972, AJ, 77, 288

Kemp, S.N., Guzmán Jiménez, V., Ramírez Beraud, P., et al. 2009, *New Quests in Stellar Astrophysics II: Ultraviolet Properties of Evolved Stellar Populations*, Springer, 91

Merritt, D. 1984, ApJ, 276, 26

Neistein, E., van den Bosch, F.C. & Dekel, A. MNRAS, 372, 933

Oemler, A. Jr. 1976, ApJ, 209, 693

Pérez-Hernández, E. 2014, *Espectroscopía de Halos de Galaxias tipo cD's*, Undergraduate thesis, University of Guadalajara

Schombert, J.M. 1988, ApJ, 328, 475





#### **5.3.4 The Butcher-Oemler Effect: Quenching vs. Ignition: A Scientific Case for TSPM and MMT**

The Butcher-Oemler effect (e.g., Butcher & Oemler 1978, 1985) has been debated for a long time (e.g., Pimbblet 2003). There are remaining issues awaiting to be explained in order to understand the gradual increment with redshift of blue galaxies in the core of rich clusters of galaxies. It is still unclear, if cluster galaxies at high redshifts are bluer because of the detonation of starburst (ignition) or the shutting-off of stellar formation (quenching).

The galaxies shutoff of star formation is one of the most important features in the understanding the galaxy evolution. There is no universal mechanism that explains quenching (Tal et al. 2014; Slater & Bell 2014); rather, exists multiple theories that can explain the observed quenching (e.g., Lin & Faber 1983; Dekel & Silk 1986; Efstathiou 1992; Birnboim & Dekel 2003; Di Matteo et al. 2005). However, it has been suggested that environmental and local properties can stimulate an specified quenching mechanism (Tal et al. 2014). For example, for low mass galaxies, process like ram-pressure, strangulation, and harassment (environmental conditions) can be used to explain the shutoff of star formation by driving cold gas away (e.g., Gunn & Gott 1972; Larson et al. 1980; Farouki & Shapiro 1981; Tal et al. 2014). Also, local galaxy properties can activate the quenching by heating up the galaxy gas (Guo 2014; Tal et al. 2014). These process can be originated by AGN feedback (e.g., Kauffmann et al. 2004; Bower et al. 2006; Guo 2014), strong virial shocks in halos (the halo quenching model, Birnboim & Dekel 2003; Dekel & Birnboim 2006), quasar activity (that will generate outflows that deplete the gas content in galaxies, Sanders et al. 1988; Di Matteo et al. 2005), cosmological starvation (in massive galaxies, e.g., Feldmann & Mayer 2015), or stellar feedback. Whatever process domains, it is directly dependent with the galaxy mass (Woo et al. 2013).

In addition, cluster galaxies can be divided in two categories, satellite galaxies and central galaxies. The central galaxies are the most massive galaxies of a clustered system, and usually reside in the potential center of their systems. Satellite galaxies are the remaining galaxies that surround central galaxies, typically with eccentric orbits (van den Bosch et al. 1999). According with the sub-halo mass function, masses of satellite galaxies are much lower than central galaxies (Giocoli et al. 2008; Boylan-Kolchin et al. 2010). Therefore, the quenching in satellite galaxies is more susceptible to be activated from environmental conditions ("environmental quenching", e.g., Peng et al. 2010, 2012; Woo et al. 2013; Tal et al. 2014). In contrasts, the quenching efficiency for central galaxies is given by local factors that directly depend on their masses ("mass quenching", e.g., Birnboim & Dekel 2003; Peng et al. 2010; Woo et al. 2013; Guo 2014; Feldmann & Mayer 2015). In fact, it is observationally known that central galaxies suffer a star formation quenching when their halo masses reach a specific mass cut (Brammer et al. 2011; Tal et al. 2014). In addition, observations of Local Group dwarf galaxies and satellite galaxies have demonstrated that there is a mass dependence with



their quenching efficiency, where galaxies with lower masses present a higher quenching fraction (Wetzell et al. 2013; Slater & Bell 2014).

Therefore, the star formation efficiency in quiescent galaxies also directly depends on their total dark halo masses (e.g., Peng et al. 2010; Woo et al. 2013; Feldmann & Mayer 2015). This is clearly seen in the relative stellar mass versus halo mass relationship (SMHR), that has a star formation efficiency peak around  $10^{11}$  Msun (e.g., Yang et al. 2012; Leauthaud et al. 2012; Behroozi et al. 2013; Woo et al. 2013; Tal et al. 2014). This relationship represents the transition function between the theoretical halo mass function and the observed stellar mass function (e.g., Vale & Ostriker 2006; Rodríguez-Puebla et al. 2012; Yang et al. 2012). This connection was proved by the application of abundance matching techniques (AMTs, Vale & Ostriker 2006) that relate theoretical halo masses with observed galaxy luminosities or masses. This technique consists to match the observed galaxy abundances, with the expected abundances from a cumulative theoretical halo mass function. In addition, since dark halos of satellite galaxies suffer tidal disruptions more severely than massive galaxies due to their low gravitational potentials; then, it is expected that the mass profiles of their stellar bodies suffer the same tidal stripping as their host dark matter halo profiles (Arnaboldi 2014). On the other hand, quenched central galaxies continue growth their masses via mergers. Therefore, it is expected that the dark matter halo profiles of central galaxies differ from their stellar mass profiles. Hence, dynamical evolution of cluster galaxies and their interaction among their galaxy companions creates a dependence with the truncation of their mass profiles.

The study of the evolution of the quenching efficiency along a big mass range (from dwarfs satellite to big central galaxies) will characterize the evolution of the SMHR. This characterization not only retrieves important constraints to some cosmological models (since it fixes the actual halo mass function), but also indicates the evolution of the stellar mass function, and retrieves the co-evolution of the host dark matter halo profiles with their inner stellar bodies.

Hence, we want to characterize the SMHR and its evolution by studying the star formation process in quiescent galaxies in high-density environments. To achieve this aim, we propose to observe a sample of about 30 rich clusters of galaxies, selected from optical (e.g., Gilbank et al. 2011) and by the Sunyaev-Zeldovich effect (SZE) signal (Planck Collaboration et al. 2014). The selected clusters should be in the range  $0.3 \leq z \leq 0.7$ . Cluster galaxies should be sampled down to  $M^* + 2$  mag, within the first turn-around radius (e.g., Tully 2015; Ibarra-Medel 2015). TSPM+Megacam in two bands for object selection, and weak lensing analysis, follow-up observations with TSPM+BINOSPEC will allow us to determine cluster membership and to measure galaxy properties. We are interested in galaxy masses, chemical evolution, and star formation rates. The scientific drivers of the proposed observations are as follows:

- To characterize the evolution of the dark matter halos from low mass to massive galaxies in clusters or groups by using observations and simulations.





- To estimate from a direct or indirect observation the baryonic and dark matter content of clustered galaxies.
- To perform a detailed study of the stellar populations in cluster galaxies and follow their star formation histories (SFH) and trace its dependence with radius.
- To study the quenching evolution and its dependence with their host galaxy halo mass using cosmological hydrodynamic simulations such as the Eris and Illustris simulation (Guedes et al. 2011; Vogelsberger et al. 2014b).

Data from this project will allow us to perform a detailed study of the matter content and their quenching in cluster galaxies by using high-performance techniques such as gravitational lensing techniques, scaling laws (SLs), caustic techniques (phase space diagrams, e.g., Kaiser 1987; Rego & Geller 1989; Diaferio & Geller 1997), and stellar population synthesis. Therefore we can explore the kinematic, stellar and dark matter mass profiles of cluster galaxies in addition of their star formation activities from observational and simulated data.

**Selection of Cluster Galaxies.** To distinguish from field galaxies, whatever the data is from a simulation or observation, I will use spectroscopic data (or projected LOS galaxy velocity data) to perform multiple membership selection criteria, such as the  $3\sigma$  algorithm (Yahil & Vidal 1977), rendering techniques (by over density selection, Ibarra-Medel et al. 2014), and caustic selection (see §3.2, below, and Serra et al. 2011; Alpaslan et al. 2012). The selection criterion based in the  $3\sigma$  algorithm is an iterative selection process that retrieves a robust membership indicator. For each iteration, this approach estimates the average velocity and the velocity standard deviation for a galaxy sample. Hence, it is possible to define two velocity limits and selects all galaxies that lie within it. Therefore, once each iteration retakes, this procedure selects a new galaxy sub-sample. This process finishes when the velocity limits are the same as the immediate predecessor sub-sample. When the system converges, the background contribution must be zero.

The iterative and convergence nature of this scheme provides robustness to the membership selection criterion. This process pretends to select galaxies that are gravitationally bounded to the cluster. Also, We have developed a cluster membership technique to look for galaxy numerical over densities. In this cluster galaxy membership criterion, the algorithm selects the three-dimensional numerical over density region that encloses a virialized region. Therefore, galaxies within this region represent the members of a self-gravitational structure. This method can be employed to provide a selection criterion for observed galaxies from large spectroscopic surveys and/or simulated galaxies from cosmological simulations. The method looks for these over densities using an adaptive method based on the Delaunay Tessellation Field Estimator (DTFE, Schaap & van de Weygaert 2000). The DTFE creates a continuous density field using a Delaunay tessellation, this tessellation uses all galaxy positions as their vertexes (e.g., Schaap 2007). Then, the sum over all tetrahedral volumes that are adjacent to a galaxy position is equivalent to the volume of the representative Voronoi cell of this galaxy (Platen et al. 2011). Hence, the inverse of the volume of the representative Voronoi cell times



4 (the number of spatial dimensions plus one) returns the numerical density estimator at this galaxy position. This tool maps the three-dimensional shape of a cluster and its substructures without any other assumption than the selection of a density threshold. By using halo occupation distribution (HOD) models, the method selects a threshold that maps virialized structures. Therefore, galaxies selected within these three dimensional numerical density contours represent members of gravitationally bounded structures.

**Analysis of Caustics.** We also plan to use caustic techniques; these techniques can trace the dark matter component without assuming a virial equilibrium. The caustics represent the maximum velocity along the line-of-sight (LOS) that a galaxy (or star) can reach without escaping from a gravitationally bounded system (galaxy cluster or stellar system). Therefore, the relation between the escape velocity and the caustics describes directly the potential profile of the system and therefore their total mass (Diaferio 1999). The caustic technique was employed by Serra et al. (2010) to compute the line-of-sight velocity dispersion profile for four dwarf spheroidal galaxies. Hence, with the use of SLs, lensing and caustic techniques, it is possible to constrain and/or recover a detailed profile of the dark matter content in galaxies and galaxy groups. See Figure 13, where we show the application of the technique that we have developed to identified substructures, and determine masses through caustic analysis.

**Weak Gravitational Lensing.** The high quality data from TSPM+Megacam will allow us to measure the deformation of background galaxies to estimate the cluster's dark matter distribution using the gravitational lensing technique. This technique uses the lens effect that is produced by massive objects, when their gravity bends the light path of foreground objects (Einstein 1936). Therefore, it is possible to model the amount of unseen dark matter that is needed to reproduce the observed shear (for weak lensing) or bend (for strong lensing) on the shape of background galaxies. Hence, with the use of software that implements parametric methods and Bayesian statistics such as LENSTOOL (Kneib et al. 2011). With this study, we will be able to reconstruct the dark halos profiles using strong and weak lensing techniques. In addition, we can use SLs to trace the dynamical mass within galaxies. These SLs assume that the galactic internal dynamics ( $\sigma$  or  $V$ ), in association with the galactic scale ( $R$ ), traces the dynamical galaxy mass ( $M_d$ ). Since the Mass-to-Light ratio ( $M/L$ ) connects the light with its mass, the light of a galaxy also correlates with  $\sigma$  and/or  $R$ . For example, Faber & Jackson (1976) proposed a SL involving the luminosity and velocity dispersion in early-type galaxies. Furthermore, Tully & Fisher (1977) found the corresponding SL for spiral galaxies that relates the maximum rotational velocity of the disk with the luminosity of a galaxy. The Tully-Fisher and Faber-Jackson relationship was previously used by Geha et al. (2006) to estimate the mass content of extremely low-mass dwarf galaxies. On the other hand, SLs depends that galaxies being in a virial equilibrium (without any external gravitational perturbation) to be valid.

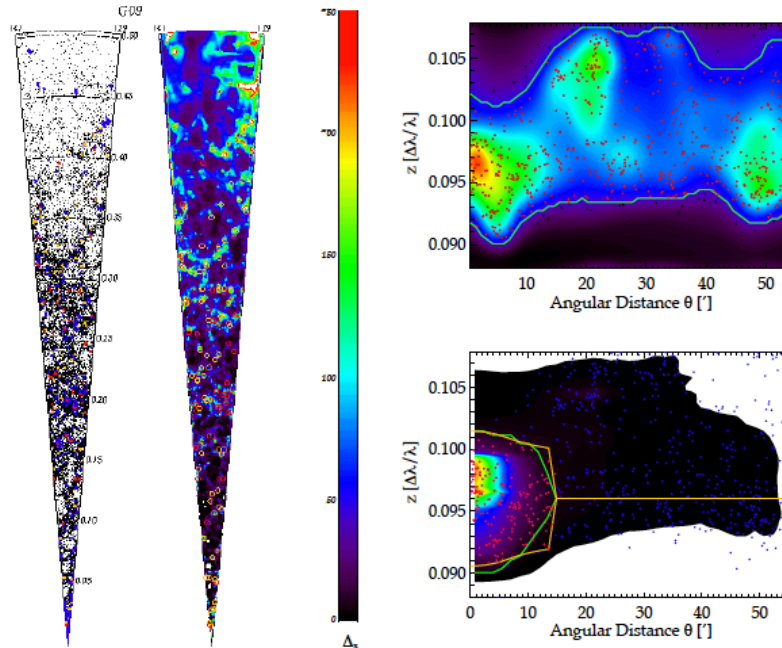


**Figure 15:** Right: This figure depicts examples of the techniques that we have developed to study the galaxy distribution of GAMA fields G09 with its continuous overdensity field in cone plot diagrams (redshift vs. right ascension). A similar analysis can be performed in the proposed observations with TSPM+Megacam and follow-up observations with TSPM+BINOSPEC. The right panel shows color-coded overdensities according to the galaxy number overdensity value. In the cone plots, the yellow points and circles are the selected clusters using a sigma-clipping algorithm. The red points and circles are the clusters whose multiplicities are greater than 10. For the discrete galaxy distribution cone plots, the blue points are all the overdensity detections. Top-Left: Example of the application of the caustic method with substructures. Bottom-Left: The same case once we clean the substructure contribution. The colors represent the continuous galaxy number density normalized at the maximum density of the region. The blue points represent the galaxies on the redshift space and the red points are the galaxies located within the caustic curves. The yellow line is the final location of the caustic amplitude.

**Stellar populations.** Spectra obtained with BINOSPEC will have enough resolution to study of stellar populations, stellar mass content, and quenched fraction in clustered galaxies, and AGN fraction. To achieve this aim, we plan to use the spectral stellar libraries of Bruzual & Charlot (2003) to perform a spectral energy distribution (SED) fit from observed galaxies. These libraries use a Salpeter stellar initial mass function (IMF), and return the values of single stellar populations for six metallicity values and 127 ages. Consequently, we will use stellar population synthesis codes (such as the STARLIGHT code, Cid Fernandes et al. 2005) that use photometric magnitudes or spectral data to reconstruct the galaxy SED. In addition, galaxy spectra demand the use of aperture corrections, since fibers cover a physical and fixed size, generating a possible bias. On the other hand, it is possible to avoid this bias by using photometric magnitudes that contain the 90% of the total galaxy flux to reconstruct the galaxy SED.



**Confrontation of models with observations.** Finally, we plan to use cosmological hydrodynamical simulations to study the quenching activation in central and satellite galaxies for low to high redshift. In the past year, the state of the art in cosmological simulations presents an alternative to studying the evolution of the dark matter in conjunction with their visible matter (e.g. the Illustris simulation, Vogelsberger et al. 2014a,b). Therefore, these type of simulations provide the perfect tool to explore the co-dependency between dark matter halos and their stellar mass contents. These type of studies return valuable information that complements the observational data of quenching galaxies. Also, these simulations provides information to understand the process of the observed quenching lag in satellite galaxies (Feldmann & Mayer 2015), the effects to take (or not to take) into account AGN feedback, SMBHs, ram-pressure or other process that can suppress the star formation in quiescent galaxies.

**Perspective.** Galaxy evolution and its relation with the environment is a key issue in cosmology. TSMP and its host instrumentation will allow us to tackle galaxy evolution in rich clusters of galaxies at intermediate redshifts with unprecedented detailed. This observations may help to settle the quenching or ignition controversy, and as a corollary, the BOE.

- Alpaslan, M., Robotham, A. S. G., Driver, S., et al. 2012, MNRAS, 3012  
Arnaboldi, M. 2014, Astronomical Society of the Pacific Conference Series, 486, 16  
Behroozi, P. S., Wechsler, R. H., & Conroy, C. 2013, ApJ, 770, 5  
Birnboim, Y., & Dekel, A. 2003, MNRAS, 345, 349  
Bower, R. G., Benson, A. J., Malbon, R., et al. 2006, MNRAS, 370, 645  
Boylan-Kolchin, M., Springel, V., White, S. D. M., & Jenkins, A. 2010, MNRAS, 406, 896  
Brammer, G. B., Whitaker, K. E., van Dokkum, P. G., et al. 2011, ApJ, 739, 24  
Bruzual, G., & Charlot, S. 2003, MNRAS, 344, 1000  
Butcher, H., & Oemler, A., Jr. 1978, ApJ, 226, 559  
Butcher, H. R., & Oemler, A., Jr. 1985, ApJS, 57, 665  
Cid Fernandes, R., Mateus, A., Sodre, L., Stasinska, G., & Gomes, J. M. 2005, MNRAS, 358, 363  
Dekel, A., & Birnboim, Y. 2006, MNRAS, 368, 2  
Dekel, A., & Silk, J. 1986, ApJ, 303, 39  
Delaunay, 1934, B. Bull. Acad. Sci. URSS, VI, Classe Sci. Mat. pp 793-800  
Diaferio, A., & Geller, M. J. 1997, ApJ, 481, 633  
Diaferio, A. 1999, MNRAS, 309, 610  
Di Matteo, T., Springel, V., & Hernquist, L. 2005, Nature, 433, 604  
Driver, S. P., Hill, D. T., Kelvin, L. S., et al. 2011, MNRAS, 413, 971  
Efstathiou, G. 1992, MNRAS, 256, 43P  
Einstein, A. 1936, Science, 84, 506  
Faber, S. M., & Jackson, R. E. 1976, ApJ, 204, 668  
Farouki, R., & Shapiro, S. L. 1981, ApJ, 243, 32  
Feldmann, R., & Mayer, L. 2015, MNRAS, 446, 1939  
Geha, M., Blanton, M. R., Masjedi, M., & West, A. A. 2006, ApJ, 653, 240  
Gilbank, D. G., Gladders, M. D., Yee, H. K. C., & Hsieh, B. C. 2011, AJ, 141, 94



- Giocoli, C., Tormen, G., & van den Bosch, F. C. 2008, MNRAS, 386, 2135  
Guedes, J., Callegari, S., Madau, P., & Mayer, L. 2011, ApJ, 742, 76  
Guo, F. 2014, ApJ, 797, LL34  
Gunn, J. E., & Gott, J. R., III 1972, ApJ, 176, 1  
Ibarra-Medel, H. J., Lara-López, M., López-Cruz, O. & the GAMA team. 2014, arXiv:1410.0748  
Ibarra-Medel, H. J. 2015, Ph.D. Thesis, INAOE.  
Kaiser, N. 1987, MNRAS, 227, 1  
Kauffmann, G., White, S. D. M., Heckman, T. M., et al. 2004, MNRAS, 353, 713  
Kneib, J.-P., Bonnet, H., Golse, G., et al. 2011, Astrophysics Source Code Library, 1102.00  
Larson, R. B., Tinsley, B. M., & Caldwell, C. N. 1980, ApJ, 237, 692  
Leauthaud, A., Tinker, J., Bundy, K., et al. 2012, ApJ, 744, 159  
Lin, D. N. C., & Faber, S. M. 1983, ApJ, 266, L21  
Peng, Y.-j., Lilly, S. J., Kovac, K., et al. 2010, ApJ, 721, 19  
Peng, Y.-j., Lilly, S. J., Renzini, A., & Carollo, M. 2012, ApJ, 757, 4  
Pimblet, K. A. 2003, PASA, 20, 294  
Planck Collaboration, Ade, P. A. R., Aghanim, N., et al. 2014, A&A, 571, AA29  
Platen, E., van de Weygaert, R., Jones, B. J. T., Vegter, G., & Calvo, M. A. A. 2011, MNRAS, 416, 2494  
Regos, E., & Geller, M. J. 1989, AJ, 98, 755  
Rodríguez-Puebla, A., Drory, N., & Avila-Reese, V. 2012, ApJ, 756, 2  
Tal, T., Dekel, A., Oesch, P., et al. 2014, ApJ, 789, 164  
Tully, R. B., & Fisher, J. R. 1977, A&A, 54, 661  
Salpeter, E. E. 1955, ApJ, 121, 161  
Sanders, D. B., Soifer, B. T., Elias, J. H., et al. 1988, ApJ, 325, 74  
Schaap, W. E. 2007, Ph.D. Thesis,  
Schaap, W. E., & van de Weygaert, R. 2000, A&A, 363, L29  
Serra, A. L., Diaferio, A., Murante, G., & Borgani, S. 2011, MNRAS, 412, 800  
Serra, A. L., Angus, G. W., & Diaferio, A. 2010, A&A, 524, A16  
Slater, C. T., & Bell, E. F. 2014, ApJ, 792, 141  
Tully, R. B. 2015, AJ, 149, 54  
Vale, A., & Ostriker, J. P. 2006, MNRAS, 371, 1173  
van den Bosch, F. C., Lewis, G. F., Lake, G., & Stadel, J. 1999, ApJ, 515, 50  
Vogelsberger, M., Genel, S., Springel, V., et al. 2014b, MNRAS, 444, 1518  
Vogelsberger, M., Genel, S., Springel, V., et al. 2014a, Nature, 509, 177  
Wetzel, A. R., Tinker, J. L., Conroy, C., & van den Bosch, F. C. 2013, MNRAS, 432, 33  
Woo, J., Dekel, A., et al. 2013, MNRAS, 428, 3306  
Yahil, A., & Vidal, N. V. 1977, ApJ, 214, 347  
Yang, X., Mo, H. J., et al. 2012, ApJ, 752, 41

## 5.4 Future instrumentation

### 5.4.1 Wide-field imaging Fourier transform spectroscopy: a instrumentation proposal for the TSPM

**Rationale.** Many physical processes in astronomy are still hampered by the lack of spatial and spectral resolution, and also restricted to the field-of-view (FoV) of current 2D spectroscopy



instruments available worldwide. It is due to that that many of the ongoing or proposed studies are based on large-scale imaging and/or spectroscopic surveys. Under this philosophy, large aperture telescopes are devoted to the study of intrinsically faint and/or distance objects, covering small FoVs, with high spatial resolution, while smaller telescopes are devoted to wide-field explorations. The future astronomical surveys, however, should be addressed by acquiring un-biases, spatially resolved, high-quality spectroscopic information for a wide FoV. Therefore, we aim to explore a possible instrument for the future 6.5m Telescopio San Pedro Mártir (TSPM), that would provide un-biased wide-field (few arcmin) spectroscopic information, with the flexibility of operating at different spectral resolutions ( $R \sim 1 - 20000$ ), with a spatial resolution limited by the atmosphere (seeing), and thus to be used in a wide range of astronomical problems. This instrument would make use of the Fourier Transform Spectroscopic technique, which has been proved to be feasible in the optical wavelength range (350-1000 nm) with designs such as SITELLE (CFHT). The proposed instrument would be designed for and installed in the future 6.5m TSPM, based on the experience acquired during the development and integration of a similar prototype instrument being currently built at INAOE for the 2.1m telescope at the Observatorio Astrofísico Guillermo Haro (OAGH) in Cananea, Mexico (*OFIUCO: Optical Fourier-transform Imaging Unit for Cananea Observatory*). We describe here the basic technical description of a Fourier transform spectrograph with important modifications from previous astronomical versions, as well as the technical advantages and weakness, and the science cases in which such an instrument can be implemented.

There are basically two traditional approaches to obtaining spectral information on extended astrophysical objects: narrow-band imagery and integral field dispersive spectroscopy. Imagery with filters allows the observer to map a target in selected wavelength ranges and to extract the required physical information by comparing the relative flux of the sources in these bands. Images of the targets in the different band passes must be obtained one after the other with a CCD detector, rejecting each time all photons excluded by the selected filters (up to 99.8%). Moreover, narrow-band imagery does not provide a high enough spectral resolution to determine kinematic information.

Dispersive spectroscopy with slits allows a much finer spectral resolution at the expense of spatial information on the targets. Extensively used since the mid-19th century to obtain the spectrum of individual stars or small slices of extended objects, dispersive spectroscopy has been transformed by the advent of multi-object spectrographs (MOS) in the 1990's: multiple slitlets or optical fibers are positioned at the location of the targets in a wide field of view (FoV), the light of which is then sent to a disperser and recorded on a CCD (e.g. 2dF, Colles et al. 2001). Major breakthroughs have also been obtained in astronomical instrumentation over the last decade by combining imagery and spectroscopy into a single experimental observation technique that produces cubes of data, which is typically referred as 2D spectroscopy.



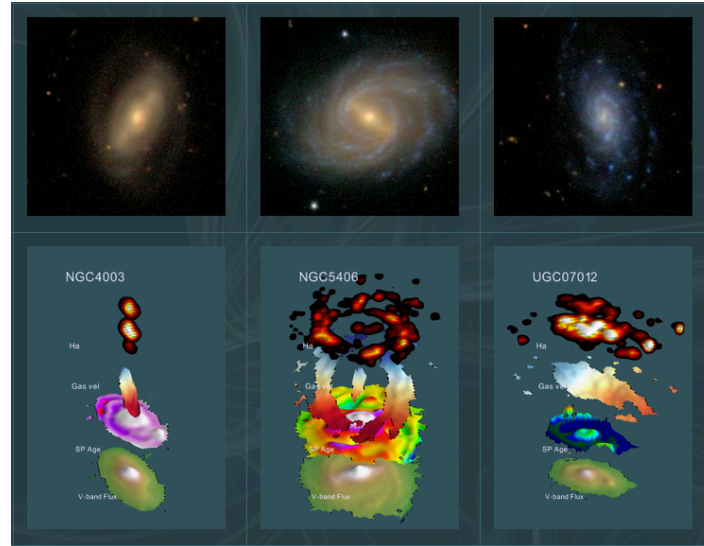


**Figure 16:** Example of galaxies observed as part of the CALIFA survey based on the integral field spectroscopy (IFS) technique. The top-row shows RGB composite images from SDSS. The bottom-row shows observables derived from the IFS datacubes, from bottom to top: V-band flux, stellar populations age map, gas velocity and H $\alpha$  emission maps (figure adapted from Sánchez et al. 2012).

This technique has revolutionized data collection by allowing to obtain spectra of a large number of objects dispersed in a large field using deployable fibres or to spatially sample relatively small (few arcsec) objects using integral field units or IFU (e.g. GMOS, Allington-Smith et al. 2002; SAURON, Bacon et al. 2001; PINGS, Rosales-Ortega et al. 2010; CALIFA, Sánchez et al. 2012). However, the vast majority of imaging spectrometers used on telescope to date are build on dispersive approaches which must sacrifice detector pixels to retrieve the spectral content instead of scene elements. Given the limitations of modern array detectors, different instrument concepts convey different trades that each enhances the possibility of discovery for a given science program category.

Nonetheless, the ongoing and planned 2D spectroscopy surveys in the coming decade are motivated by some of the most compelling questions on stars, Galaxy/galaxy formation, evolution and cosmology. There is an acute need for large-scale surveys in both hemispheres with wide-field, highly-multiplexed spectrographs. Several 2D spectroscopy survey instruments are already in rapid development around the world, and are anticipated to be in use well before the end of this decade. These include complex single and multi-object IFUs for mapping individual galaxies, as well as a new generation single-fiber MOS instruments devised to obtain thousands of integrated galaxy spectra, some even extending into the near IR.



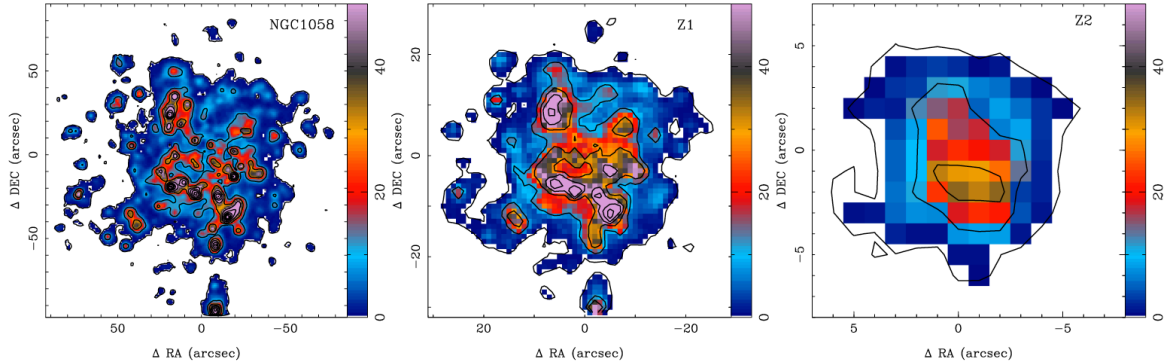


**Figure 17:** Left: IFS Ha image of NGC1058 from the PINGS sample. Middle-Right: simulated IFS observations of NGC1058 at different redshifts, Z1 associated with the CALIFA survey ( $z \sim 0.02$ ) and Z2 with a hypothetical higher redshift survey, e.g. SAMI 1.6"/fibre, or MaNGA 3"/fibre (figure adapted from Mast et al. 2014).

On the other hand, given the worldwide trends in the use of astronomical infrastructure, in the forthcoming decades large aperture telescopes ( $>20\text{m}$ ) will be devoted to the study of intrinsically faint and/or distance objects, covering small FoVs, with high spatial resolution, while smaller telescopes ( $<8\text{m}$ ) will be devoted to wide-field explorations. In this context, one can speculate about the most efficient use of 2-6m class telescopes worldwide (including the TSPM) and their related instruments in 10-15 years, as they would need to necessarily find synergies with the new generation of large telescopes both ground-based and space ones. One possibility might be by conceiving an instrument that, within a reasonable budget, could be capable of acquiring un-biased, spatially resolved, high-quality spectroscopic information for really wide FoVs (10-30 arcmin). Such telescope-instrument binomial would represent a natural complement to the new generation of ground and space telescopes in the next decades, and would set a milestone in the history of observational astronomy. Such binomials would impact in large number of research programs and scientific cases, and will naturally extend to numerous other areas of broad community interest, setting a transformational era that will certainly help to unravel many of the fundamental puzzles of contemporary astrophysics.

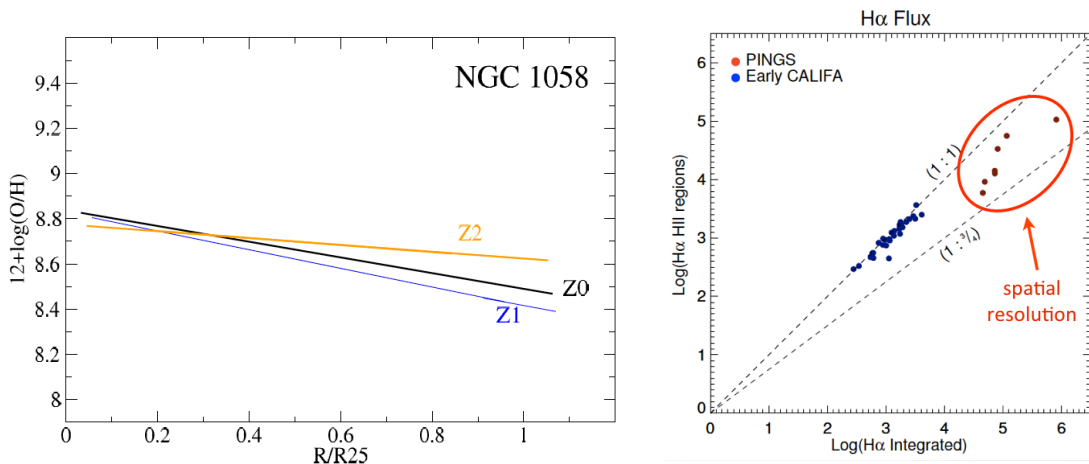




*Figure 18: Left: Linear regressions of the oxygen abundance gradient of NGC1058 for the three redshift regimes, note the wrong gradient derived for Z2 (figure adapted from Mast et al. 2014). Right: Comparison of H $\alpha$  flux obtained from the integrated spectra of a sample of spiral galaxies to the sum of H $\alpha$  flux of individual HII regions, the 1-to-1 correspondence disappears once the IFS observations have enough spatial resolution to discriminate diffuse emission (figure adapted from Castellanos-Durán et al. in prep).*

**Beyond MOS and fibres: wide-FoV, high-spatial resolution spectroscopy.** In the extragalactic context, the CALIFA, SAURON and ATLAS3D (Cappellari et al. 2011) surveys represent the benchmark for current and future 2D spectroscopy surveys on nearby galaxies (see Fig. 16). MaNGA (Drory et al. 2015) and SAMI (Croom et al. 2012) will observe thousands of galaxies using IFS, providing important statistical information (although with a coarse spatial resolution), while MUSE (Bacon et al. 2004) will become the most powerful IFS, seeing-limited instrument in the world. However, many physical processes in astronomy are still hampered by the lack of spatial and spectral resolution. As shown by Mast et al. (2014), there can be an important information loss due to spatial resolution degradation of IFS surveys at different redshifts. It is worth noting that the important figure of merit is the ratio between the spaxel size and the typical scale-length at a certain redshift. The loss of information due to spatial degradation might cause an incorrect interpretation of common observables in the considered framework. The spectroscopic blending of local structures might not result in global trends or averaged values, as shown in Fig. 17 and Fig. 18.

As mentioned before, current 2D instrument/survey concepts convey different trades for a particular science program. The vast majority of spectrometers are based on dispersive approaches that must *sacrifice* detector pixels to retrieve the spectral content instead of scene elements. A revolutionary approach would consist in an instrument capable of simultaneously obtaining spatially resolved spectra on extended areas (few arcmin) with a 100% filling factor, with a spatial resolution limited by the atmosphere (seeing), and a flexible spectral resolution (up to  $R \sim 10^4$ ) over a wide spectral range in a mid-class (4-8m) telescope. Nowadays, the only instrument based on a dispersive approach with such capabilities is (the complex and largely expensive) MUSE-VLT spectrograph (see Fig. 19). Therefore, if one wants to devise wide-FoV, high spatial resolution 2D spectroscopy instruments within a reasonable budget, new technologies have to be sought. The technique known as imaging Fourier transform spectroscopy (IFTS) is very promising on that regard.

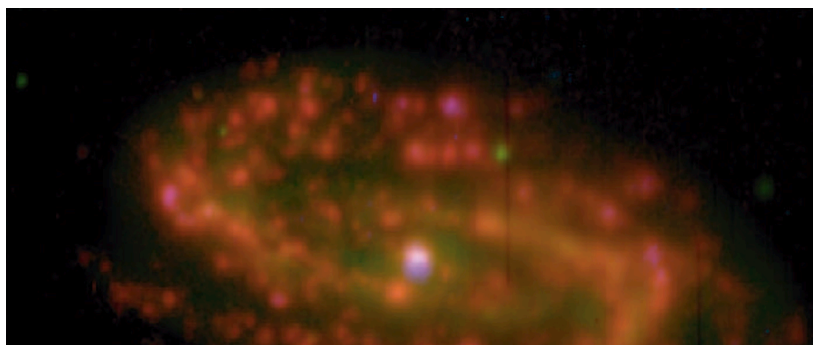




**Figure 19:** True color image created from continuum subtracted narrow-band images of the IFS mosaic of NGC6754, illustrating the power of the combined large FoV and high spatial resolution of MUSE. The mosaic is composed of two  $\sim 1$  arcmin pointings aligned east-west, with an overlapping area of  $\sim 16$  arcmin<sup>2</sup>. Different seeing conditions for the for the East ( $\sim 0.8$ ) and for the West ( $\sim 1.8$ ) pointings are also clear. The final dataset comprises 200k individual spectra. Each red structure corresponds to a single HII region.

**The IFTS concept.** An astronomical imaging Fourier transform spectrometer (IFTS) is basically a Michelson interferometer inserted into the collimated beam of an astronomical camera system. Contrary to conventional integral field dispersive spectrographs, all detector pixels are used for imagery as with the Fabry-Pérot, but instead of acquiring spectral slices one by one (thus rejecting every other wavelength) to cover the entire waveband of interest, an “all in one” approach is used. Likewise, all wavelengths from the field are simultaneously transmitted to either one or both of the interferometer outputs in which the array detectors sit. This configuration results in a large light gathering power since no light is lost except through items common to any optical design: substrate transmission, coatings efficiency, and quantum efficiency of the detectors.

Fig. 20 shows how a Fourier Transform Spectrometer works: the core of the instrument is a classical Michelson interferometer, the incoming beam from the telescope is first split into two equal parts by a beam splitter. Half the light is transmitted through the beam splitter, bounces back on a moving mirror and interferes, in the beam splitter, with the other half-beam that has, in the meantime, been reflected by the beam splitter to a fixed mirror and bounced back. Initially, the optical path travelled by the two beams is the same; we are at the Zero Path Difference (ZPD) position. The two beams are in perfect phase when they combine and the interference is completely constructive: the detector receives the sum of the two beams while none of the light goes back to the source. The moving mirror is then slightly displaced, creating small offset in optical paths between the beams. These are not in phase anymore, the interference is not entirely constructive and the detector receives a bit less light while the difference goes back to the source. Typical displacements vary between 175 nm and a few micrometers, depending on the wavelength range and the desired spectral resolution.

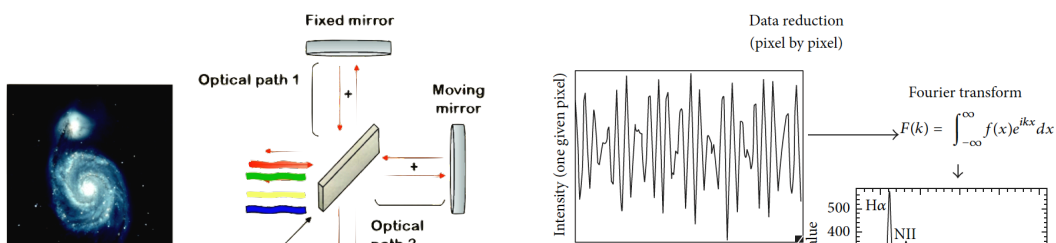




**Figure 20:** Left: The Michelson interferometer consists of a beam splitter used to separate the incoming beam into two equal parts, two mirrors on which the halves of the original beam are reflected back, a moving mechanism to adjust the position and orientation of one of the mirrors, and a metrology system (IR laser and detector) to monitor the mirror alignment. The result of an exposure is a data cube in the 3D space: R.A., Dec, Optical Path Difference (OPD). By scanning the OPD and taking images at every step, one gets a datacube composed of one interferogram for every pixel. Right: For a given pixel, the recorded intensity varies as a function of the OPD. An inverse Fourier transform of the signal produces a spectrum for every pixel in the image. The final result is a data cube in the 3D space: R.A., Dec, wavelength, with one spectrum per pixel of the detector, i.e. thousands of spectra per pointing. (Figures adapted from Drissen+ 2010, 2014).

Eventually, after a sufficiently large mirror displacement, the interference will be totally destructive: no light will be recorded on the detector; the entire beam will go back to the source. In practice, an interferogram is obtained by first moving the mirror to a predetermined position away on one side of the ZPD, moved by equidistant steps to the same position on the other side of the ZPD. The original frequency, or wavelength, of the incoming light beam is thus recovered by calculating the Fourier transform of the time dependent signal recorded by the detector

**IFTS versus dispersive spectrographs.** An IFTS has two advantages over any system feeding a dispersive slit. The first is that, because an IFTS builds up the datacube frame-by-frame, the total number of available datacube elements is an entire CCD times the number of samples. By comparison, on a slit system the area of the slit limits the observed total angular area on the sky. Another way to look at this is that, for image slicers and fiber-fed spectrographs, all three dimensions of the datacube obtained are limited to a single CCD image. The other advantage of an IFTS is that the spectral resolution is flexible; it is not necessary to change gratings to "tune" the observing to the science or the observed object's faintness. The grating efficiency is analogously replaced by the modulation efficiency of the interferometer (see below) that would typically reach values higher than 80% over most of the instrument waveband.

**IFTS versus Fabry-Pérot interferometer.** The IFTS must be distinguished from filter systems including imaging Fabry-Pérot (FP) spectrographs or tunable filters. An IFTS accept all the light at all wavelengths. It only creates one interference between the two branches of a photon and records the phase difference. On the other hand, an FP creates multiple branches by multiple reflections inside a cavity creating constructive interferences only for a narrow band of wavelengths, rejecting most of



the light. Also, the passband is periodic and one order has to be selected, limiting the spectral range to a few angstroms. FP systems are better suited for narrow band observations of faint extended objects as they cut all the out-of-band noise to which IFTS would be sensitive. Moreover, on the spectral coverage, the Fabry-Pérot is considered more as a line profiler than a true spectrometer due to its limited spectral coverage.

**IFTS drawbacks.** The light gathering power of the IFTS is unsurpassed since it can almost be made to match the CCD performance in terms of waveband and FoV. Its optical design is similar to that of most focal reducers for astronomy, after considering the desired, science-driven, pixel sampling and total FOV, as well as field aberration. The design only has to allow a sufficient length of collimated beam space to insert the flat optics interferometer. The control of the chromatic aberration is however of greater challenge when compared to classical astronomical imaging cameras. This is because all wavelengths are imaged and sampled simultaneously as opposed to imaging with filters in which the telescope can be refocused to the central wavelength of the filter used. This can easily become a limiting factor for the spectral coverage of the instrument which otherwise is mostly limited by the beam splitter efficiency band. The interferometer is then designed to prevent vignetting of the selected FoV and acts as a panchromatic modulator for each individual beam associated with every pixel. Calibration of the obtained data cubes is obviously pixel dependent and much care must be taken in this operation.

The greatest disadvantage of the IFTS is the difficulty of observing fluctuating sources. Since an FTS inherently uses time domain multiplexing of the spectral data, with spectral intensity vs. modulation frequency translated into spectral intensity vs. wavenumber, any significant temporal fluctuations in the observed light intensity within the frequency range corresponding to the spectral features of interest represents noise in the derived spectrum. Furthermore, periodic fluctuations produce line shifts of the observed spectral features, with the implication that it is very difficult, for example, to measure AC modulated calibration sources. Under certain circumstances however, this aspect of an IFTS may be used to advantage. For example, it is possible to use the broadening of ordinarily narrow spectral features as a measure of the degree of temporal fluctuation of the source term, and this can be used to distinguish transient or erratic spectral features.

#### ***5.4.1.1 Technical challenges in the construction of an IFTS system***

As any professional optical instrument, an IFTS must include high-quality optics that allows a higher transmittance in the considered working wavelength. The performance of an IFTS is characterized by the modulation efficiency (ME), i.e. the capacity of the interferometer to modulate incident light, defined as:

$$ME = \frac{I(\text{modulated light})}{I(\text{incident light})}$$





The ME can be seen as the analog of diffraction grating efficiency in dispersive spectrographs. The ME depends upon several factors, the most demanding from the technical point of view being:

- The surfaces quality of the optical components of the interferometer (mirrors, beam splitter, etc.) at a given wavelength. The less optical quality, the less ME. One has also to consider the number of reflections within the instrument. It is required a surface optical quality (peak-to-valley) greater than  $\lambda/20$ .
- Alignment of the moving mirror and stability of the OPD during an exposure, which highly depend on the quality of the metrology system, the most important challenge for an IFTS system in the optical range. Any tiny variation in any direction, angle or alignment of the mirrors, would reduce the spatial coherence (interference) between the two recombined beams, effect that is more problematic at shorter (bluer) wavelengths. The system requires monitoring the distance and alignment of the components several thousand times per second, combined with a fast correction by the use of actuators.

An additional factor is the CCD readout time. Given, that an interferogram is acquired through a series of hundreds of short exposures, the required time to read the CCD limits the global efficiency of the instrument, and thus the system requires a fast, low-noise readout CCD ( $\sim 2$ s.) Nonetheless, the IFTS technique has been proved to be feasible in the optical wavelength range (350-1000 nm) with designs such as SpIOMM (Grandmont et al. 2003) and SITELLE (Drissen et al. 2010, currently under commissioning at CFHT), by using appropriate optical configurations, fast readout CCD detectors, and especially improved metrology and control systems.

Main advantages of an IFTS system

- A large FoV with a complete (100%) covering factor.
- Flexible spectral resolution ( $R = 1 - 10^4$ ), easily tuned (optimal for  $R \sim 2000$ ).
- Full optical wavelength coverage.
- Angular resolution limited by seeing.
- No diffuse light.
- Better precision in wavelength calibration (laser metrology system).
- High throughput, superb efficiency.

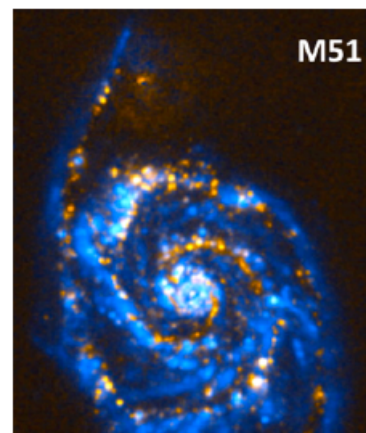
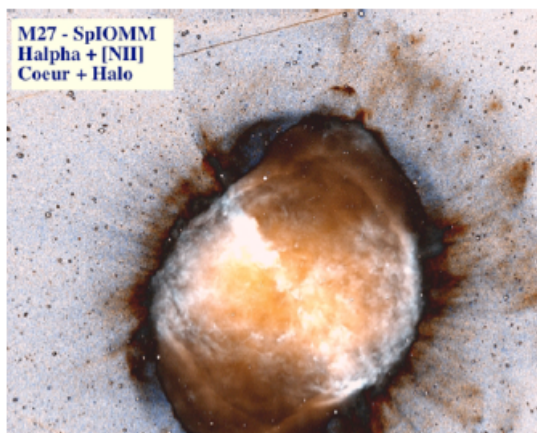




**Figure 21:** Left:  $H\alpha + [NII]$  emission line combined image of the planetary nebula M27 obtained with the IFTS prototype SpOIMM. Right: False colour image of the nearby galaxy M51 showing in blue the  $H\alpha$  emission obtained by the SpOIMM IFTS prototype and in orange the NUV emission from the GALEX space telescope. Figures adapted from Drissen et al. 2008.

An IFTS is most efficient for:

- Low spectral resolution ( $R \sim 100$ ) of very large FoV and/or crowded fields.
- Moderate resolution ( $R \sim 2000$ ) of extended sources.
- High resolution ( $R > 10000$ ) for extended, nearby, bright objects.
- Large number of relatively bright objects in the FoV.

Drawbacks

- Not suitable for low SB objects (high spectral resolution modes)
- Control of chromatic aberration (high quality optics)
- Very precise mechanical scanning (flexures)
- Pixel-by-pixel calibration

#### **5.4.1.2 Science with an IFTS instrument in a 6.5m class telescope: the case for TSPM**

The current large-format astronomical surveys (e.g. SDSS, 2dF) provide multi-wavelength imaging on very broad fields, which are then combined with spectroscopic observations of a previously selected, magnitude-limited targets. Given the large amount of information that they provide, these surveys have contributed enormously to the development of modern astrophysics, however the present several restrictions. The most important being that the spectral information is restricted to a specific spatial region of the target, in the case of galaxies normally the central one (covered by the fibre), which prevents the study of properties that show a spatial variation (e.g. chemical abundances in spiral galaxies, dust properties, metallicity and age gradients of the stellar populations, etc.). This combined with the impossibility of covering spectroscopically a large number of targets given the limited number of fibres and spectrographs in a given instrument.





Two-dimensional spectroscopy came to revolutionize the field by allowing the spectroscopic observation of spatially-resolved objects. However, in general, this method offers a very short FoV ( $< 1$  arcmin) with poor spatial and spectral resolution, which hampers the possibility to observe a large number of targets. That is why an IFTS would be the ideal instrument in case the target occupies a large fraction of the FoV of the instrument, or if one requires observing a large number of sources in a crowded FoV. The niche of opportunity of an astronomical IFTS is thus covering a very large FoV, with a spatial resolution limited by seeing), with a flexible, moderate-to-high spectral resolution ( $R \sim 2000 - 10000$ ) and a wide spectral range coverage.

The potential scientific cases to be explored by an IFTS instrument in the optical wavelength range are the following:

- *Evolution of cluster of galaxies.* The large FoV of an IFTS would allow to cover spatial regions corresponding to the virial radius of nearby clusters ( $z < 0.04$ ) in reasonable observing times (0.25 to 1 degree FoV). The potential of an IFTS is perfect considering the high density of galaxies in the central regions of clusters, which would provide great statistics considering the large number of objects in such fields. Observations with an IFTS would allow to detect spectroscopically tidal and other environmentally features which are common in these dense environments and that can shed light on the physical processes governing the evolution of cluster galaxies.
- *Galactic HII regions.* Photoionized nebulae are essential to determine the chemical composition of the interstellar medium in galaxies, including the primordial helium abundance. Linked to this problem is the existence of abundance discrepancy problem measured through collisionally excited lines (CEL) or recombination lines (RL). The large FoV offered by the IFTS the best opportunity for obtaining the required spectral information of nearby Galactic HII regions with a complete spatial coverage, as well as the study of the impact of shock fronts originating from massive stellar winds and the kinematics of HII regions.
- *Nearby galaxies.* With its high efficiency and large field of view an IFTS will be the ideal instrument to study the chemical abundances, kinematics and stellar populations of nearby galaxies. Deep, high-resolution observations of large samples of nearby galaxies with a IFTS will revolutionize the study of galaxy chemical evolution and provide new frontiers in the study of the kinematics and stellar populations of nearby galaxies.
- *Galaxies across the Universe.* Because the IFTS can be used without predefined filter in the whole visible waveband, they can be extremely useful to study the intermediate-to-high  $z$  Universe in a relatively unbiased way. As an example, the IFTS will allow detection of Lyman- $\alpha$  emission in objects at  $2 < z < 7$ . The IFTS will sample the redshift space uniformly on a wide field allowing spectroscopic redshift determination and line profile analysis of many galaxies in a single observation.



- *Properties of open stellar clusters.* Although hundreds of open clusters are known in the Galaxy, only for very few of them their main properties (size, distance and reddening) have been estimated. The angular extension of the cluster (of the order of 1 deg in some cases) is a limitation for obtaining spectroscopic data of a very large number of stars, and in cases of important crowding, the multi-fiber or multi-slit spectroscopy are not able to observe all the objects in the field at once. Again, an IFTS will allow obtaining spectroscopic information on crowded stellar clusters with complete spatial coverage.

Therefore the required parameters for the IFTS are the following:

- *Field of View of 15-30 arcmin circular.* This field of view will allow mapping in a single exposure most galaxy groups in the local Universe and in few exposures most galaxy clusters (up to  $z = 0.02$ ). In addition, this will allow studying in close detail nearby galaxies with very high spatial resolution.
- *Spectral range from 360 – 1000 nm.* The lower limit is imposed by the importance of detecting the [OII] 372.7,3.729 nm doublet for studies of galaxy evolution. The upper limit will be imposed by the decreasing of the total throughput of the system (optics + CCD) at near IR wavelengths. In any case, most of the emission and absorption lines of interest for galactic structure and evolution at optical wavelengths will be covered. For this reason the optics and CCD of IFTS will be optimized for optical wavelengths, and this naturally imposes the upper wavelength limit at 1 micron. The required lower limit in  $\lambda$  implies that the minimum OPD sampling must be  $\Delta x = 180$  nm.
- *Resolving Power  $1 < R < 20000$ .* The spectral resolution of an IFTS is a function of the field of view as well as of the total OPD sampled. In this case, the desired field of view of 15-30 arcmin is this last factor the one that limits the spectral resolution. For most scientific cases (as the ones explained above)  $R = 20000$  is largely enough at any wavelength in the allowed spectral range. For a resolving power  $R = 20000$  at 650 nm the total scanned OPD would be of 7.8 mm.

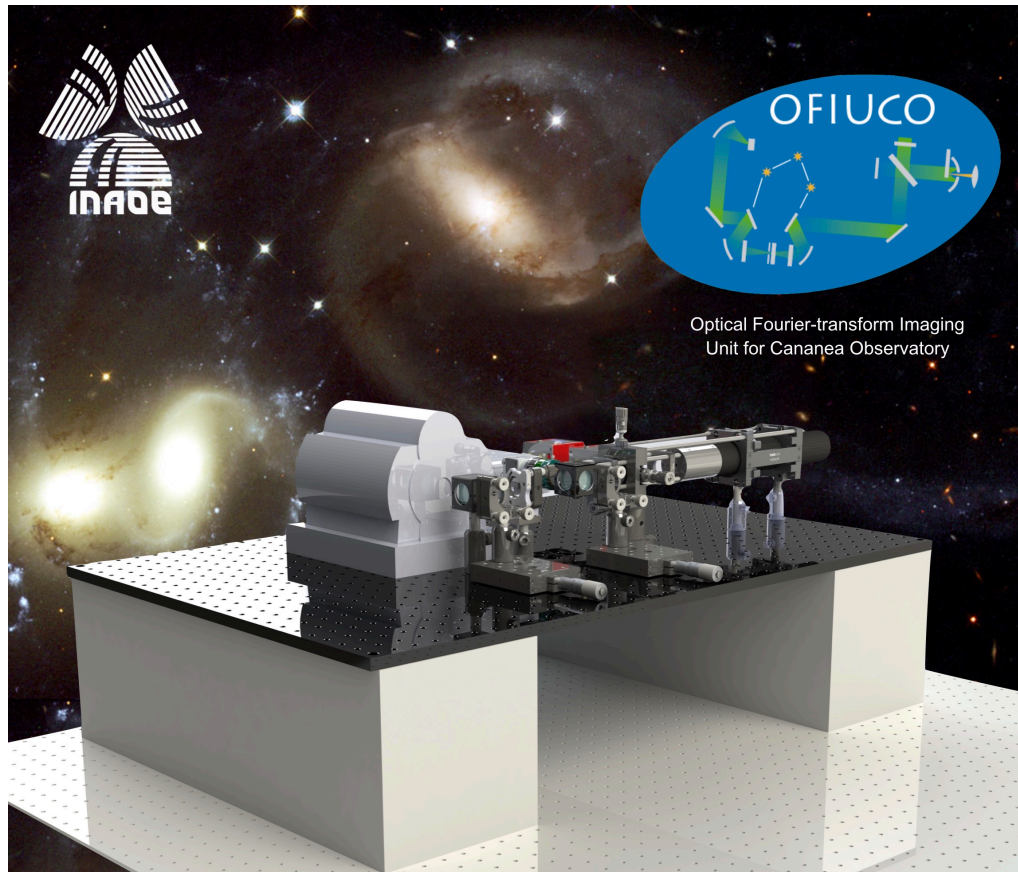


**Figure 22:** 3D design render of OFIUCO: Optical Fourier-transform Imaging Unit for Cananea Observatory (PI F. Rosales-Ortega), the IFTS prototype currently being designed and integrated at INAOE. The design includes a beam splitter, one fixed mirror, one moveable mirror with an actuators system, two CCD ports, and a metrology system.

**A second-generation instrument proposal for TSPM.** We have presented the IFTS concept as a viable approach to integral field spectroscopy. A working IFTS instrument would combine high-resolution imagery and spectroscopy at levels unmatched by any other astronomical instrument. Such instrument would acquire spectra within images that are between 100 and 1000 times larger than is possible with conventional spectrographs. The science niche for the IFTS approach must take into account its main advantages (very wide field of view, high throughput, seeing-limited image quality, and flexible spectral resolution) and disadvantages (spectrally distributed noise, and necessary compromise between spectral coverage and resolution).



Given this niche of opportunity, we are building at INAOE-Mexico a pilot instrument based on the IFTS concept designed for and tested at the 2.1m telescope of the Observatorio Astrofísico Guillermo Haro (OAGH) in Cananea, called *OFIUCO: Optical Fourier-transform Imaging Unit for Cananea Observatory*. This instrument will provide un-biased wide-field (10 arcmin) spectroscopic information, with a spatial resolution limited by seeing ( $\sim 1.4$  arcsec), and flexible spectral resolution ( $R \sim 500\text{--}8000$ ), see Fig. 22. The design and development of this prototype instrument has been founded by the Mexican Council for Science and Technology (CONACyT).

The development process of this pilot instrument would allow us to understand the technical issues of this technology, interpret the data, prepare the reduction and analysis pipelines, train students and postdocs in the use of the data, and address a set of suitable astronomical problems. The experience acquired during the design, integration and testing of this prototype would be of paramount importance in order to explore a potential, second generation IFTS instrument for the future Telescopio San Pedro Mártir (TSPM) in Mexico. The ability to provide high spectral resolution across a large area of space will provide Mexican astronomers with a considerably larger data set in a fraction of the time currently possible. An IFTS instrument could collect the same amount of data in a single night that would require weeks of observations with a conventional instrument, i.e. a huge improvement for telescope efficiency, where observing time is a scarce resource, often restricted to few hours per project.

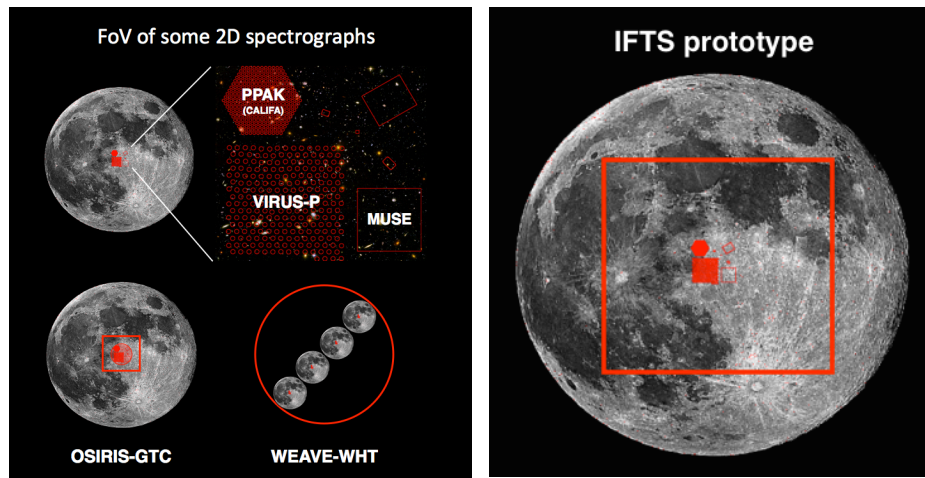


**Figure 23:** Left: Field-of-View of some 2D spectrographs compared to the angular size of the Moon (30 arcmin). Bottom-left: The red square/circle represent the nominal (7 arcmin) and usable (3 arcmin) FoV of the OSIRIS-GTC tunable filter instrument respectively, compared to the size of the Moon. The FoV of the OSIRIS-GTC MOS is 2 arcmin, with a very limited spectral coverage. Bottom-right: the 2 $\sigma$  FoV of the WEAVE-WHT instrument in which 1000 low spatial resolution fibres (1.3-2.6 arcsec) can be positioned, with low effective coverage. Right: Comparison of the 15 arcmin FoV for the proposed IFTS instrument for the 2.1m OAGH telescope to the angular size of the Moon (see main text).



The arrival of such an instrument to the 6.5m-class TSPM, under exceptional skies, could mark a milestone in the astronomical observing techniques, allowing for a wide variety of science projects, promoting the competitiveness of the TSPM, and positioning the Mexican astronomical infrastructure as a leading contender in the world arena.

- Allington-Smith et al. 2002, PASP, 114, 892  
Bacon et al. 2004, SPIE, 5492, 1145  
Cappellari et al. 2011, MNRAS, 413, 813  
Colless et al. 2001, MNRAS, 328, 1039  
Croom et al. 2012, MNRAS, 421, 872  
Drissen et al. 2010, SPIE, 7735, 77350B  
Drissen et al. 2014, Advances in Astronomy, 293856  
Grandmont et al. 2003, SPIE, 4842, 392  
Rosales-Ortega et al. 2010, MNRAS, 405, 735  
Sánchez et al. 2012, A&A, 538, 8  
Sánchez et al. 2015, A&A, 573, A105

#### 5.4.2 A (Spectro-)Polarimeter Unit for the TSPM: EspectroPol

**Rational:** Light is the fundamental source of information in astronomy and astrophysics. It is therefore understandable that studying its characteristics would grant us a large amount of information on the nature and particularities of the objects emitting it. The property behind this study is the polarization, which describes the geometry of the electromagnetic waves arriving to the observer. The waves being composed of both the perpendicularly oriented electrical and magnetic fields, a polarization analysis would therefore give valuable information on both components. The polarization of light is divided between the linear and circular modes (note that an elliptical mode also exists), each measured differently and originating from different phenomena. The polarization states needed to describe any astronomical system are set by the Stokes parameters I (total intensity), Q & U (linear polarization) and V (circular polarization). The latter allowing us to obtain the degree  $p$  and angle  $\Theta$  of polarization such as:  $p = (Q^2 + U^2 + V^2) / I$  and  $\Theta = \tan^{-1}(U/Q)$ .

Among the physical processes of interest directly obtained from polarimetric studies we can cite the magnetic fields. The latter are known to play an important role in a wide range of astrophysical objects along the HR diagram. The most obvious example is that of our Sun. Indeed, a large fraction of our knowledge of stellar magnetic activity is made via the analogy with the solar activity. The latter is seen through the presence of sunspots (intense concentration of magnetic field), coronal mass ejection, flares and magnetic reconnection which release a large amount of energy in the interplanetary medium. Those phenomena are not proper to the Sun, and solar type stars display a similar internal structure: an internal radiative zone and an external convective one. It is believed that the dynamo





effect, responsible for the generation of global magnetic fields, occurs in the interface region between both zones called "tachocline" (Parker 1993). Therefore all solar type stars should display a magnetic activity. However such activity can also be found in other type of stars: the fully convective ones at the bottom of the HR diagram or the hot ones with a spectral type A and B locate in the upper part of the HR diagram.

The different internal structure of these stars has led to the search for new magnetic fields generation models such as the fossils fields (Moss 1997) where the fields are remnants from the stellar formation era, the presence of a dynamo acting in the convective nucleus (Charbonneau & MacGregor 2001). A non-solar type dynamo process has been invoked to explain the fields found in M and L type star (on the other side of the main sequence) and the action of binary stars (amplifying and maintained the fields) was presented for evolved stars such as cold ( $< 10\,000\text{K}$ ) Post-AGBs and planetary nebulae (Nordhaus et al. 2007). If progresses have been made in the development of theoretical models, data analysis techniques and magneto-hydrodynamical codes; more accurate and more numerous observational data are still missing.

For instance, detecting and measuring magnetic fields in the so-called weak field regime is a difficult task as observationally speaking the Zeeman signature, indicative of the presence of the field, shown with the Stokes V data is (extremely) weak (so the name). In this regime, the magnetic splitting is small compared to the thermal and pressure broadening and is generally below  $\sim 10\text{th}$  kG level depending of the studied absorption lines. Such challenging detection threshold hampers the accurate study of magnetic fields in a large number of objects such as evolved stars, some massive stars, etc. One of the best known (and more used) high resolution spectropolarimeter is ESPaDOnS on the 3.6m CFHT (Hawaii, <http://www.ast.obsmpifr/projets/espadons>). With an access primarily reserved to the CFHT and Gemini consortium members (and collaborators), a sometimes high oversubscription (up to 5-6 depending on the agency) and a "limiting" magnitude up to 13-14 mag in V band for spectroplarimetric observations to use reasonable Stokes-V exposure time: a proper analysis of the (weak) magnetic field along the HR diagram is therefore a long and arduous task (fainter objects can be detected, up to mag  $V = \sim 17$ , but the polarimetric observing time would become prohibitive).

Alongside circular polarization, linear polarization also provides a huge amount of information on astrophysical objects. Hence it has been shown by Brown et al. (1978) that the Stokes Q and U (through their polarization degree) can be used to unveil the geometry of any object scattering (or polarizing) the light. In addition, if the studied objects are binaries, the polarization degree will be non-null. In this case the Stokes parameters Q and U will depend on the orientation of the two stars with respect to the observer. If these sources are moving within a certain orbit, we will observe a variation of the linear polarization in function of the geometry of the orbit and its orientation with respect to the observer: linear polarization provides a direct measurement of the inclination of the system.





On the other hand, stellar objects showing synchrotron emission display a polarization degree which is linked to distribution of the magnetic field: the most organized fields produce a higher degree of polarization, and the variation of this degree indicate changes in the structure of the magnetic field. Assuming that the emission of a relativistic jet results from shocks propagation, the compression produced by the shocks increase the level of organization of the magnetic field lines as well as the degree of polarization. Therefore a correlation between the brightness variability and the degree of polarization would likely indicate the hypothesis shock propagation. Furthermore, a lack of correlation would indicate that such variability would have a different origin. Linear polarization studies can help investigate astrophysical phenomena such as magnetic fields, shocks, jets, synchrotron emission, morphology and binarity in various objects (blazars, binary stars, protoplanetary discs, etc). The accurate detection and measurement of the Stokes Q and U using a large aperture (as polarimetric studies are notoriously "photon hungry") would therefore allow the precise calculation of the polarization parameters for a larger set of objects.

The implementation of a polarimetric unit such as EspectroPol on the TSPM will significantly contribute to boost scientific investigations in a wide range of astrophysical areas. Indeed:

- The large 6.5m aperture will provide more light which will be useful to palliate the loss inherent to this observing technique (due to the optical path and elements in the way) and to reach fainter targets which were otherwise would not be considered.
- The possibility of exploring stars along the whole HR diagram using high resolution circular spectropolarimetry would be a huge breakthrough as it would open a new door in the detection and analysis of (weak) magnetic fields for the community involved in the TSPM (and particularly the Mexican one). Totally unexplored groups of objects would now be accessible.
- The characteristics of the polarimeter here proposed is such that its versatility due to the fact that it is fiber-fed, allows its adaptation to any kind of instruments (e.g. mostly any spectrograph). The range of applications is therefore ample: from the detection of objects' geometry to the study of binary systems and tomagnetic fields analysis to cite a few.
- The TSPM will be part of the small group of (highly demanded) telescopes providing spectropolarimetry and be one of the largest, as comparison:
  1. William Herschel Telescope (4.2 metros) ISIS: <http://www.ing.iac.es>
  2. Canada-France-Hawaii Telescope (3.6 metros) ESPaDOnS: <http://www.cfht.hawaii.edu>
  3. Telescope Bernard Lyot (2.2 metros) NARVAL: <http://www.ast.obs-mip.fr>
  4. ESO La Silla Telescope (3.6 metros) HARPS: <http://www.eso.org/sci>
  5. Large Binocular Telescope (2 x 8.4 m ) PEPESI: a high-resolution echelle spectrograph with two polarimeters, <http://www.aip.de/groups>
  6. BTA-6m SCORPIO: <https://www.sao.ru/hq/lsvfo/devices/scorpio>



#### 5.4.2.1 *EspectroPol: science with the TSPM*

**Magnetic Fields in evolved intermediate mass stars:** Our global understanding of stellar magnetism in evolved intermediate mass stars such as AGB and Post-AGB stars is relatively poor. Such discoveries are of great importance in order to investigate the dynamical ability of magnetic fields in driving outflows, shaping the envelopes (leading subsequently to asymmetrical Planetary Nebulae) but also controlling the mass loss and influencing the chemistry of evolved stars. At larger scale, correlating the galactic distribution of these magnetic stars with existing (theoretical) models predicting the variation of the mass, morphology and chemistry of evolved stars in the Galaxy would then give us valuable information regarding the role of these Fields. This would also provide a unique and powerful prognostic tool. Little is known about the magnetic characteristics of the central stars: most importantly the field strength.

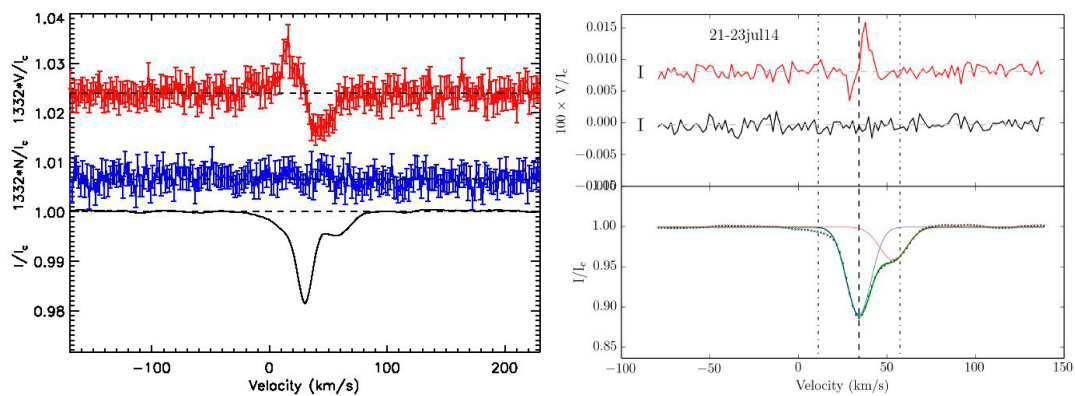


**Figure 24:** Clear Zeeman signature in the Stokes V spectra (red) of U Mon (left) with  $V_{\text{mag}}=5.8$  and R Sct (right) with  $V_{\text{mag}}=5.2$ . The null spectrum (blue) shows a rather flat shape probing the authenticity of the polarization signal. Finally the double peak in the Stokes I spectra (black) representing the full intensity indicates the shock process occurring in the atmosphere of the PAGBs (Sabin, Wade & Lebre, 2015).

The few spectropolarimetric observations of planetary nebulae central stars realised so far, were all inconclusive (Leone et al. 2011,2014; Steffen et al. 2014). Our group used the high resolution spectropolarimeters ESPaDOnS at CFHT and Narval at TBL to investigate the presence of magnetic field at the stellar surface of a set of different types of bright Post-AGBs. Using the Least-Squares Deconvolution (LSD) technique to analysed the data we detected for the first time a clear Zeeman signature in the Stokes V profiles of the PAGB U Mon (Fig. 24, left). The LSD analysis indicated a definite detection and a longitudinal magnetic field of  $10.2 \pm 1.7$  G (Sabin, Wade & Lebre, 2015). Additional observations allowed us to unveil a magnetic field at the surface of the PAGB R Sct (Fig.24, right). In both cases, we were also able to identify a likely relationship between the magnetic field and the shock processes in the PAGBs. Monitoring a long a portion of their pulsation cycle would allow to characterise this relation.



The general faintness of these evolved stars ( $\text{mag } V < \sim 10$ ) makes it difficult to detect and assess a proper magnetic field diagnostic in these stars. In the case of planetary nebulae, one has in addition to overcome the presence of a large number of emission lines. The use of a polarimetric unit adapted via fiber to any high resolution spectrograph mounted on the 6.5m will allow to achieve this goal.

**Spectropolarimetry of AGN:** Active Galactic Nuclei (AGN) are divided in type 1 and type 2 objects based on the presence or not of the so-called Broad Line Region (BLR). Depending on their luminosity and distance, these objects are also classified as either Seyfert galaxies (for the nearby and less luminous objects  $M_B > -23$ ) or Quasars (distant objects with  $M_B < -23$ ). To explain the type 1/type 2 dichotomy, the Unified Model (Antonucci 1993) assumes that the BLR in type 2 AGN is blocked from our line of sight due to the presence of a dusty and clumpy torus surrounding the central Super Massive Black Hole (SMBH). This obscured material makes UV, optical and soft X-ray emission anisotropic. Broad permitted emission lines are typically seen without significant obscuration in type 1 AGN. The Sloan Digital Sky Survey (SDSS) has identified a number candidates of type 2 AGN for objects for low- (Reyes et al 2008) and highredshifts (Alexandroff et al 2013). Optical spectropolarimetry of type 2 AGNs give us the opportunity to observe its central regions along several lines of sight when the light from its central part is heavily extinct (Zakamska, et al. 2005).

Although the AGN central emission is obscured, some of the light of the BLR is scattered by material outside of the obscuring torus and can reach the observer. This scattered radiation is polarized, thus observation of the polarized flux can offer evidence of the existence of obscured AGN. Following the pioneering work by Antonucci & Miller (1985) for NGC 1068, there have been several attempts (e.g. Zakamska et al. 2005) to detect broad emission lines in type 2 AGN with both optical spectropolarimetry. The presence of dim broad wings in the permitted narrow lines will be interpreted as evidence of a not totally obscured BLR, i.e. the presence of a clumpy torus. Conversely, the detection of a broad polarized emission lines will be an evidence of scattering by electrons outside the dust torus plane. X-ray observations of Seyfert 2 galaxies have shown extremely short ( $\sim 4$  hours) flux variability timescales (Elvis et al. 2004), which have been explained as evidence of holes in a clumpy torus of dust that allows to observe the central region. Optical microvariability has also been reported by Polednikova et al. (2015; 2016), which also favors the presence of optically thin gaps in a clumpy obscuring medium.

- Alexandroff, Rachael et al. 2013, MNRAS, 435,3306  
Antonucci, R. R. J. 1993, ARA&A, 31, 473  
Antonucci, R. R. J. & Miller, J. S. 1985, ApJ, 297, 621  
Charbonneau, P., & MacGregor, K. B., Astrophysical Journal, 2001, 559, 1094  
Elvis, M. et al. 2004, ApJ, 615, L25  
Leone, F. et al., ApJ, 731,33,2011  
Leone, F.;et al., A&A,563,43,2014  
Moss D., Monthly Notices Royal Astron. Society, 1987, 226, 297



**TSPM Science Document**

Code: SCI/TSPM-PDR/001

Issue: 1.B

Date: 20/10/2017

Page: 86 of 86

Nordhaus J. et al., MNRAS, 2007, 376,599  
Parker, E. N., Astrophysical Journal, 1993, 408, 707  
Polednikova, J. et al. 2015, A&A, 578, A121  
Polednikova, J. et al. 2016, MNRAS, 460, 3950  
Reyes, R. et al. 2008, AJ, 136, 2373  
Sabin, L.; Wade, G. A.; Lèbre, A., MNRAS,446,1988,2015  
Steffen, M. et al., A&A, 550,88,2014  
Zakamska, N. L. et al. 2005, AJ, 129, 1212